ISSN:2795-1707
www.hist.edu.np

Journal of Science Techonlogy & Management

HIST - Engineering College
Himalayan Institute of Science & Technology
(Affiliated to Purbanchal University)

Journal of Science Technology & Management

(Peer Reviewed Journal)

Volume 2 **Number1** **Aug./Sep. 2022**

Publisher

HIST Engineering College

New Baneshwor, Kathmandu

Tel. No.: 01-01-4794951, 01-5202726

E-mail: info@hist.edu.np

Website: www.hist. edu.np

Sensitivity Analysis of a Surge Tank in a Hydropower System using Method of Characteristics

Khem Prasad Bhattarai[1]†, Kamal Prasad Pandey[2]

[1]Institute for Integrated Hydro-Environment Research, Kathmandu, Nepal
[2]Hydro Lab Pvt. Ltd., Lalitpur, Nepal
† Corresponding author. Phone: +977-9849151175, Email: kpbhattarai2019@gmail.com

Abstract

Hydropower system frequently encounters hydraulic transients due to changes in flow characteristics of the system. These transients could be catastrophic if proper transient controlling devices are not provided. Thus, a detailed study of the behaviour of the hydraulic transient of the hydropower system becomes crucial for the safety of the system against the negative effects of transients and also the optimization of transient protection devices. In large hydropower systems, surge tanks are the important structures that control the effects of transients. Detailed analysis of hydraulic transients is extremely important to optimize the system for safe and effective functionality. This paper presents the 1-D numerical modelling approach of the hydraulic transient analysis in a hydropower system with a simple surge tank by using Method of Characteristics (MOC). Matlab codes are prepared to simulate load rejection and load acceptance cases. The numerical model is validated by using Hytran software, a commercial software designed for transient analysis. Various sensitivity analyses were carried out to draw important conclusions, which assist in the optimized design of surge tanks ensuring the safety of the system against the worst transient event that may occur in the system. The analysis revealed that the larger diameter of the surge tank significantly reduces the mass oscillations in the surge tank, while the larger diameter of the headrace tunnel and smaller wave speed in the conduit also contribute, to reducing the mass oscillations in the surge tank to a relatively small amount. Thus, this study helps in understanding the behaviour of mass oscillation in surge tanks for different hydraulic parameters, and assists in the optimized design of surge tanks.

Keywords

Hydraulic transients; Method of Characteristics; Sensitivity analysis; Surge tank; Water hammer, Surge analysis

1. Introduction

Hydropower is a cheap, environment-friendly, and efficient renewable source of energy as compared to fossil fuels. It converts the potential energy of stored water or kinetic energy of fast-flowing water into electric energy, which can be used in various modern energy devices. As the demand for electricity is increasing day by day, hydropower is one of the most fascinating and suitable solutions to address the energy crisis (Sharma, Tiwari, & Sood, 2013).

Despite being an efficient, renewable, and environmentally friendly source of energy, large hydropower generation also, have some disadvantages. The construction of dams and diversion of river channels renders severe negative social, biological, and environmental impacts. In addition, the failure of dams and hydropower components causes huge loss of life and property. Thus, special attention is required to establish a safe and stable design with the least impact on the surrounding environment. One of the major sources of instability for hydropower projects, along with other pressurized water flow systems, is the hydraulic transients caused by the changes in flow conditions in the system, which is the major topic of analysis and discussion of this study.

In any pressurized flow system, hydraulic transient occurs whenever there is a disturbance in the steady state condition of the system resulting in variations of pressure and discharge in the system. The highly fluctuating pressure wave travels along the waterway threatening the safety and stability of the system. The control of hydraulic transients in pressurized systems like water supply, wastewater, and hydropower system, is a major concern for engineers regarding the safe and effective operation of the system throughout the life span of the project. Uncontrolled hydraulic transients in the system have led to several cases of accidents in hydropower stations in the past (Adamkowski, 2001; Arrington, 1999; Bonin, 1960; Schmitt, Pluvinage, Hadj - Taieb, & Akid, 2006). Several methods, models and software have been developed for analysis of hydraulic transients like the graphical method, the algebraic method, the implicit method, the wave characteristic method, the Method of Characteristics (MOC), Zielke model, Brunone model, Surge2012, Hytran, etc. (Boulos, Karney, Wood, & Lingireddy, 2005; Chaichan & Al-Zubaidi, 2015; Izquierdo & Iglesias, 2004; Salmanzadeh, 2013; Sam Ani & Khayatzadeh, 2002; Shani & Gupta, 2017). Among such methods, MOC is a popular method, owing to its advantages over other methods in producing accurate results with shorter computational time, and convenience to use in computer modelling (Chaudhry, 1979; Wylie, Streeter, & Suo, 1993). In this study, MOC is used, considering the steady-state friction along the pipe as initial condition. A generalized hydropower system is considered and transient events are generated for full load rejection and full load acceptance conditions. The effect of several hydraulic parameters on the mass oscillation in surge tank are analysed for optimum design of surge tank for the system.

The MOC is frequently used by researchers for the transient analysis of pressurized systems. Calamak et al. developed a computer program using MOC, which accurately predicted pressures for various simulations in case studies having Pelton and Francis turbine (Calamak & Bozkus, 2012). Nambiar et al. studied the characteristics of valves in pipeline systems and carried out optimization of valves by implementing the MOC in a computer software (Nambiar et al., 2015). Bhattarai et al. and Dhakal et al. employed MOC for transient analysis in hydropower system and performed optimization of surge tank (Bhattarai, Zhou, Palikhe, Pandey, & Suwal, 2019; Dhakal, Zhou, Palikhe, & Bhattarai, 2020). Garg and Kumar carried out the hydraulic transients analysis for a simple reservoir-pipeline-valve arrangement in Matlab using MOC (Rahul Kumar Garg, Arun Kumar, 2018). Tiwari et al. performed the numerical simulation of the hydraulic transients in a hydropower system using MOC and concluded that the valve maneuver time and pattern have negligible effect on the mass oscillation in surge tank, while its effect is significant for the water hammer pressure in the system (Tiwari, Tamot, Palikhe, Bhattarai, & Pandey, 2021). Ma et al. and Zhou et al. explored the head loss coefficient characteristics for different kinds of throttles in surge tank through experimental and simulation based investigations (Ma et al., 2022; Zhou, Palikhe, Cai, & Liu, 2020). Yu et al. performed the transient analysis of a long-diversion type hydropower project with differential surge tank having several pressure reduction orifices to effectively reduce the pressure difference on the two sides of the breast wall (Yu, Zhang, & Zhou, 2014). Several researchers attempted to perform the sensitivity analysis of the hydraulic transient behaviour of pressurized pipeline flow (Chaichan & Al-Zubaidi, 2015; Diao, Zhang, & Yang, 2016; Emadi & Solemani, 2011; Wan & Li, 2016; Zhou & Karney, 2014).Thus, optimal parameter

selection requires sensitivity analysis, which may be useful for future researcher in deciding the parameters for optimization as well as analysis of results.

2. Methodology

The governing equations for the physics of the hydraulic transients are the continuity equation and the equation of motion, also known as the Saint-Venant equations. These equations have no analytical solution, and can be most accurately solved by the MOC (Chaudhry, 1979; Wylie et al., 1993). The Saint-Venant equations form a pair of quasi-linear hyperbolic partial differential equations in terms of two independent variables, distance and time, and two dependent variables, discharge and piezometric head. The MOC, as proposed by Wylie et al., is applied to solve the governing equations, which are conveniently handled numerically (Wylie et al., 1993). Several researchers have employed MOC for the numerical analysis of highly pressurized pipeline system due to its simplicity, high accuracy, capability of handling several boundary conditions and convenience in computer modelling (Afshar & Rohani, 2008; Bhattarai et al., 2019; Shani & Gupta, 2017).

The MOC uses the initial steady state condition to predict the flow characteristics at any given time and distance. The two characteristics lines, C^+ and C^-, intersect at point P, as shown in Figure 1. Thus, solving the Saint-Venant equation by MOC and applying the initial steady state condition, the values of the piezometric head and discharge at any required position and time in the x-t grid can be obtained.

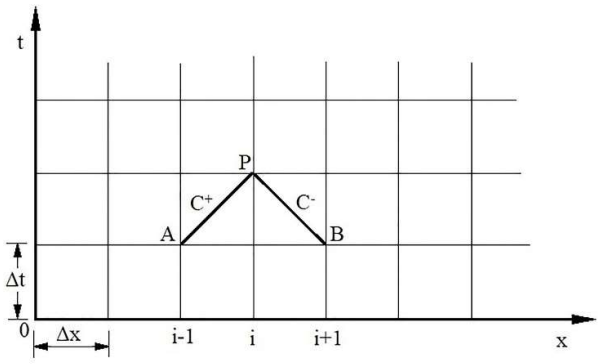

Figure 1. Characteristic Lines in x-t Grid (Bhattarai et al., 2019)

2.1. Boundary Conditions

Upstream Reservoir

The hydropower system considered for this study consists of an upstream reservoir, and it is assumed that water level in the reservoir remains constant for the short transient event.

$$H_{P_1} = H_R \tag{1}$$

where, H_{P_1} and H_R are the piezometric head and water level in the reservoir, respectively.

Surge Tank

The hydropower system of this study consists of a simple surge tank at the end of headrace tunnel. The equations representing the boundary conditions of the simple surge tank are presented below (Wylie et al., 1993).

$$H_P = Z_S \tag{2}$$

$$Z_S = \mathrm{W}(Q_S + Q_{S0}) + Z_{S0} \tag{3}$$

$$Q_1 = Q_2 + Q_S \tag{4}$$

$$W = \frac{\Delta t}{2A_S} \tag{5}$$

where, Q_1, Q_2 and Q_S are the discharge in pipe 1, pipe 2 and surge tank, respectively; H_P is the piezometric head at the bottom of the surge tank, and Z_S is the water level in the surge tank; Q_{S0} and Z_{S0} are the discharge and water level in the surge tank for previous time step, respectively; and A_S is the cross-sectional area of surge tank. Equations (2)-(5) are solved along with the characteristic equations to determine the variables at the surge tank boundary for each time step.

Downstream Valve

A valve is used at the end of penstock pipe in the hydropower system to control the flow passing into the turbine as per the load acceptance and rejection in the system. The equations representing the valve boundary condition are presented below. These equations are solved with the positive characteristic equation to evaluate the variables at the valve boundary.

$$Q_{P_{N+1}} = -BC_V + \sqrt{(BC_V)^2 + 2C_V C_P} \tag{6}$$

$$C_v = \frac{(Q_0\tau)^2}{2H_0} \tag{7}$$

Where, $Q_{P_{N+1}}$ is the discharge passing through valve; τ is the valve opening; Q_0 is the flow during steady state; and H_0 is the operating head in the system.

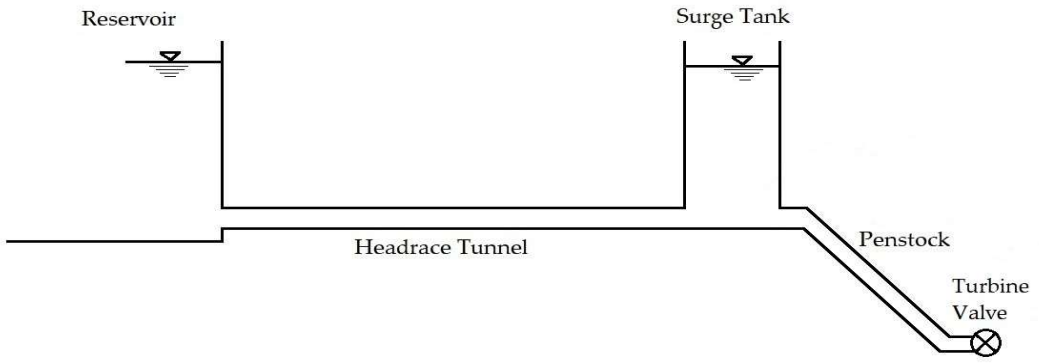

Figure 2. Generalized Layout of a Hydropower System

3. Model Setup and Validation

The hydropower system considered in this study consists of an upstream reservoir, headrace tunnel, simple surge tank, penstock pipe, and turbine valve as shown in Figure 2. The 1-D numerical model of the hydropower system was prepared by using MOC via coding in Matlab. The time step (Δt) of 0.008 seconds and position step (Δx) of 10 meters, considered in the analysis, are based on the Courant's condition with wave speed of 1200 m/s. Friction losses in the conduit are considered to establish the initial steady state in the system, while the minor losses are neglected. The transient condition of full load acceptance and full load rejection were modelled with valve opening/closure time of 30 seconds. Initially, steady state condition is run for 100 seconds, and then, linear valve opening/closure is performed in 30 seconds to study the transient behaviour of the system. The total time of operation is 600 seconds. The results obtained for the system were compared with the results obtained from the Hytran software, a commercial software for hydraulic transient analysis, for the same system and same input parameters. Figure 3 shows the results of the model prepared via coding in Matlab and via Hytran software for linear valve closure and opening conditions, which demonstrates high accuracy of the model prepared for this study. Thus, the model prepared in Matlab coding is validated by using Hytran software simulations, and further analysis were carried out using the validated Matlab model of the given hydropower system.

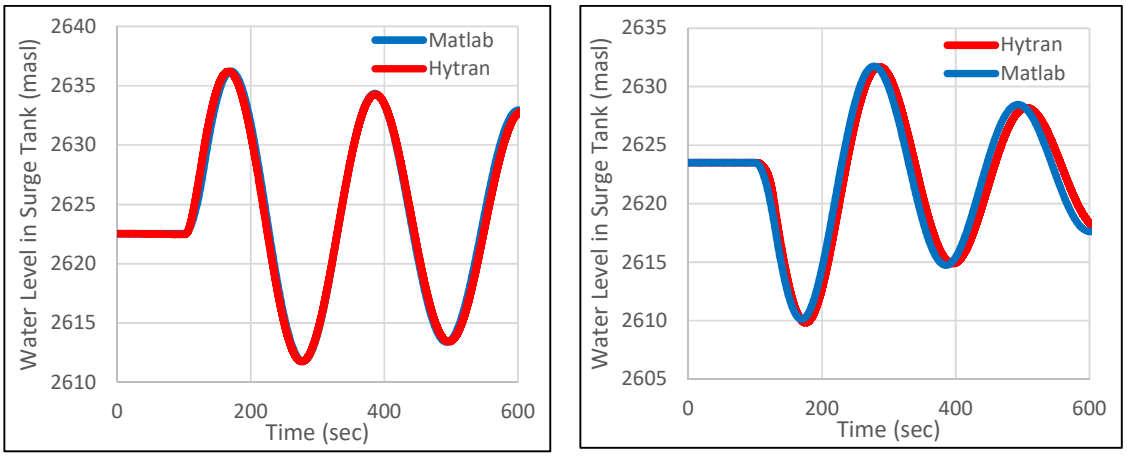

(a) (b)

Figure 3. Surge Analysis Comparison of Matlab Numerical Model and Hytran Software for Gradual Closure of Valve (a) and Gradual Opening of Valve (b)

4. Results and Discussions

The transient analysis reveals various important characteristics of the hydropower system such as mass oscillation levels in the surge tank, pressure variations throughout the waterway, etc., and thus, assists in designing a safe system through analysis of critical cases. The full load acceptance and full load rejection conditions for the given hydropower system, which gives the maximum and minimum water level in the surge tank, are crucial to investigate the worst transient effect on the system. This study presents the sensitivity analysis of surge tank based on the hydraulic parameters like diameter of surge tank, headrace tunnel (*HRT*), penstock pipe, coefficient of friction of *HRT* and penstock pipe, and wave speed in the conduit.

4.1. Surge Tank Diameter (D_S)

Surge tank diameter (D_S) is the most important factor, which influence the mass oscillation in the surge tank, and hence, determines the maximum water level (Z_{max}) and the minimum water level (Z_{min}) in the surge tank. The analyses were carried out for different values of D_S from 3 m to 20 m with increment of 0.5 m for the given hydropower system. The Z_{max} and Z_{min} obtained in the surge tank during the valve-closure and valve-opening conditions, respectively, were plotted against the respective D_S as presented in Figure 4. The analysis revealed that larger values of D_S decreases the Z_{max}, and increases the Z_{min}. Thus, larger values of D_S are preferable to reduce the height of surge tank. It is apparent from Figure 4 that the change in water level is higher in the initial stage and gradually decreases with increasing D_S.

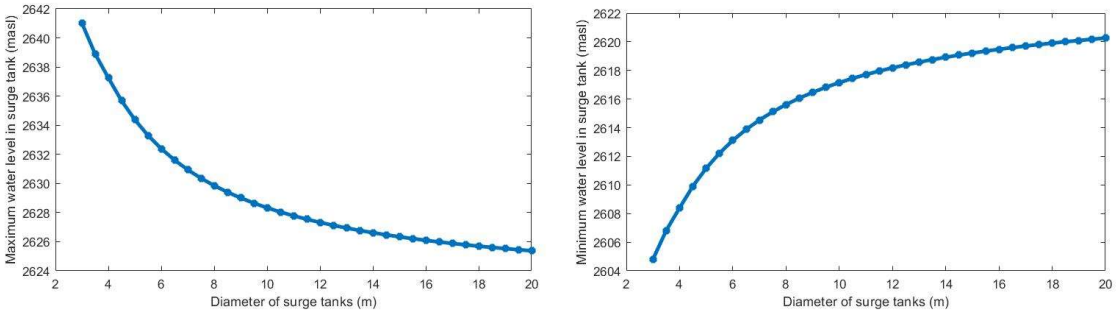

Figure 4. Maximum and Minimum Water Level Variation in Surge Tank with Changing D_S

4.2. Headrace Tunnel Diameter (D_{HRT})

The RoR type hydropower projects largely depends upon the head of the project to generate large amount of hydroelectricity, which is created by transporting the discharge through headrace tunnel (*HRT*) with surge tank at the end, with respect to the existing geographical constraints. The surge analysis for valve-closure and valve-opening was carried out with varying diameters of headrace tunnel (D_{HRT}) from 3 m to 5 m with increment of 0.2 m. The Z_{max} and Z_{min} in the surge tank, obtained for the cases of valve-closure and valve-opening respectively, were plotted against the respective D_{HRT} for the hydropower system as shown in Figure 5. The results revealed that the Z_{max} decreases with increasing D_{HRT}, and Z_{min} increases with increasing D_{HRT}. This indicates that larger D_{HRT} is favourable to decrease the mass oscillation levels in the surge tank, and thus, reduce the height of the surge tank. However, larger D_{HRT} significantly increases the cost of the project, and therefore, the cost of the *HRT* must be addressed while deciding the diameter of the *HRT* for the hydropower project.

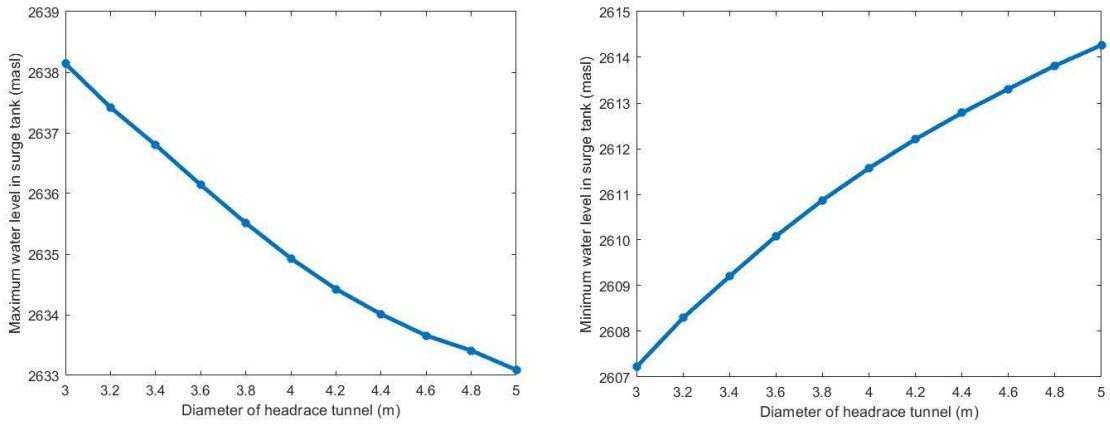

Figure 5. Maximum and Minimum Water Level Variation in Surge Tank with Changing D_{HRT}

4.3. Penstock Pipe Diameter (D_P)

Penstock pipe are used as a high pressure conduit that connects the *HRT* with the turbines in the powerhouse, and delivers discharge at very high velocity. Surge analysis for different values of diameters of penstock pipe (D_P) were carried out ranging from 1.0 m to 3.0 m with increment of 0.2 m. The Z_{max} and Z_{min} in the surge tank, obtained for the cases of valve-closure and valve-opening respectively, were plotted against the respective D_P for the hydropower system as shown in Figure 6. The results shows that the change in Z_{max} and Z_{min} is insignificant (only few centimetres). Nevertheless, the increasing D_P significantly increases the cost of the project, and thus, D_P must be decided considering the cost, while the transient effect of D_P is minimal.

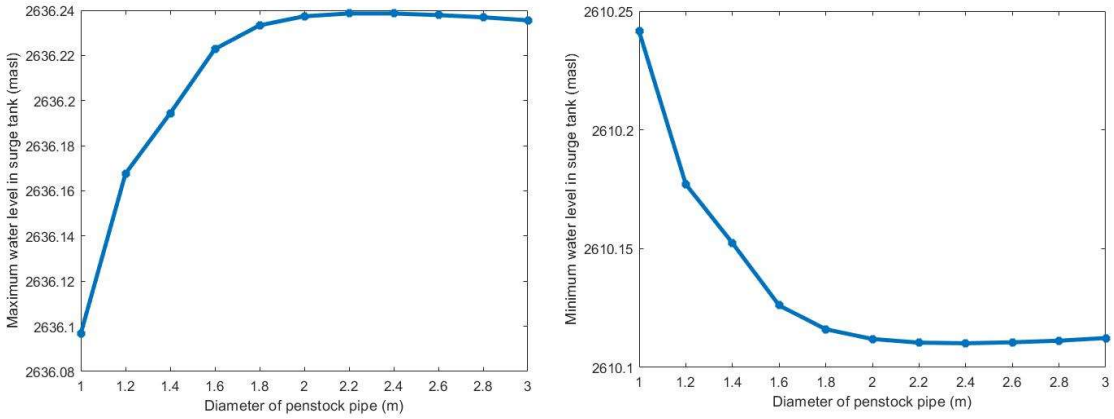

Figure 6. Maximum and Minimum Water Level Variation in Surge Tank with Changing D_P

4.4. Coefficient of Friction of Headrace Tunnel (f_{HRT})

The degree of roughness of the surface of the *HRT* determines the coefficient of friction of headrace tunnel (f_{HRT}). Surge analysis was performed for varying f_{HRT} from 0.012 to 0.024 with increment of 0.002. The Z_{max} and Z_{min} in the surge tank, obtained for the cases of valve-closure and valve-opening respectively, were plotted against the respective f_{HRT} for the hydropower

system as shown in Figure 7. The result shows that the Z_{max} and Z_{min} have minimal variation with changing f_{HRT} with both values decreasing with increasing $f_{HRT.}$

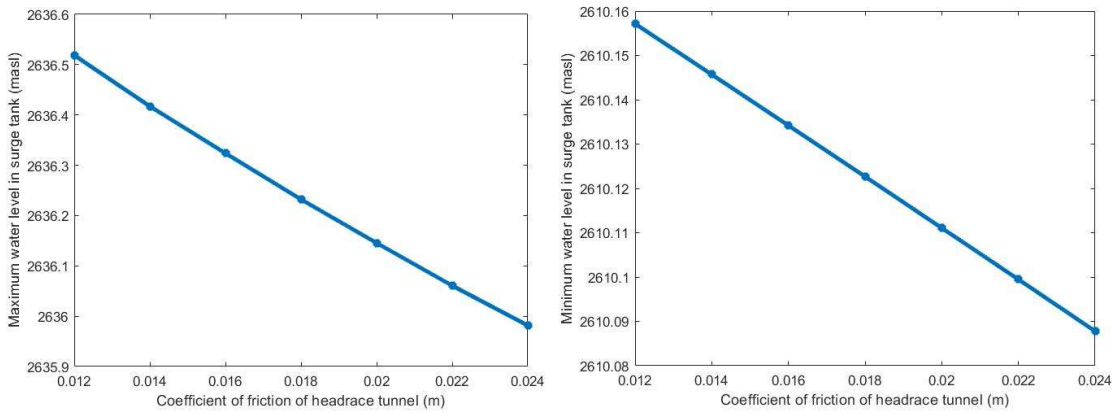

Figure 7. Maximum and Minimum Water Level Variation in Surge Tank with Changing f_{HRT}

4.5. Coefficient of Friction of Penstock Pipe (f_P)

The coefficient of friction of pipe f_P determines the friction loss occurring in the conduit. Different values of f_P were adopted for surge analysis, ranging from 0.01 to 0.015 with increment of 0.0005. The Z_{max} and Z_{min} in the surge tank, obtained for the cases of valve-closure and valve-opening respectively, were plotted against the respective f_P for the hydropower system as shown in Figure 8. The result shows that with increasing f_P, the decrease and increase in Z_{max} and Z_{min}, respectively, are minimal. Thus, changing f_P changes the friction in the penstock pipe; however, the height of the surge tank remains unaffected.

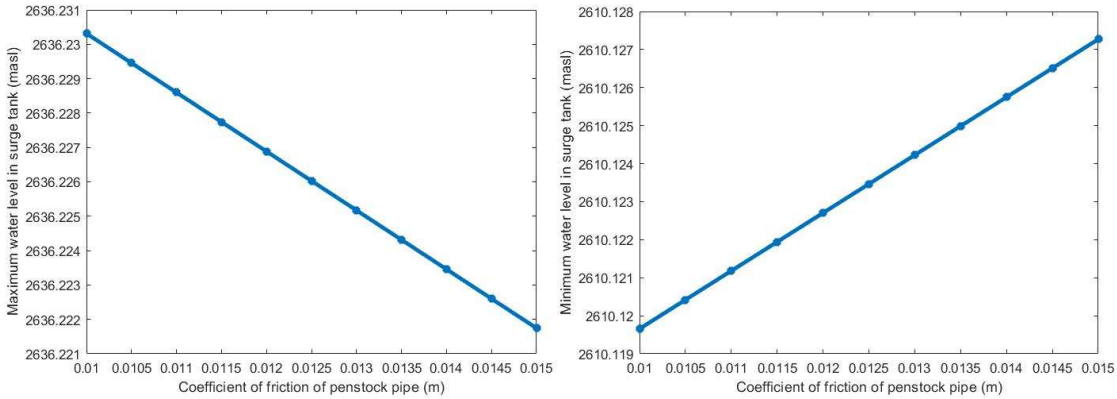

Figure 8. Maximum and Minimum Water Level Variation in Surge Tank with Changing f_P

4.6. Wave Speed (a)

The wave speed is an important parameter during water hammer phenomenon. The wave speed mainly depends on the type of material and wall thickness in the conduit. Surge analysis was performed for various values of wave speed ranging from 1000 m/s to 1400 m/s with increment of 50 m/s and the change in Z_{max} and Z_{min} was observed. The graph between the Z_{max} and Z_{min} during valve-closure and valve opening, respectively, were plotted against the respective wave speed values as presented in Figure 9. The graph indicates that for larger values of wave speed,

Z_{max} increases and Z_{min} decreases. Thus, lower values of wave speed are favourable to decrease the mass oscillation levels in surge tank. However, the change in water level observed is quiet small.

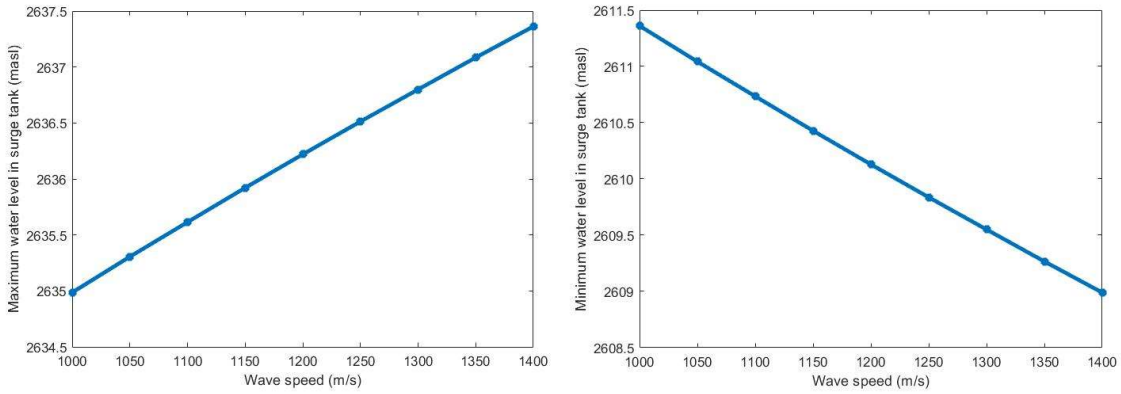

Figure 9. Maximum and Minimum Water Level Variation in Surge Tank with Changing Wave Speed

5. Conclusions

Surge tank is an important structure for the control of harmful transient effects in any hydropower system. Load acceptance and rejection are very frequent events in hydropower projects, which generates hydraulic transients in the system. Besides, accidental incidents may cause severe cases of transients in the system, threatening the safely of the project. Thus, an optimized design of surge tank is vital for effective performance and safety of the system throughout the life of the project. This study presents the sensitivity of the mass oscillation in the surge tank during the worst transient cases for the given hydropower system. Various hydraulic parameters were studied and following conclusions were made.

1. Larger D_S decreases the mass oscillations in the surge tank, and thus, the height of surge tank could be significantly reduced. However, the reduction in surge tank height gradually decreases as the D_S increases.
2. The mass oscillation in the surge tank can be decreased slightly by increasing D_{HRT}, and decreasing the wave speed in the conduit.
3. The mass oscillation in the surge tank has almost negligible effect on changing D_P, f_{HRT} and f_P.

Acknowledgement

Authors acknowledge the encouragement and support provided by Technoquarry Consults Pvt. Ltd. for the successful accomplishment of the study.

Reference

Adamkowski, A. (2001). Case study: Lapino powerplant penstock failure. *Journal of Hydraulic Engineering*, *127*(7), 547–555.

Afshar, M. H., & Rohani, M. (2008). Water hammer simulation by implicit method of characteristic. *International Journal of Pressure Vessels and Piping*, *85*(12), 851–859.

Arrington, R. M. (1999). Failure of water-operated needle valves at Bartlett dam and Oneida station hydroelectric plant. In *3rd ASME/JSME Joint Fluids Engineering Conference* (pp. 18–22).

Bhattarai, K. P., Zhou, J., Palikhe, S., Pandey, K. P., & Suwal, N. (2019). Numerical modeling and hydraulic optimization of a surge tank using particle swarm optimization. *Water*, *11*(4), 715.

Bonin, C. C. (1960). Water-hammer damage to Oigawa power station. *Journal of Engineering for Power*, *82*, 111–119. https://doi.org/10.1115/1.3672721

Boulos, P., Karney, B., Wood, D., & Lingireddy, S. (2005). Hydraulic Transient Guidelines. *Journal of the American Water Resources Association*, *97*(5), 111–124.

Calamak, M., & Bozkus, Z. (2012). Comparison of performance of two run-of-river plants during transient conditions. *Journal of Performance of Constructed Facilities*, *27*(5), 624–632.

Chaichan, M. T., & Al-Zubaidi, D. S. M. (2015). Control of hydraulic transients in the water piping system in Badra-Pumping Station No. 5. *Al-Nahrain University, College of Engineering Journal*, *18*(2), 229–239.

Chaudhry, M. H. (1979). *Applied Hydraulic Transients*. New York: Van Nostrand Reinhold.

Dhakal, R., Zhou, J., Palikhe, S., & Bhattarai, K. P. (2020). Hydraulic Optimization of Double Chamber Surge Tank Using NSGA-II. *Water*, *12*(2), 455.

Diao, X. F., Zhang, X. H., & Yang, Y. Y. (2016). Sensitivity analysis of restricted orifice in the hydropower station. In *2016 5th International Conference on Civil, Architectural and Hydraulic Engineering (ICCAHE 2016)*. Atlantis Press.

Emadi, J., & Solemani, A. (2011). Maximum water hammer sensitivity analysis. *World Academy of Science, Engineering and Technology*, *49*, 416–419.

Izquierdo, J., & Iglesias, P. L. (2004). Mathematical modelling of hydraulic transients in complex systems. *Mathematical and Computer Modelling*, *39*(4–5), 529–540. https://doi.org/10.1016/S0895-7177(04)90524-9

Ma, W., Yan, W., Yang, J., He, X., Yang, J., & Yang, W. (2022). Experimental and numerical investigation on head losses of a complex throttled surge tank for refined hydropower plant simulation. *Renewable Energy*, *186*, 264–279.

Nambiar, P., Dsouza, B., Dsouza, A., Chaudhari, P., Bandal, S., Jadhav, K., & Dmello, B. (2015). Surge analysis in piping systems analysis of valve characteristics. In *2015 International Conference on Technologies for Sustainable Development (ICTSD)* (pp. 1–4). IEEE.

Rahul Kumar Garg, Arun Kumar, U. (2018). Analysis of Hydraulic Transients in a Reservoir-Valve-Pipeline Arrangement by Analysis of Hydraulic Transients in a Reservoir-Valve-Pipeline Arrangement by Using Method of Characteristics (MOC), (April).

Salmanzadeh, M. (2013). Numerical method for modeling transient flow in distribution systems. *International Journal of Computer Science and Network Security*, *13*(1), 72–78.

Sam Ani, H. M. V, & Khayatzadeh, A. (2002). Transient flow in pipe networks. *Journal of Hydraulic Research*, *40*(5), 637–644.

Schmitt, C., Pluvinage, G., Hadj-Taieb, E., & Akid, R. (2006). Water pipeline failure due to water hammer effects. *Fatigue & Fracture of Engineering Materials & Structures*, *29*(12), 1075–1082.

Shani, T., & Gupta, T. (2017). Hydraulic transient flow analysis using method of characteristics. *International Journal of Innovative Research in Science, Engineering and Technology*, *6*(7), 14812–14827. https://doi.org/10.15680/IJIRSET.2017.0607323

Sharma, N. K., Tiwari, P. K., & Sood, Y. R. (2013). A comprehensive analysis of strategies, policies and development of hydropower in India: Special emphasis on small hydro power. *Renewable and Sustainable Energy Reviews*, *18*, 460–470.

Tiwari, S., Tamot, S., Palikhe, S., Bhattarai, K. P., & Pandey, V. P. (2021). Impact of Valve Maneuver Pattern and Operation Time in Course of Water Hammer: An Analysis based on Numerical Simulation of Hydraulic Transient. *Nepal Journal of Civil Engineering*, *2*(1), 11–25.

Wan, W., & Li, F. (2016). Sensitivity analysis of operational time differences for a pump–valve system on a water hammer response. *Journal of Pressure Vessel Technology*, *138*(1), 11303.

Wylie, E. B., Streeter, V. L., & Suo, L. (1993). *Fluid Transients in Systems*. Englewood Cliffs, NJ: Prentice Hall.

Yu, X., Zhang, J., & Zhou, L. (2014). Hydraulic transients in the long diversion-type hydropower station with a complex differential surge tank. *The Scientific World Journal*, *2014*.

Zhou, J., & Karney, B. W. (2014). Optimal Design of Pressure Relief Valves in Hydropower Stations Optimal Design of Pressure Relief Valves in Hydropower Stations, (May 2012).

Zhou, J., Palikhe, S., Cai, F., & Liu, Y. (2020). Experimental and simulation-based investigations on throttle's head loss coefficients of a surge tank. *Energy Science & Engineering*, *8*(8), 2722–2733.

Numerical Modelling of Flow Pattern and Characteristics in Overflow Spillway with Flip Bucket and Undersluice Spillway with Downstream Plunge

Ishwar Dahal[1]†, Dr. Santosh Bhattarai[2]†, Arun Bhujel[1], Prabin Neupane[1]

[1]M.Sc. Student, Department of Civil Engineering, Institute of Engineering Pulchowk Campus, Tribhuvan University, Nepal
[2]Assistant Professor, Department of Civil Engineering, Institute of Engineering Pulchowk Campus, Tribhuvan University, Nepal

† Corresponding author. Email: Ishwardahal77@gmail.com, santoshsumi9@gmail.com

Abstract

Flow over spillways and flip bucket of high dam are complex hydraulic phenomenon. Estimation of flow characteristics in such complex hydraulic structures are challenging and shall need higher accuracy. Innovative approach using numerical modelling technique are nowadays common in design of spillway and associated structures. For understanding the flow pattern including water surface profile and flow characteristics including velocity of flow and pressure distribution during flow, numerical modelling using FLOW-3D simulation software has been used. For numerical modelling, a high dam with three main overflow spillway with flip bucket structure and three undersluice spillway with downstream plunge have been used. The undersluice spillway is submerged hydraulic structure during different cases of simulation in numerical modelling. FLOW-3D software was used which uses Reynold's averaged Navier Stokes equation coupled with Re-Normalizaion Group (RNG) turbulence model for flow simulation. For overflow spillway, five different simulations were carried out for design head over crest (Hd) upstream of reservoir which are Hd, 0.75Hd, 0.5Hd, 0.25Hd and partial opening of radial gate (9.5 meters). For undersluice spillway; four different simulations were carried out for design head over undersluice crest (Hd') which are Hd, 0.75Hd', 0.5Hd' and 0.25Hd'. Results of different simulations demonstrate that the Numerical Modelling is accurate in prediction of water surface profile, velocity, pressure and flow depth in spillways, flip bucket and downstream plunge; the integrated approach used is cost effective and efficient in optimizing the design of these hydraulic structures.

Keywords

Spillway, Flip Bucket, FLOW-3D, Numerical Modelling, Turbulence

1. Introduction

Numerical Modelling technique is used in design of hydraulic structures to estimate the flow characteristics and flow pattern in different type of hydraulic structures in recent days. Spillway are proposed for safe passage of flood from upstream of reservoir formed by dam construction which on its downstream part consist of energy dissipating structure. Hydraulic phenomenon and performance of overflow spillway, gated spillway and undersluice are crucial to understand and quantify to safely pass the flood discharge without affecting the dam body itself and downstream reach of the dam. For high dams, as the spillway may have to encounter higher velocity in flip bucket area and there may be possibility of low pressure zone; accurate estimation of water surface profile, velocity and pressure is necessary in design of dam hydraulic structures.

Numerical modelling of hydraulic phenomenon and performance using Computational Fluid Dynamics (CFD) with Volume of Fluid (VOF) approach is well verified method in spillway and flip bucket of high dam structures. Numerical modelling is a cost effective, economic and time saving approach in comparison to the physical modelling of hydraulic structures as they don't need any advance equipment and space for modelling. About 109 m high dam with overflow spillway comprising of flip bucket and undersluice spillway comprising of downstream plunge has been modelled in FLOW-3D CFD software to study the flow pattern, water surface profile during different conditions, velocity field and pressure filed at different sections of spillway and flip bucket. The three overflow spillway consists of radial gates of size 13.5 m × 22 m (B × H) and three breast wall undersluice spillway of size 7 m × 13 m (B × H) are modelled for numerical simulation. Both spillway consists of ogee profile at the crest area and flip bucket in overflow spillway and downstream plunge in undersluice spillway. The crest level of the overflow spillway is at 891 m amsl and sluice spillway is at 860 m amsl.

Numerical Simulation of physical phenomenon to ensure the performance of hydraulic structures is well verified method using numerical models (Ghazi, Daneshfaraz, & Jeihouni, 2019). Use of appropriate numerical model always help in saving cost and time (Ebrahimnezhadian, Mohammadi, Kookhi, & Seyedi, 2017). Numerical model study has also been carried out to study the probable maximum flood in an existing service spillway and new auxiliary spillway using standard turbulence k-ε model (Li, Cain, Wosnik, & Miller, 2011). Hydraulic parameters such as pressure and velocity including the study of cavitation index has been carried out in Aydoghmush Dam's spillway and has been verified with physical model results (Barzegari, Foumani, Isari, & Tarinejad, 2019). RNG K-Epilson method for evaluation of turbulence models in modelling dam's spillway guide's wall in FLOW-3D software for performance evaluation of different cases (Behbahan & Parsaie, 2016). Use of CFD model with its performance evaluation in large scale projects using FLOW-3D simulation software has been proven for design and rehabilitation of these project hydraulic structures (Oukid, Libaud, & Daux, 2020). Measurement of the hydraulic properties; pressure, water depth and velocity with consideration of sensitivity of grid size in meshing has been carried out for open channel flow in spillways and channel chutes (Hien & Duc, 2020).

2. Study Methodology

a) Preparation of 3D Model and Export in .STL Format

For carrying out flow CFD model, initially the 3D model of the dam, spillway, undersluice spillway and flip bucket structures were prepared in Autodesk CIVIL-3D. The solid models are then used in stereolithography (or STL) format. The files in .stl format are generally represented and approximated by number of triangles. All the coordinates in the STL format are represented in Cartesian coordinate system. After the preparation of 3D Model in STL format, the model is imported to FLOW-3D software for numerical modelling.

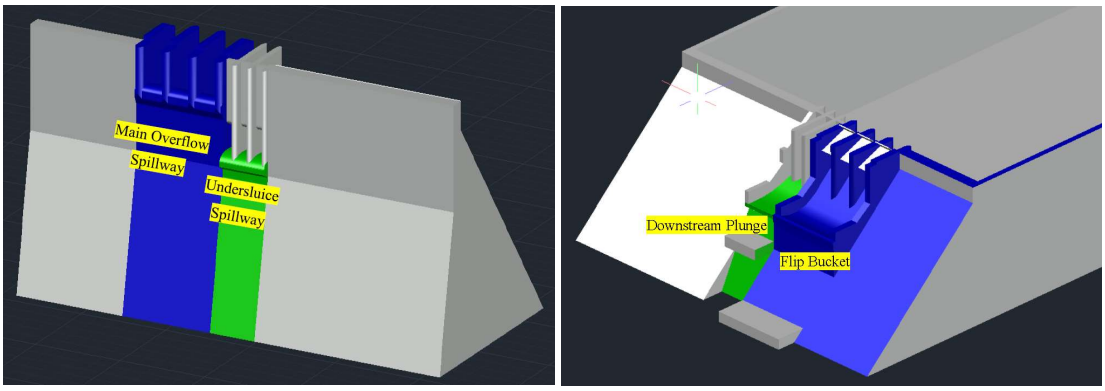

Figure 1: 3D Model of Main Overflow Spillway and Undersluice Spillway (Left Image-Front View from U/S of Dam) and Flip Bucket and Downstream Plunge (Right Image - Back View from D/S of Dam)

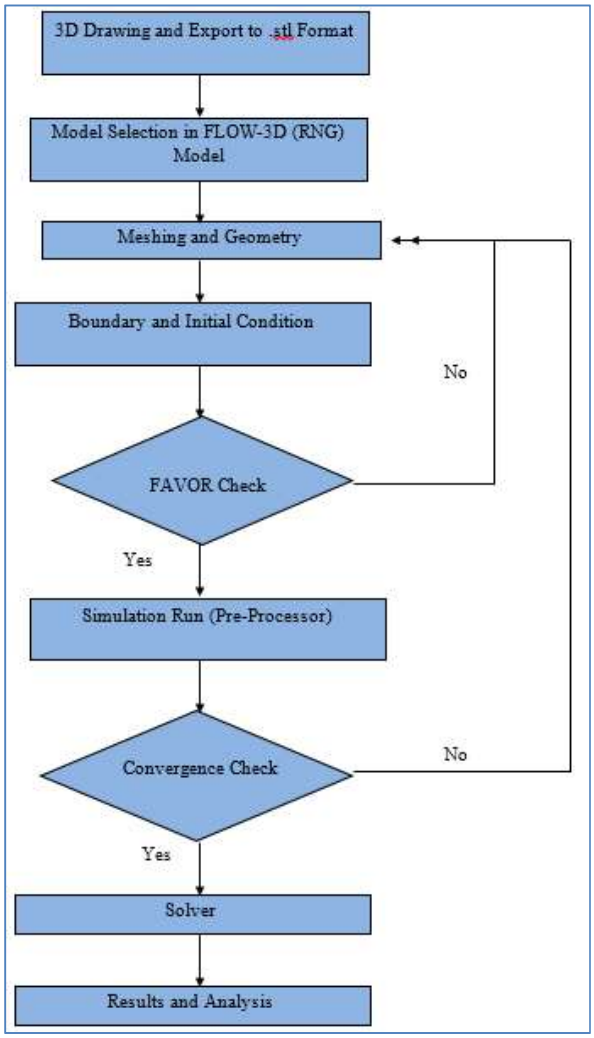

Figure 2: Study Methodology for Numerical Simulation of Dam Overflow and Undersluice Spillway

b) Model Setup and Selection in FLOW-3D

Initially, the model runtime has been selected which is 100 s and 2000000000 cycles were selected for model run. Incompressible flow with single fluid, water at 20°C and 1000 kg/m3 density was selected and the model was prepared in SI system of units. For considering the effects of viscosity and turbulence, Re-Normalization Group (RNG) method has been selected in the model setup. This method considers the smaller scales of motion in Navier Stokes Equation. For gravity, -9.81 m/s^2 value of acceleration due to gravity in Z-direction is provided as input to gravity and non-inertial frame in the model.

c) Meshing and Geometry

Non uniform orthogonal mesh has been prepared in each direction as per the requirement of the study. Multiple mesh planes were added in each X, Y and Z direction. The details of mesh planes provided during model setup are presented in Table 1 and Figure 3.

Table 1: Details of Meshing with Mesh Planes Cell Size Details

Description of Local Mesh Plane	**Mesh Plane- X direction (m)**			**Mesh Plane- Y direction (m)**				**Mesh Plane- Z direction (m)**	
Distance (m)	350	460	600	100	120	200	250	798	910
Cell Size (m)	5	1	1	5	1	1	1	2.5	2.5

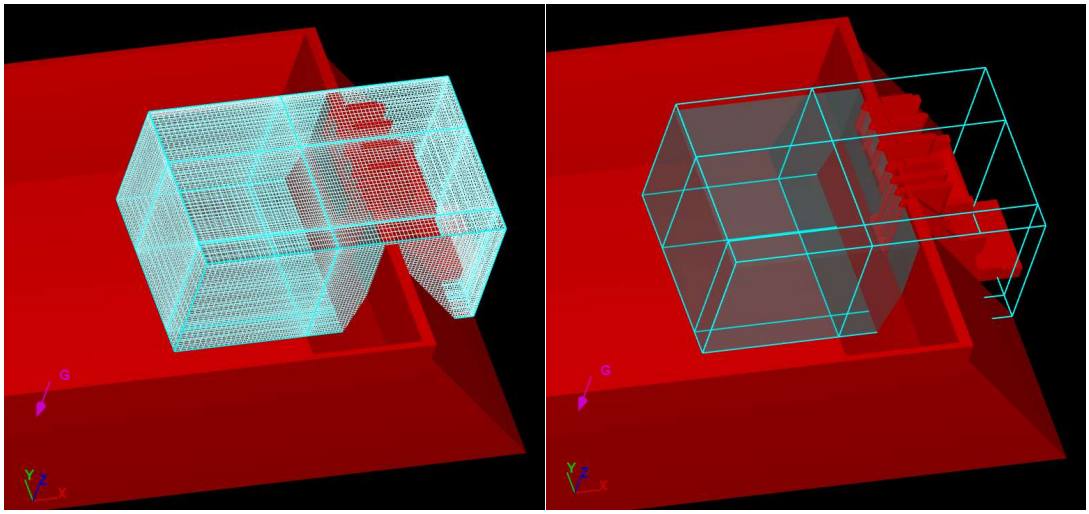

Figure 3: Meshing Details with Cells (Left) and Mesh Planes (Right) in FLOW-3D Model Setup

d) Boundary and Initial Conditions

Defining the boundary conditions and initial conditions for numerical modelling was carried out before the model run. For initial conditions, the upstream of proposed dam overflow and undersluice spillway were considered to be filled upto the level based on different cases of

simulation. Among six different boundary conditions available in FLOW-3D, following boundary conditions was used for numerical simulation.

Table 2: Boundary Conditions

S.N.	Region	Boundary Conditions	Remarks
1	Inlet	Specified pressure	
1.1	Overflow Spillway	910 m	Different H/Hd (1, 0.75. 0.5 and 0.25) Simulation Carried out; Partial gate opening case also carried out
1.2	Undersluice Spillway	910 m	
2	Outlet	0 m	For all simulations
3	Bottom	Symmetry	For all simulations
4	Other Part	Symmetry	For all simulations

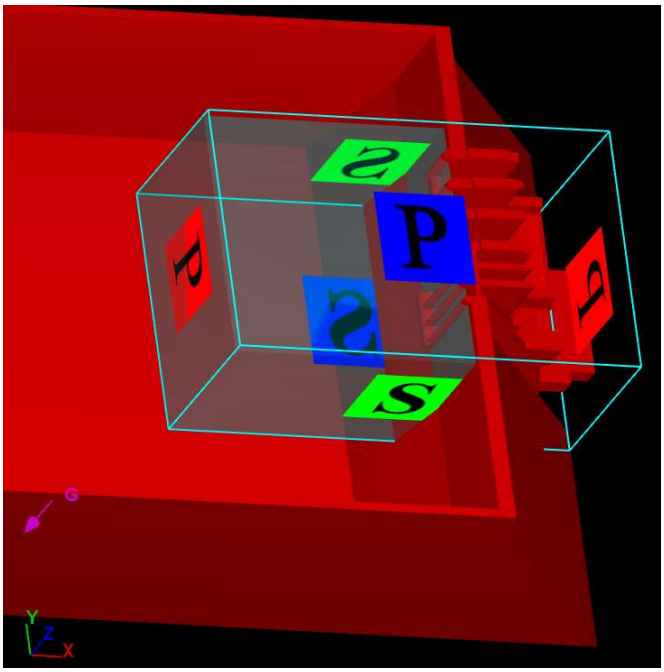

Figure 4: Boundary Conditions

e) FAVOR Check

Fractional Area/Volume Obstacle Representation (FAVOR) is used in FLOW-3D model setup to check the geometric description of the coarser or finer grids used in meshing. Complicated geometries are checked using FAVOR and in case the grid size are not sufficient or meshing need to be revised, FAVOR check provides the error. In this study, FAVOR tools indicate the provisioned meshing is sufficient for modelling with error in permissible range.

3. Results and Analysis

a) Convergence Check

The time step size and convective volume error is nearly equal to zero with respect time of simulation mean for convergence of simulation as shown in Figure 5and Figure 6. The

maximum convective error is 0.019 % at around 2.5 seconds of simulation run. Hence, the model-setup and meshing is considered okay from the convergence check.

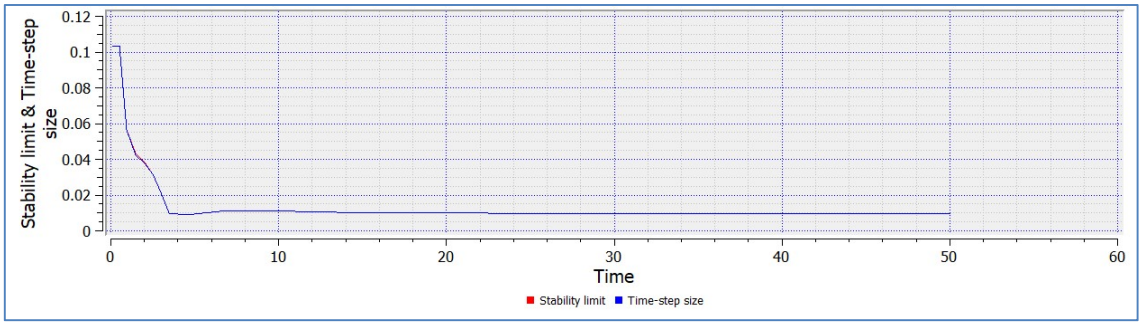

Figure 5: Stability Time vs Time Step Size

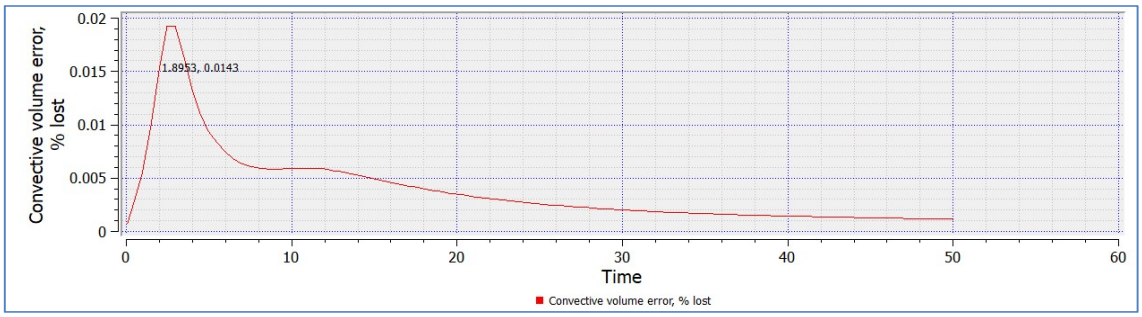

Figure 6: Convective Volume Error vs Time

b) Results and Analysis

The total head over crest (H_d) of gated overflow spillway for initial case of numerical simulation is 19 m and other cases of simulation run are 0.75 Hd, 0.5 Hd, 0.25 Hd with full opening of the radial gates and last case is of partial opening of 9.5 m of radial gate. Similarly, the total head over crest of breasted undersluice spillway (Hd') for initial case of simulation is 50 m and other cases of simulation are 0.75 Hd', 0.5 Hd', 0.25 Hd' with full opening of the undersluice gates. Different hydraulic characteristics of flow which include water surface profile, velocity and pressure field in crest area and flip bucket area of overflow spillway and undersluice spillway with downstream plunge during the different cases of simulation in FLOW-3D are presented in Table 3 and Table 4 respectively.

Table 3: Velocity and Pressure at Crest and Flip Bucket Zone of Main Overflow Spillway

Case	Location	Velocity (m/s)	Pressure (MPa)
Hd	Crest	14	0.47
	Flip Bucket	40	-0.20
0.75Hd	Crest	12.5	0.62
	Flip Bucket	35.2	-0.58
0.5Hd	Crest	11	0.71
	Flip Bucket	34.5	-0.95
0.25Hd	Crest	7.5	0.78
	Flip Bucket	31.5	-1.24
Hd (Radial Gate Opening 9.5 meters)	Crest	16.7	0.65
	Flip Bucket	34.8	-0.45

Table 4: Velocity and Pressure at Crest and Flip Bucket Zone of Undersluice Spillway

Case	Location	Velocity (m/s)	Pressure (Ma)
H_d'	Crest/Opening	24.5	1.3
	D/S Plunge	32.1	-0.86
0.75 H_d'	Crest/Opening	15	1.5
	D/S Plunge	31.9	-0.45
0.5 H_d'	Crest/Opening	14	2.19
	D/S Plunge	30	0.32
0.25 H_d'	Crest/Opening	12.5	2.3
	D/S Plunge	28.5	0.55

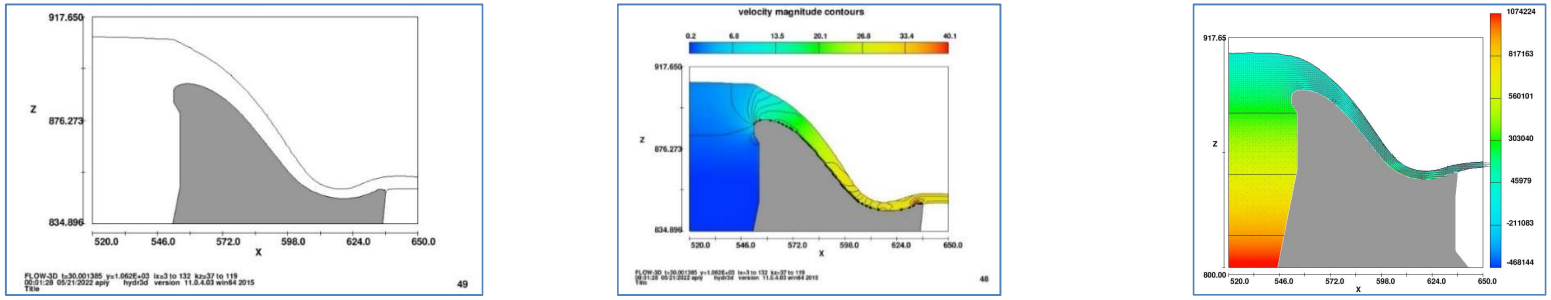

Figure 7: Free Water Surface Elevation (Left), Velocity Profile (Middle) and Pressure Profile (Right) at Hd design head at Overflow Spillway

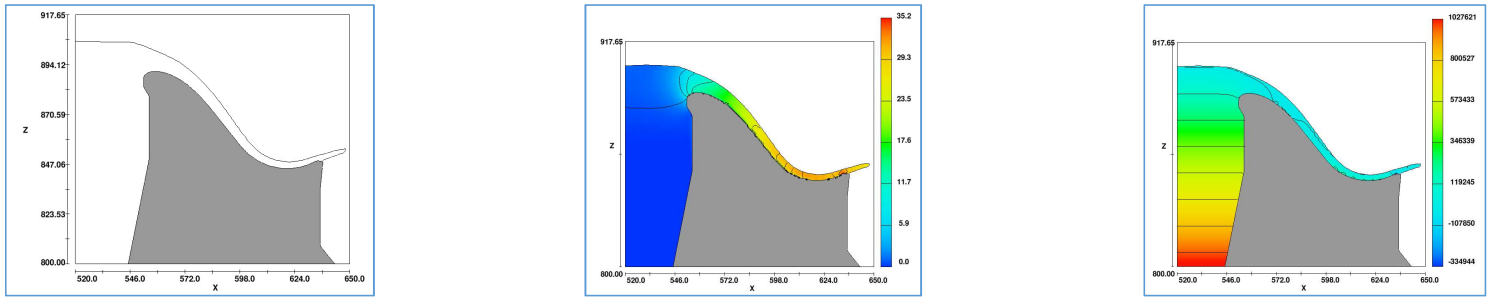

Figure 8: Free Water Surface Elevation (Left), Velocity Profile (Middle) and Pressure Profile (Right) at 0.75Hd design head at Overflow Spillway

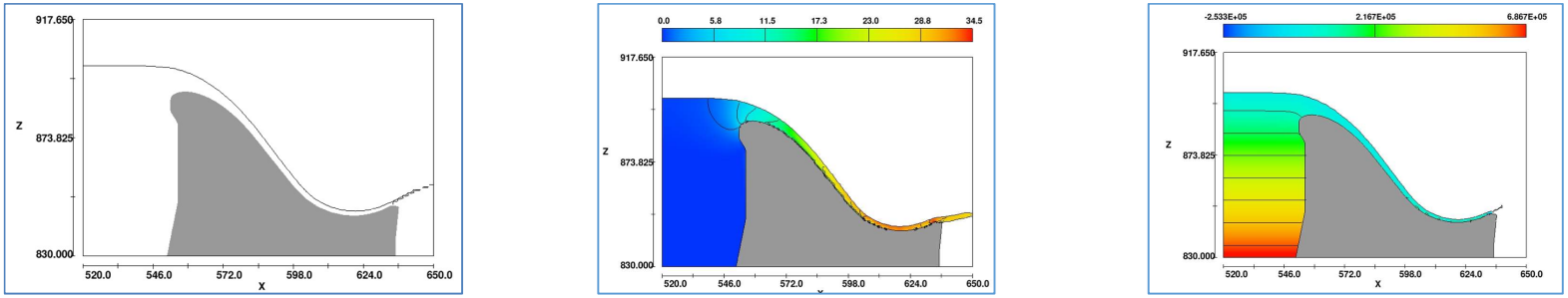

Figure 9: : Free Water Surface Elevation (Left), Velocity Profile (Middle) and Pressure Profile (Right) at 0.5Hd design head at Overflow Spillway

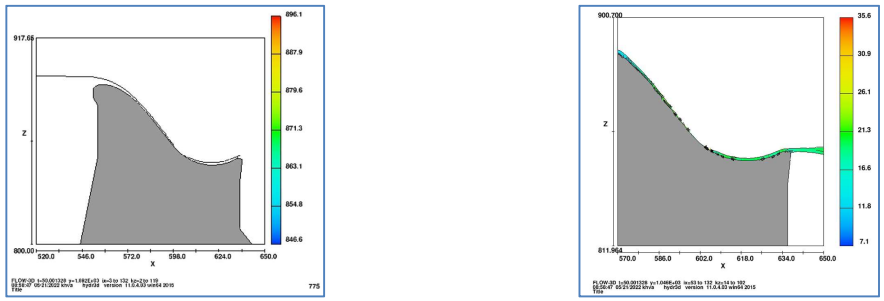

Figure 10: : Free Water Surface Elevation (Left) and Velocity Profile (Right) at 0.25Hd design head at Overflow Spillway

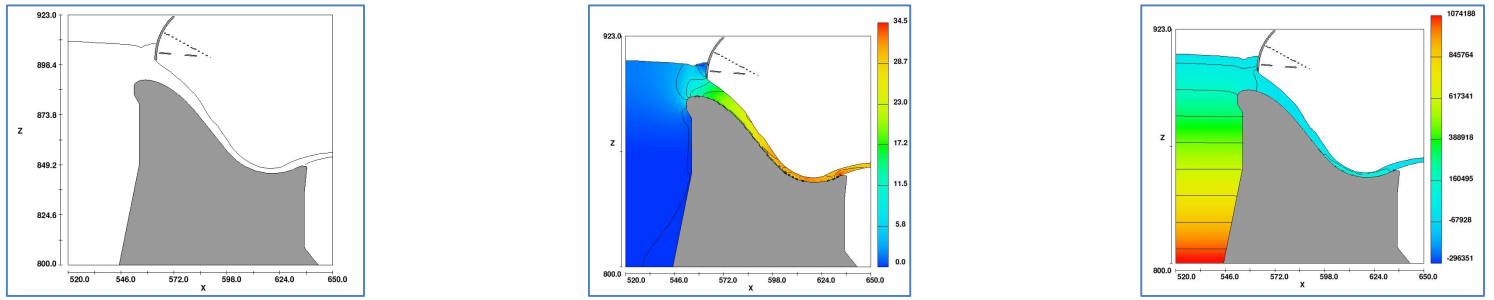

Figure 11: : Free Water Surface Elevation (Left), Velocity Profile (Middle) and Pressure Profile (Right) at Hd Design Head and Partial Opening of Radial Gate

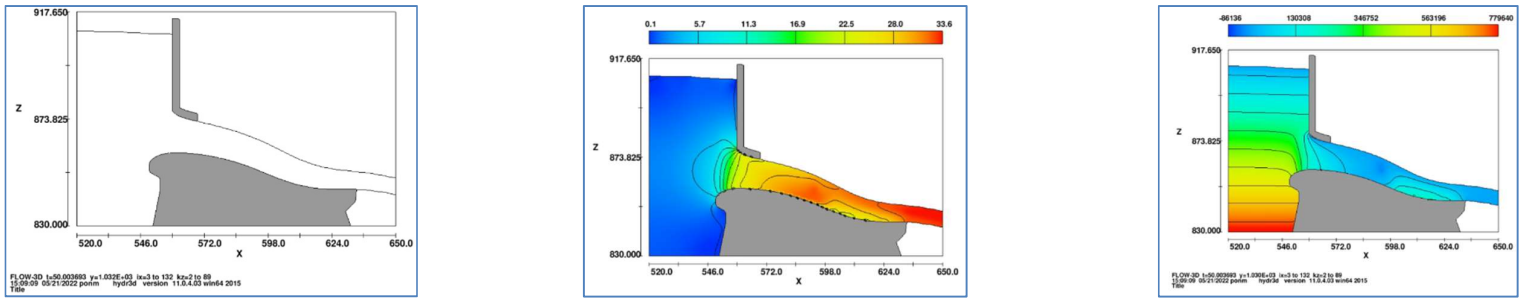

Figure 12: Free Water Surface Elevation (Left), Velocity Profile (Middle) and Pressure Profile (Right) at Hd' design head at Full Opening of Undersluice Spillway

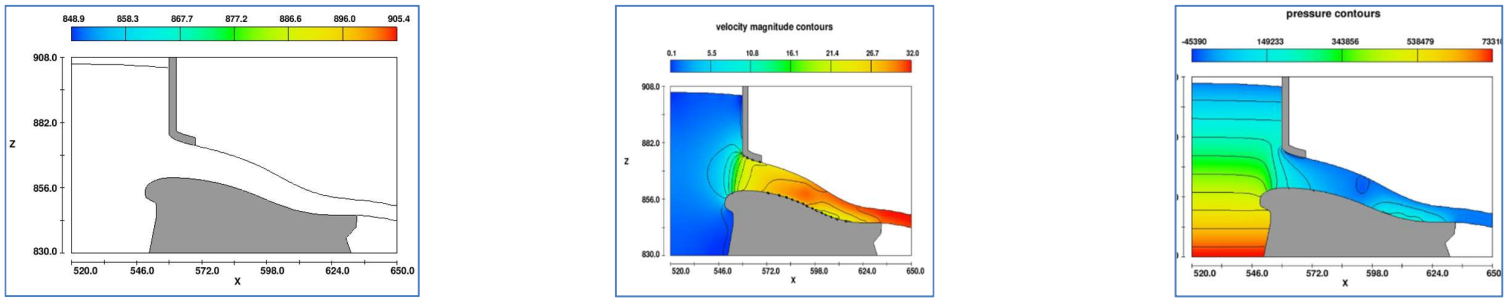

Figure 13: Free Water Surface Elevation (Left), Velocity Profile (Middle) and Pressure Profile (Right) at 0.75Hd' design head at Full Opening of Undersluice Spillway

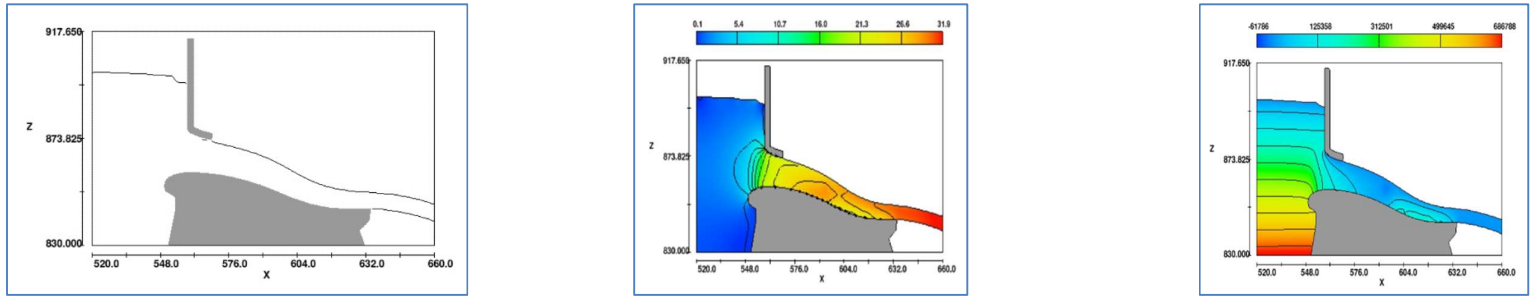

Figure 14: Free Water Surface Elevation (Left), Velocity Profile (Middle) and Pressure Profile (Right) at 0.5Hd' design head at Full Opening of Undersluice Spillway

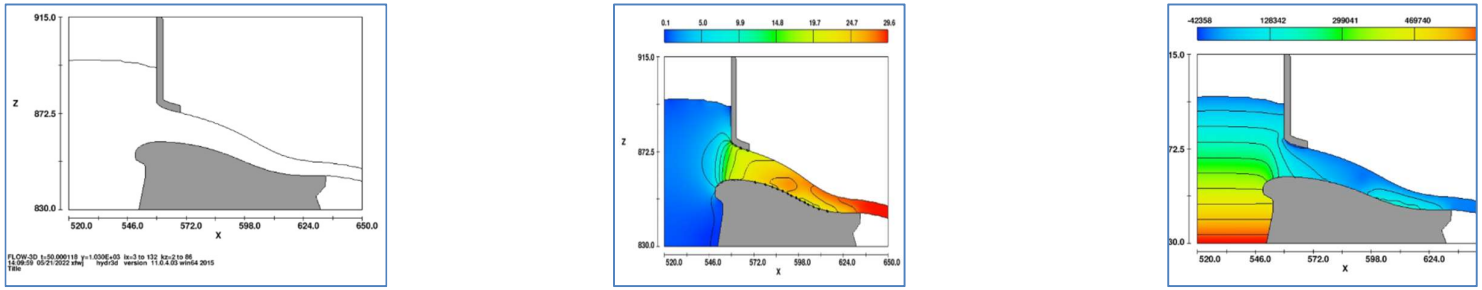

Figure 15: Free Water Surface Elevation (Left), Velocity Profile (Middle) and Pressure Profile (Right) at 0.25Hd' design head at Full Opening of Undersluice Spillway

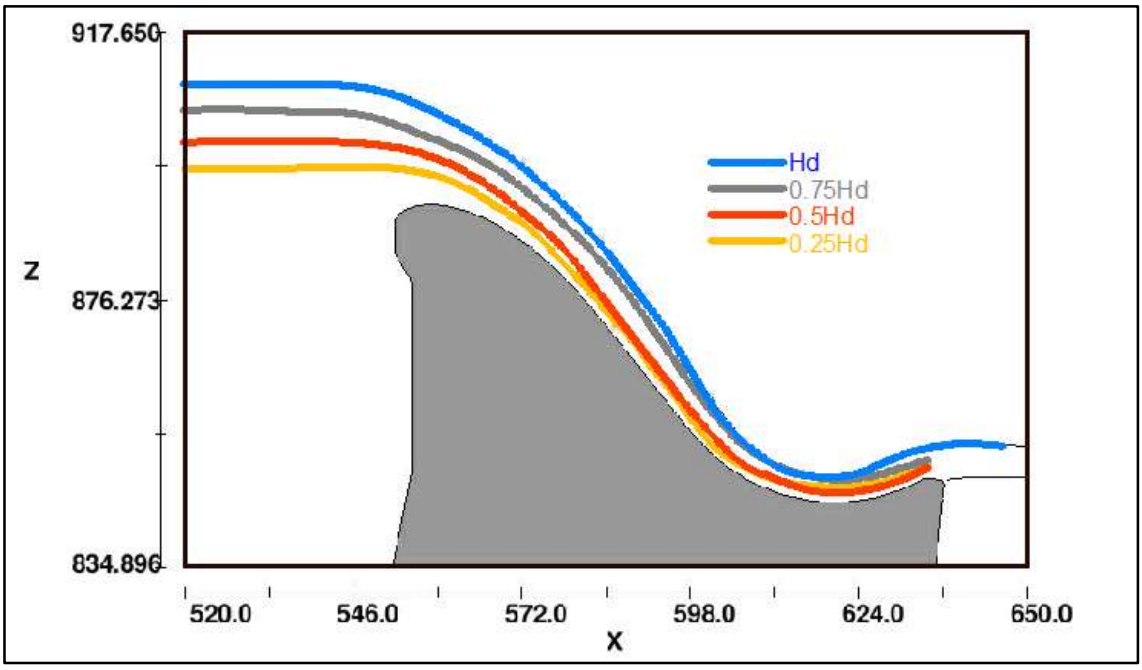

Figure 16: Comparison of Water Surface Profiles at different head over crest in overflow spillway

4. Conclusions

The study suggests the successful application of Computational Flow Dynamics (CFD) method in estimating the flow pattern and flow characteristics of high dam overflow spillways with flip bucket and high dam undersluice spillway with downstream plunge. The estimation of water surface elevation, flow velocity and pressure distribution under different head over crest conditions were carried out using numerical modelling technique in FLOW-3D CFD software. The results from these numerical simulation encourages hydraulic engineers and CFD modelers in use of this method in design and optimization of hydraulic structures with complex flow characteristics. As numerical models are less expensive and less time consuming method in hydraulic engineering of high dam spillways and flip bucket structures, it is recommended for use of this method in design of hydraulic structures.

5. References

- Barzegari, M., Foumani, R. S., Isari, M., & Tarinejad, R. (2019). Numerical Investigation of Cavitation on Spillways. A Case Study: Aydoghmush dam. *Numerical Methods in Civil Engineering*, 1-10, 10.52547/nmce.4.1.1.

- Behbahan, S. D., & Parsaie, A. (2016). Numerical modeling of flow pattern in dam spillway's guide wall. Case study: Balaroud dam, Iran. *Alexandria Engineering Journal, Volume 55, Issue 1*, 467-473.

- Cavitation in Chutes and Spillways, A Water Resources Technical Publication, Engineering Monograph No. 42.

- Ebrahimnezhadian, H., Mohammadi, M., Kookhi, R. A., & Seyedi, A. (2017). Numerical study of the passing flow over spillway with emphasis on the potential of cavitation occurrence. *Long-Term Behaviour and Environmentally Friendly Rehabilitation Technologies of Dams*, 451-458, DOI:10.3217/978-3-85125-564-5-059.

- FLOW-3D Version 9.3, User Manual, Copyright 2008, Flow Science, Inc. All rights reserved

- Ghazi, B., Daneshfaraz, R., & Jeihouni, E. (2019). Numerical investigation of hydraulic characteristics and prediction of cavitation number in Shahid Madani Dam's Spillway. *Journal of Groundwater Science and Engineering*, Vol.7 No.4: 323—332, 10.19637/j.cnki.2305-7068.2019.04.003.

- Hien, L. T., & Duc, D. H. (2020). Numerical Simulation of Free Surface Flow on Spillways and Channel Chutes with Wall and Step Abutments by Coupling Turbulence and Air Entrainment Models. *Water 12 (11)*, 1-16, 10.3390/w12113036.

- Li, S., Cain, S., Wosnik, M., & Miller, C. (2011). Numerical Modeling of Probable Maximum Flood Flowing through a System of Spillways. *Journal of Hydraulic Engineering*, 66-74.

- Oukid, Y., Libaud, V., & Daux, C. (2020). Practical capacities and challenges of 3D CFD modeling in design and rehabilitation of hydraulic structures. *Taylor Francis Online*, 55-65.

Assessing the Impact of Land Use and Land Cover Change on Surface Runoff Using SWAT Model: A Case Study of Madi River Basin, Nepal

Pragya Pokharel[1], Sabina Pokharel[1], Ram Krishna Regmi[2]†

[1]M.Sc. Student, Department of Civil Engineering, Institute of Engineering Pulchowk Campus, Tribhuvan University, Nepal
[2]Assistant Professor, Department of Civil Engineering, Institute of Engineering Pulchowk Campus, Tribhuvan University, Nepal

†Corresponding author. Phone: +977-9860267834, Email: rkregmi@pcampus.edu.np

Abstract

This study is aimed to understand the impacts of Land Use Land Cover (LULC) change on the surface runoff in the Madi river basin at basin, sub-basin, and individual land use class levels. The Madi watershed has a drainage area of 1122 km2 which is located in the central part of Nepal. Hydrological modeling using the Soil and Water Assessment Tool (SWAT) model was carried out to quantify the impact of land use and land cover dynamics on surface runoff. SWAT model was calibrated and validated between observed and simulated discharge using SWAT-CUP. Statistical parameters R2, NSE, and PBIAS were used to evaluate model performance. The impacts of LULC changes were assessed by developing three different scenarios using land use maps corresponding to the years 2000, 2010, and 2020 keeping climate data (1985-2008), soil map, and slope map the same. The results showed that the agricultural area decreased by 3.97% whereas forest area and built-up area increased by 4.21% and 0.02% respectively. For the given LULC change at the basin level, the average annual surface runoff decreased by 782 mm from scenarios S1 to S3. This situation is seen as critical for sub-basin 2 and 3. The highest surface runoff producing class was recognized to be agriculture. This scenario could be created due to high precipitation leading to a high generation of surface runoff on fragile land slopes. The outputs of this project could help in the decision-making process for sustainable generation of hydropower projects, catchment management, and land use planning.

Keywords

LULC, Surface runoff, SWAT, SWAT-CUP, Madi river basin

1. Introduction

Land use is a crucial factor that influences the hydrological responses of a river system along with the climate variables (Zhang et al., 2017; Neupane and Kumar 2015). Land use change can result in disruption of the hydrological cycle and alteration of base flow (Wang et al. 2006). Thus, study of impacts of changes in land use and land cover is required for proper planning and development in water resources (Kiros et al., 2015). It is also one of the important variables that results in global warming, alteration in stream flow pattern and global atmospheric circulation (Singh et al., 2017; Kumar et al., 2018). The human activities (Gyamfi et al., 2016) responsible for LULC changes such as agricultural expansion, burning activities or fuel wood consumption, deforestation, development of grazing land, construction works and urbanization affects the integrity of natural water resources and services in the ecosystem (Kiros et al., 2015; Singh et al., 2017).

Land use and land cover change is continuous development and its effect on the catchments is significant due to its implication on the hydrological and ecological aspects within that area. Land cover changes are considered an important factor affecting the hydrological process. Land use and land cover change is a very complex dynamic process that occurs in different forms with differences in magnitude and rate (Keyser and Kaiser 2010). The impact of LULC is seen high in the Middle Mountain and High Mountain regions than in the Terai even when the changes were small (Khanal 2002).

A study in the Madi river basin highlights that "Initiation of many small and shallow landslide and debris flow scars during and after highly localized heavy precipitation events like in the Madi watershed in between 1948-1955 has also been reported from other areas of Nepal in recent years" (Manandhar and Khanal 1988, Dhital et al. 1993, Upreti and Dhital 1983, Khanal 1998). Landslide and debris flow scars were concentrated mainly in five localities namely Siklesh, Saimarang, Bhujung, Karapu and Jita area (Khanal and Watanabe, 2004). As runoff is one of the main factors that triggers soil erosion and ultimately landslide, it becomes imperative to assess the effect of LULC change on runoff characteristics in fragile areas like Madi basin which also possess the potential for hydropower production.

Soil and Water Assessment Tool (SWAT) is a watershed model which is used to evaluate stream flow, surface runoff, and transportation of sediment and nutrients. SWAT is a hydrological model which simulates on a time step of daily or monthly (Arnold et al., 1998; Gassman et al., 2007). Thus, the critical focus of this research is to understand the pattern of precipitation and assess the impact of LULC changes on surface runoff using the SWAT model at various basin and sub-basin levels as well as individual land use class levels.

2. Materials and Methods

2.1. Study Area

The Madi watershed, with drainage area of 1,122 km^2 is located in the central part of Nepal. The basin is located in Gandaki Province of Nepal with the altitude ranging from 7,919 masl to 271 masl within a north-south distance of around 68 km (Fig.1). Geographically, the basin extends between latitude 28°33'58"N to 27°55'03"N and langitude 83°53'15"E to 84°28'02"E longitude. The outlet of the study area is taken at Byas cave of Damauli situated at 27°58'13"N latitude to 84°15'59"E longitude. The recorded mean annual precipitation in the watershed ranges from 1,795 mm at Damauli in the south to 3,743 mm at Sikles in the north. Around 70–80% of the total precipitation occurs during the four summer months (June–September). River discharge varies throughout the year influenced by both snow melt and precipitation.

2.2. Data Acquisition and Processing

Primary data required for this study are DEM, land cover data, soil data, daily precipitation data, monthly discharge data, wind data, solar data, relative humidity data, and temperature maximum and minimum data.

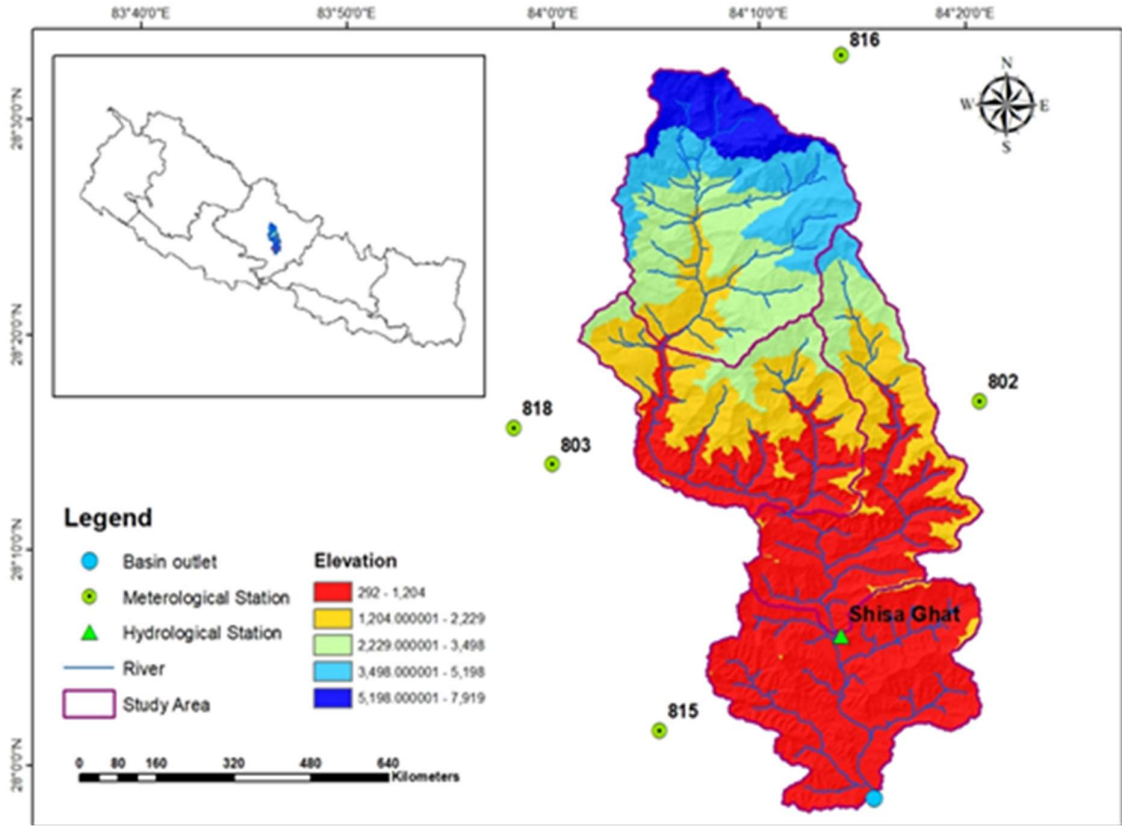

Figure 1. The spatial location of hydro-meteorological stations across the Madi river basin

2.2.1 DEM

A 30 m spatial resolution ASTER GDEM Version-3 downloaded from NASA Earth data was used for the purpose of this study.

2.2.2 Hydro-Meteorological Data

Daily meteorological data (1985-2008) were collected from the Department of Hydrology and meteorology. Similarly, monthly discharge data from (1985-2006) was collected for Shisa Ghat Station (438) which lies inside the basin shown in Fig.1. Further required input data like solar, wind, relative humidity, and temperature minimum and maximum data were extracted from 1985-2008 from the power data access viewer.

2.2.3 Soil Map

This study used Food and Agricultural Origination (FAO) developed soil map of the Globe at spatial resolution of 1:5 million.

2.2.4 Land Use and Land Cover Maps

The land use map of the study area (ICIMOD, 2010) at the spatial resolution of 30 m was used. Six land use classes were identified within the study area Table 1 and Fig.2.

Table 1. Land Use Classes and their percentage in area

S.N.	LULC classes	SWAT classes	Area coverage (km^2)		
			2020	2010	2000
1	Bare ground	BARR	103.9635	95.36	104.57
2	Built-up area	URMD	0.32	0.19	0.07
3	Cropland	AGRR	165.67	187.18	210.32
4	Forest	FRST	754.98	731.5	707.81
5	Rangeland	RNGE	94.71	106.59	247.72
6	Water	WATR	2.4	1.3	0.97

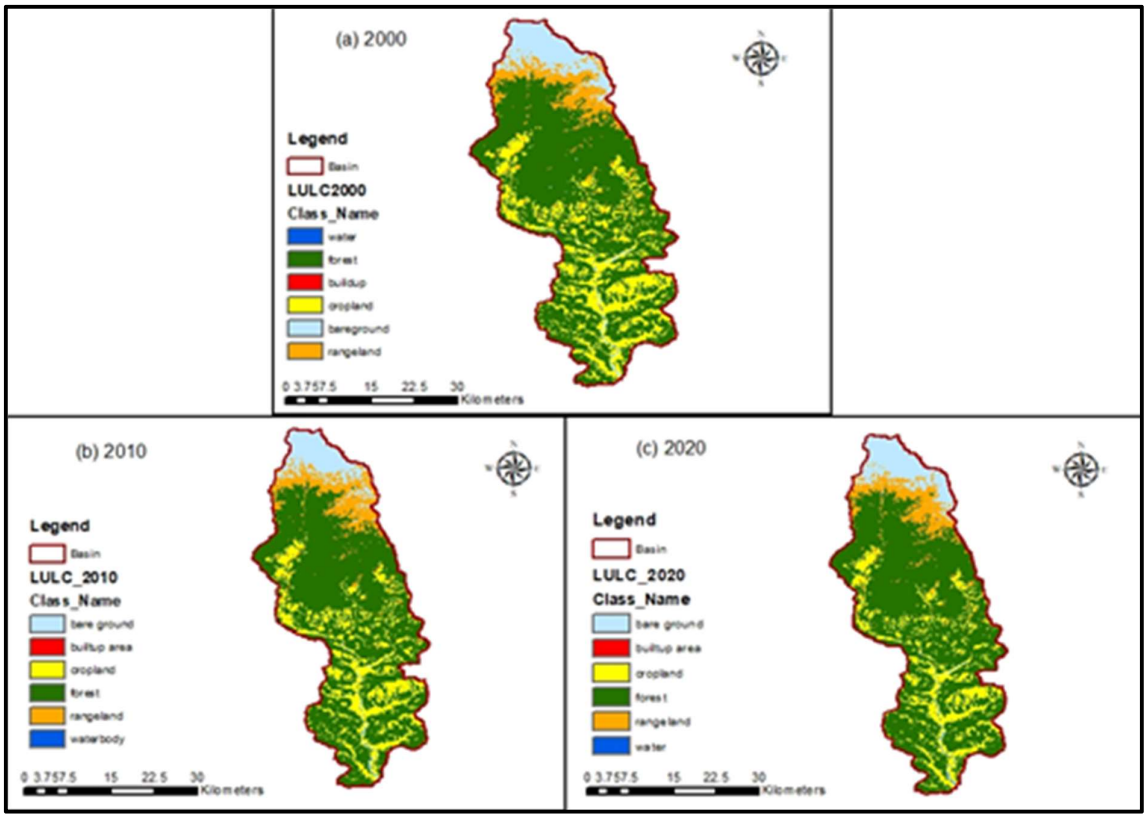

Figure 2. Land use map of Madi river basin a) 2000 year b) 2010 year c) 2020 year

3. Methodology

3.1. The SWAT Model

The SWAT model for Madi Basin was set up with the Arc SWAT 2012.10.5 interface. The calibration validation and simulation work were done with the assistance of the SWAT-CUP using the SUFI-2 algorithm. Coefficient of Determination (R2), Nash-Sutcliffe Simulation efficiency (NSE), and Percentage-Bias (PBIAS) were used during the calibration and validation of the model. The principal yield from the model was released at the Byas Cave outlet of the catchment. The model for the Madi river basin was calibrated using monthly rainfall-runoff data. The whole study area was divided into four sub-basins. 37 HRUs were created within these four sub-basins. Four slope classes were defined: 0-15%, 15-45%, 45-65

% and > 65 %. The yield from sub-basin 3 of the model was compared with the observed discharge at the respective outlet. Sub-basin delineation map of the study area is presented in Fig.3.

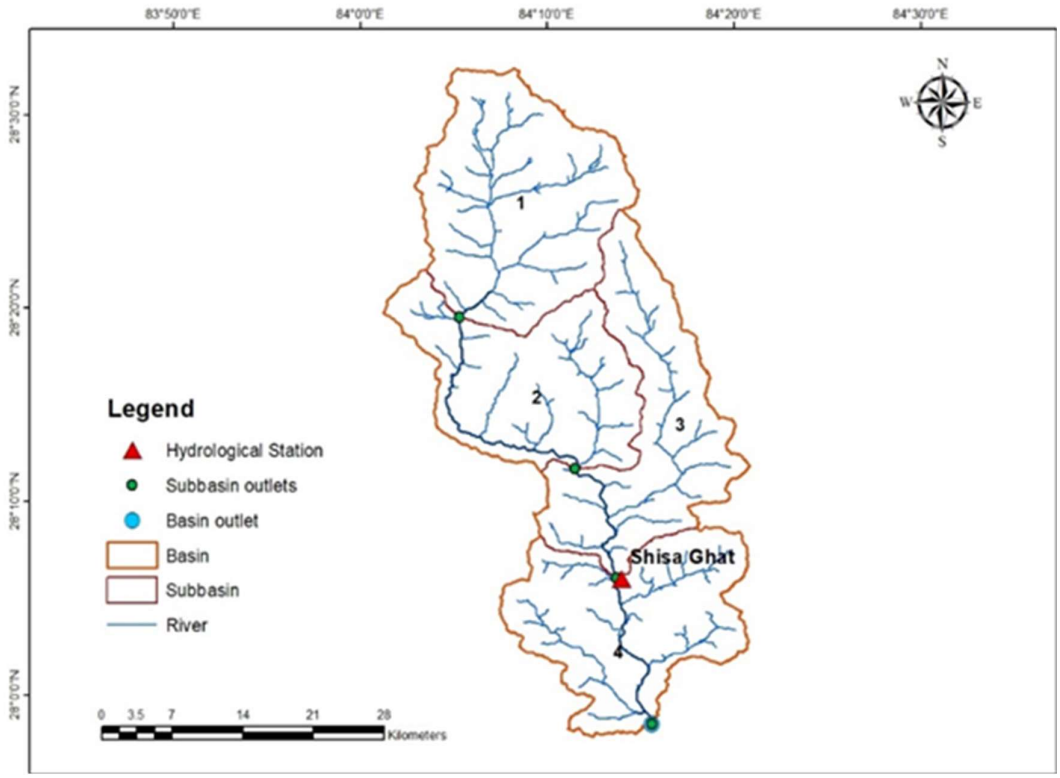

Figure 3. Sub-basin Delineation of the study area

3.2. SWAT Model Development Criteria

Three different SWAT models were developed.

Model 1 (land use map of 2000 and climate data during the 1985-2000 period, M1)

Model 2 (land use map of 2010 and climate data during the 1985-2006 period, M2)

Model 3 (land use map of 2020 and climate data during the 1985-2006 period, M3)

4. Results and Discussions

4.1. Land-use Change

Land use change was examined for three years at an interval of 10 years i.e., 2000, 2010, and 2020. From 2000 to 2010, forest cover increased by 2.11%, range land and water bodies also increased by 0.74% and 0.03% respectively while agriculture and barren land decreased by 2.06%, and 0.82% (Table 2 and Fig.4). From 2010 to 2020, agriculture further decreased by 1.91% while, barren land, forest, and water bodies increased by 0.7%, 2.1%, and 0.09% respectively (Table 2 and Fig.4). This analysis clearly showed that the agricultural area has

decreased by 3.97%, forest cover has increased by 4.21% also the range land and barren land decreased by 0.32% and 0.12 from the year 2000 to 2020 (Table 2 and Fig.4).

Table 2. Land Use change (in %)

Year	Bare Ground	Buildup	Crop Land	Forest	Rangeland	Water
2000-2010	-0.82	0	-2.06	2.11	0.74	0.03
2010-2020	0.7	0.7	-1.91	2.1	-1.06	0.09
2000-2020	-0.12	0.02	-3.97	4.21	-0.32	0.12

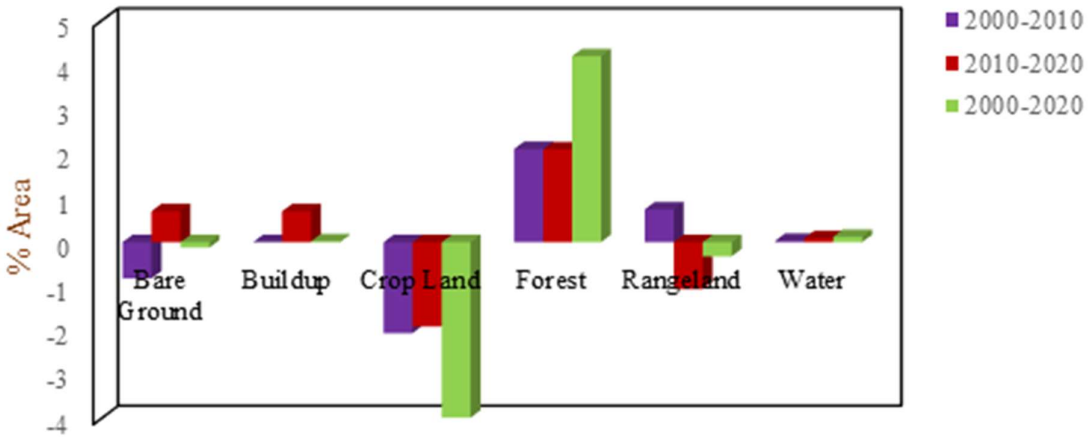

Figure 4. Land Use Change (in %)

4.2. Performance Evaluation of Calibrated SWAT Model

Out of 18 chosen parameters, 14 were found to be most sensitive and are listed in Table 4. The model was calibrated by changing the parameters for snow, elevation, runoff, groundwater, and soil in SWAT-CUP. All three models suggested very good model performance based on R2, NSE, and PBIAS values (Table 3). Therefore, based on all the three model calibration and validation results, it can be concluded that the SWAT model is applicable to the Madi river basin.

Table 3. Performance Evaluation of Developed Model

Scenario	Application	Year	P-factor	R-factor	R^2	NSE	PBIAS (%)
M1	Calibration	1985-1995	0.67	0.47	0.766	0.75	-1.5
	Validation	1996-2000	0.6	0.41	0.7667	0.74	-2
M2	Calibration	1985-1998	0.61	0.45	0.769	0.7	8.8
	Validation	1999-2006	0.6	0.3	0.754	0.69	9.9
M3	Calibration	1985-1998	0.72	0.57	0.82	0.71	9
	Validation	1999-2006	0.5	0.36	0.7513	0.7	4.5

Table 4. Parameters used in calibration and their calibrated values for different Models

S.N.	Parameter	Min Value	Max Value	Calibrated Values for all Model
1	r__TLAPS.sub	-5	5	-4.8
2	r__SFTMP.bsn	-5.03	0.80	-0.45
3	r__CN2.mgt	0.00	0.30	0.12
4	v__ALPHA_BF.gw	0.00	1.00	0.99
5	v__GW_DELAY.gw	30.00	450.00	225.05
6	v__GWQMN.gw	0.00	2.00	1.10
7	v__GW_REVAP.gw	0.00	0.20	0.13
8	v__ESCO.hru	0.80	1.00	0.90
9	v__CH_N2.rte	0.00	0.30	0.22
10	v__CH_K2.rte	5.00	130.00	72.59
11	v__ALPHA_BNK.rte	0.00	1.00	0.09
12	r__SOL_AWC(1).sol	-0.30	0.14	0.13
13	r__SOL_K(1).sol	0.93	1.11	0.93
14	r__SOL_BD(1).sol	-0.50	0.60	-0.49

Note: r_ relative change in parameter value; v_ replace with existing parameter value

Calibration and validation of the model is performed with the observed monthly flow at Shisa Ghat (Fig.5 to Fig.7).

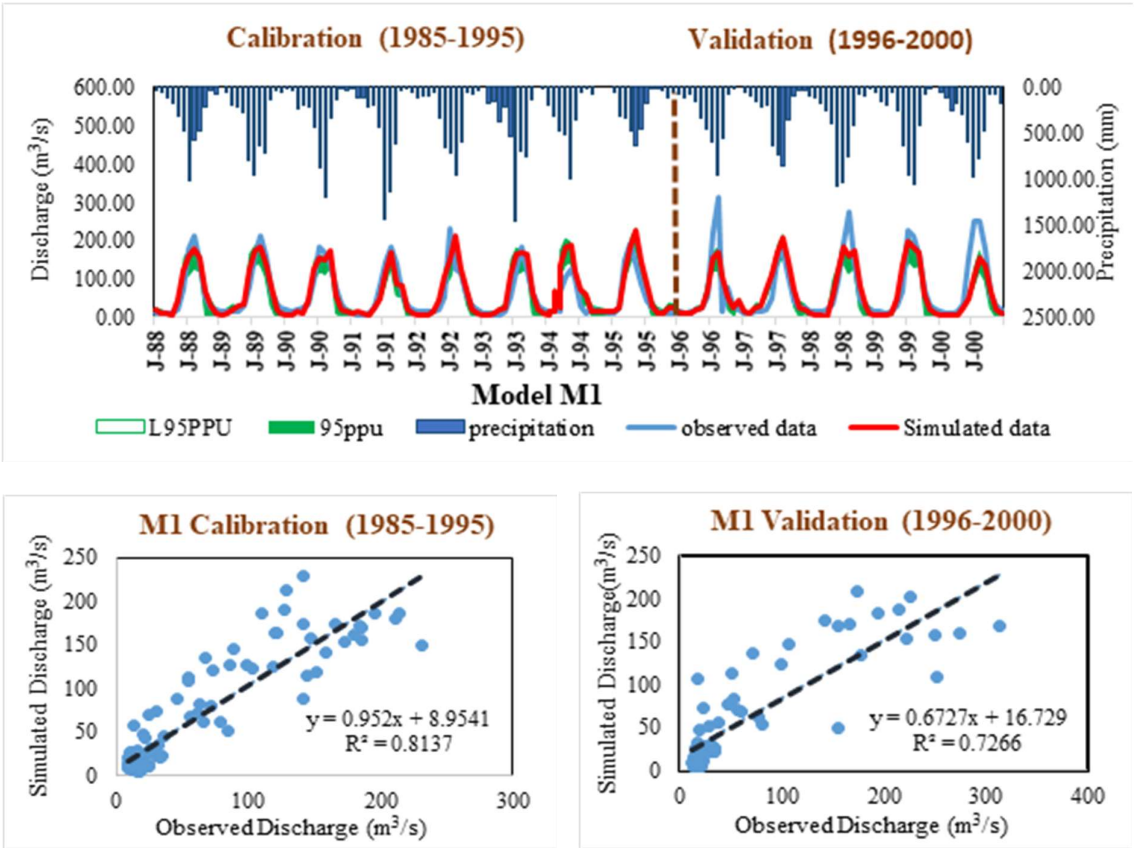

Figure 5. Observed and Simulated Monthly Discharge Hydrograph with scatterplot at Shisa Ghat Outlet for Model M1

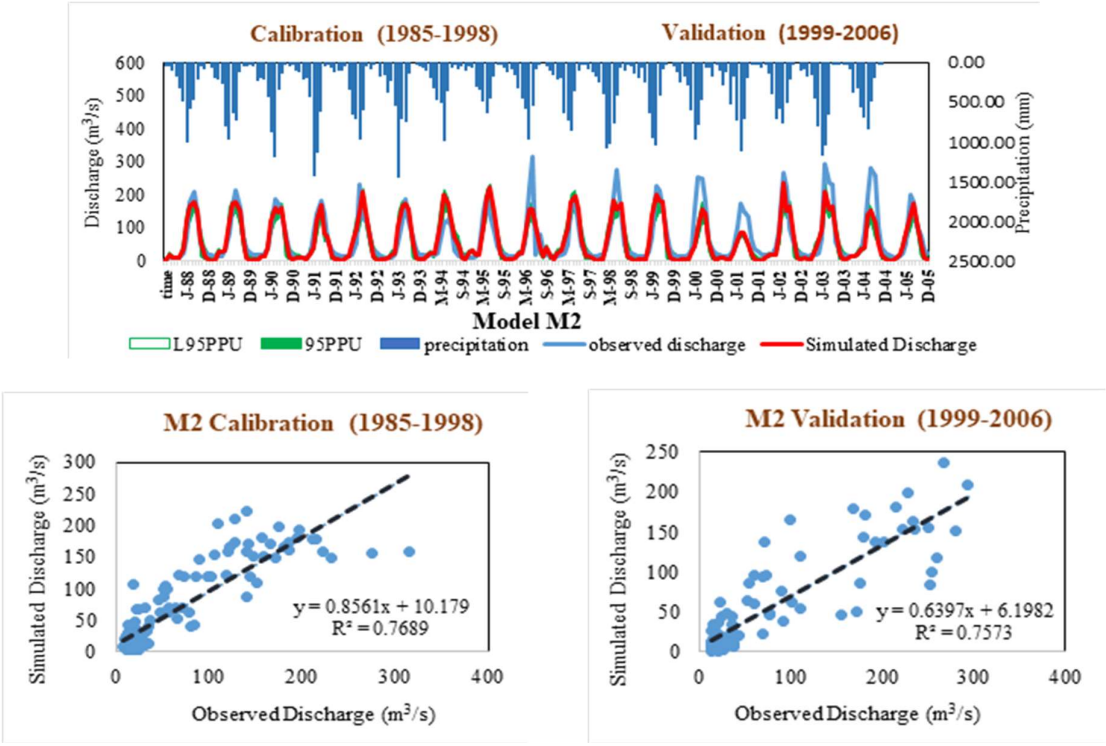

Figure 6. Observed and Simulated Monthly Discharge Hydrograph with scatterplot at Shisa Ghat Outlet for Model M2

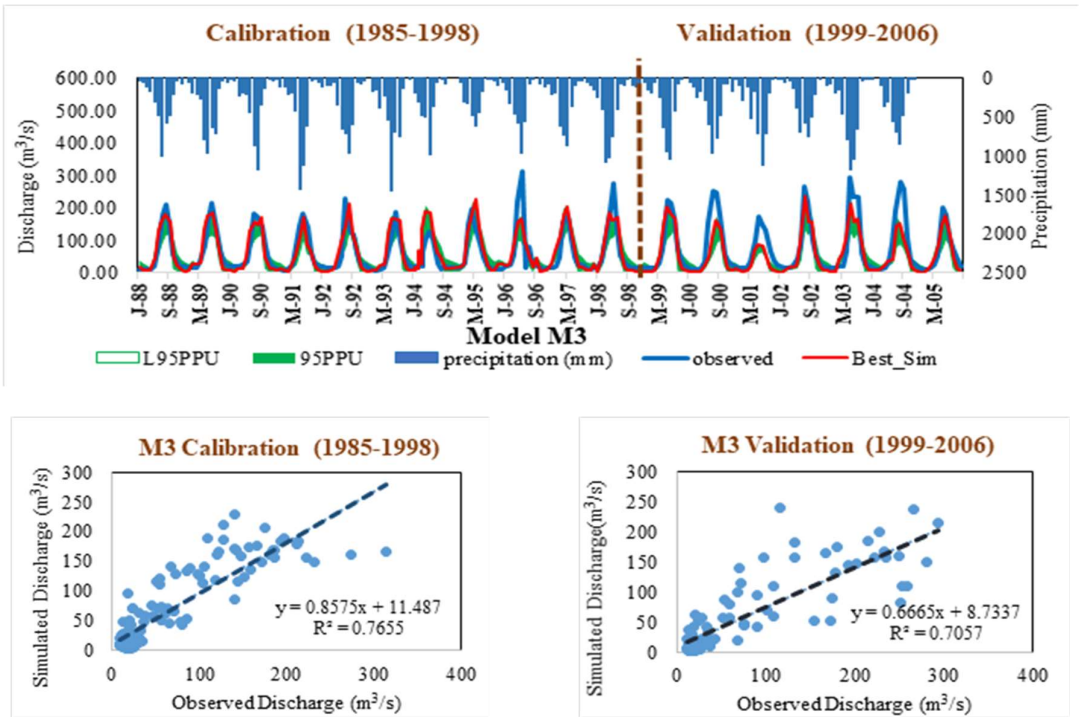

Figure 7. Observed and Simulated Monthly Discharge Hydrograph with scatterplot at Shisa Ghat Outlet for Model M3

4.3. Impact of LULC Change on Runoff at Basin Level

Three different scenarios were developed corresponding to respective models. They are:

Scenario 1 (Land Use map of 2000 and climate data during 1985-2008 period, S1) Scenario 2 (Land Use map of 2010 and climate data during 1985-2008 period, S2) Scenario 3 (Land Use map of 2020 and climate data during 1985-2008 period, S3)

The impact of LULC changes indicates, that for average annual precipitation of 2912.19 mm, the surface runoff has decreased rapidly from the first scenario (S1) to the second scenario (S2), and decreased gradually from the second scenario (S2) to the third scenario (S3) (Table 5). The possible reasons for decreasing surface runoff from S1 to S3, in the study area could be due to the expansion of forest area and built-up area and reduction in the agricultural area, barren land, and range land (Table 5). However, the LULC change has a low impact on surface runoff from scenarios S2 to S3. The surface runoff was highest in scenario S1 and decreases in scenarios S2 and S3. Around 782.6 mm (38.23%) surface runoff has decreased from scenario S1 to scenario S3 (Table 5).

Table 5. Change in Surface Runoff under different scenarios

Scenario	Rainfall (mm)	Surface Runoff (mm)
S1	2921.1985	2047.19975
S2	2921.1985	1323.31125
S3	2921.1985	1264.544875

4.4. Impact of LULC Change on Runoff at Sub-Basin Level

The change in annual average surface runoff is analysed at the sub-basin level. Scenario S3 has the lowest runoff among all the sub-watersheds, while the runoff in scenario S1 is the highest. The sub-basin 1 has the highest elevation and is located on the upper side of the Madi basin which covers a portion of the Annapurna Himalayan range. The elevation varies for these sub-basins from 272 masl to 7919 masl (Fig.1). Sub-basin 1 receives less rainfall than all other basins as a large portion of this basin falls under the arctic zone (above 4,500 masl), sub-alpine and alpine zone (between 3,000 and 4,500 m), and a small portion under cool temperate zone (between 2,000 and 3,000 m). The majority of precipitation occurs in the form of snowfall. Hence, generating the lowest surface runoff for all scenarios can be seen. Sub-basin 2 and 3 falls under warm temperate zones (between 1,000 and 2,000 m) and sub-tropical zone (below 1,000 masl) generates the highest surface runoff. For sub-basin 3 we can see the rising trend in runoff from scenario S1 to S2 and the sudden fall in scenario S3. These sub-basins occupy the middle portion of the study area. While the sub-basin 4 lies at a lower elevation and falls under the subtropical zone and is located on the lower side of the basin with relatively less surface runoff that is decreasing gradually over the scenarios S1 to S3 (Fig.8).

Table 6. Variation in Runoff (in mm) at Sub-Basin Level due to Land-use Change

Scenario	S1	S2	S3
Sub-basin 1	600.1215	296.4815	300.597
Sub-basin 2	3254.333	2252.661	2081.549
Sub-basin 3	2943.063	3051.9	1905.792
Sub-basin 4	1391.282	1460.15	770.242

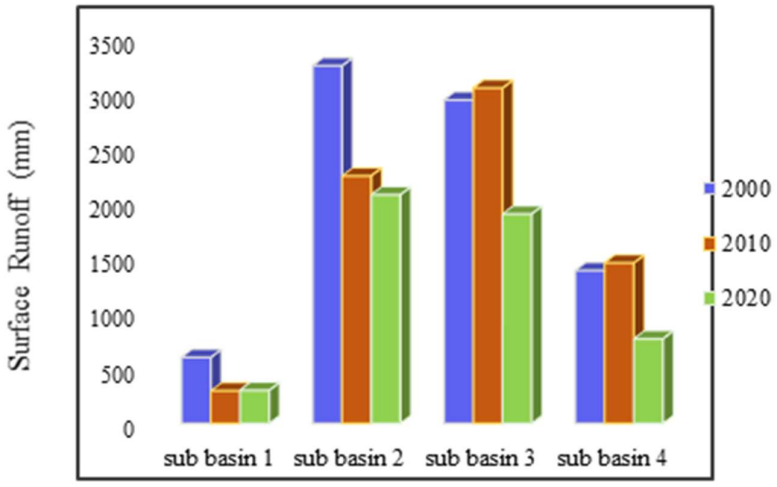

Figure 8. Variation in Runoff at Sub-Basin Level due to Land-use Change

4.5. Impact of LULC Change on Runoff by Individual Class

It could be seen from Table 7 that overall surface runoff is decreasing in all the classes from scenarios S1 to S3. The surface runoff was 3097.121 mm for the agriculture class in scenario S1 which has decreased to 2226.58 mm in scenario S2 and 796.51 mm in scenario S3. Around 1301 mm of surface runoff is decreased from scenario S1 to scenario S3 for the agriculture class. The agriculture class is the land use class that is producing the highest runoff in the basin (Table 7). For barren land, the surface runoff is decreased by about 203mm from scenarios S1 to S3 (Table 7 and Fig.9b). Fig.9c shows the variation of surface runoff for the forest land use class. The surface runoff for forest class decreases by around 772 mm from scenario S1 to S2 whereas for scenario S3 it increases by around 26 mm from scenario S2. For range land class the surface runoff decreases between scenario S1 and S2 from 617.906 mm to 195.563 mm respectively but for scenario S3 there is an increase in surface runoff of 5 mm from scenario S3 (Fig.9d).

Table 7. Surface Runoff and Curve Number by Individual LULC classes under different Scenarios

Land-use	Scenario	Rainfall (mm)	Surface Runoff (mm)	Curve Number
Agriculture	S1	3531.701	3097.121	91.988
	S2	3531.701	2226.588	92.699
	S3	3097.967	1796.511	98.235
Barren	S1	1018.498	725.108	96.172
	S2	1143.350	591.159	96.398

Land-use	Scenario	Rainfall (mm)	Surface Runoff (mm)	Curve Number
	S3	1018.498	521.550	98.259
Forest	S1	3118.906	2022.570	84.855
	S2	3026.145	1250.305	85.395
	S3	3209.436	1276.077	94.433
Rangeland	S1	1014.531	617.906	89.736
	S2	1018.790	195.563	90.257
	S3	1058.786	200.965	97.740

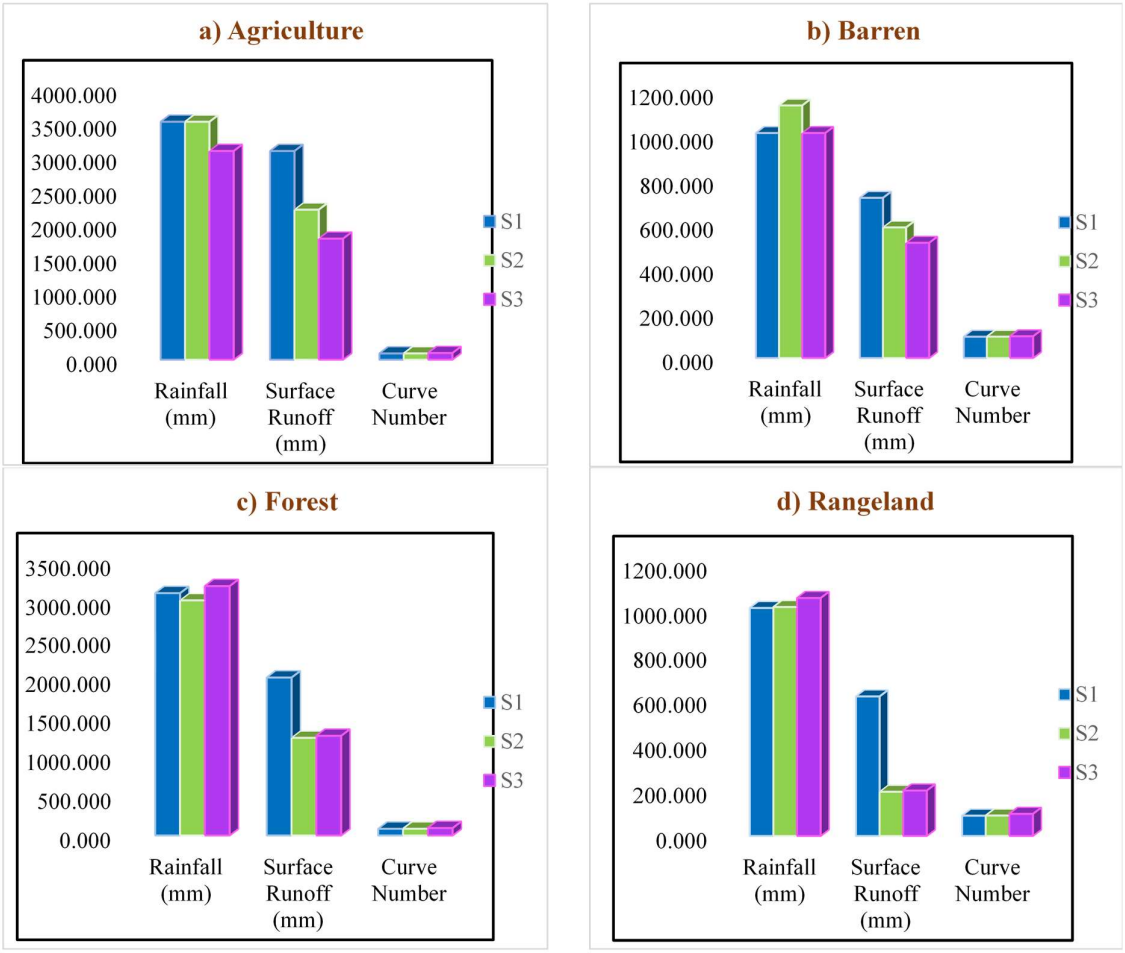

Figure 9. Change in Surface Runoff, and Curve Number for LULC classes under different scenarios (a) Agriculture (b) Barren land (c) Forest (d) Rangeland

5. Conclusions

The Madi basin lies in the high mountain as well as the hilly region. During the summer season, it receives heavy rainfall by the summer monsoon. These changes can be identified by assessing the change in LULC of a region using hydrological modeling and the SWAT model has been proven to quantify successfully the hydrological process in the Madi river basin.

Following are the conclusions from this study:

• The land use change of the Madi River Sub-basin shows around 4.21% increment in the forest cover and around 3.97% decrement in agricultural land. Further, there is seen decrement in rangeland and bare ground by 0.32% and 0.12% respectively. The surface runoff has decreased by 783 mm in the basin from the year 2000 to 2020.

• This study reveals that an increase in forest area and decrease in the agricultural area has decreased surface runoff. It could be seen that overall surface runoff is decreasing in the Madi river basin as a consequence of agricultural land reduction.

• Proper control measures shall be taken for addressing problems triggered by slope, precipitation, river edge cutting. One of the measures could be control through the embankment along the edge. Further catchment management practices should be developed in future that adopts methods like agriculture intensification rather than expansion to prevent possible damage that could be brought by runoff.

• The reduction in surface runoff reduces the stream flow eventually in the basin as it indicates that there occurs increased proportion of precipitation that infiltrates the soil and decrease in the amount that runs off directly into rivers. This might conclude that people particularly from the ridge and upper slopes in the Middle Mountains might migrate to the valley and lower slopes because of increasing shortage of drinking water. As a result, agricultural lands in the place of origin would be abandoned and left idle. This could be the main reason in agricultural land reduction in Madi basin.

• Due to reduction in the amount of runoff, the streamflow levels during storm events will be reduced, thereby reducing flood and landslide risk and the need for structures such as dams in Madi Basin at best case scenario. However, critical focus is required for sub-basin 2 and 3 while carrying out sustainable generation projects like hydropower because it has highest contribution in surface runoff despite majority of the area is covered by forest.

• These results are expected to be helpful for the sustainable watershed management, generation management and provide useful information for land use planning and ecosystem services strategies in future for Madi river basin.

References

Abbaspour, K.C., 2011. SWAT-CUP4: SWAT Calibration and Uncertainty Programs A User Manual, EAWAG Swiss Federal Institute of Aquatic Science and Technology, 1-103.

Abbaspour, K.C., Rouholahnejad, E., Vaghefi, S., Srinivasan, R., Yang, H., and Kløve, B., 2015. A continental-scale hydrology and water quality model for Europe: Calibration and uncertainty of a high-resolution large-scale SWAT model. Journal of Hydrology 524, 733–752

Arnold, J.G., Kiniry, J.R., Srinivasan, R., Williams, J.R., Haney, E.B. and Neitsch, S.L., 2012. SWAT Input/Output Documentation, Version 2012. Texas Water Resources Institute, TR-439.

Arnold, J.G., Srinivasan, R., Muttiah, R.S., and Williams, J.R., 1998. Large area hydrologic modeling and assessment part I: Model development. Journal of the American Water Resources Association, 34, 73-89.

Arnold, J.G.; Srinivasan, R.; Muttiah, R.S.; Williams, J.R. Large Area Hydrologic Modeling and Assessment Part I: Model Development. J. Am. Water Resour. Assoc. 1998, 34, 73–89.

Fan, Min; Shibata, Hideaki (2015). Simulation of watershed hydrology and stream water quality under land use and climate change scenarios in Teshio River watershed, northern Japan. Ecological Indicators, 50(), 79–89. doi:10.1016/j.ecolind.2014.11.003

Gyamfi, C., Ndambuki, J. M., Salim, R. W., 2016. Simulation of sediment yield in a semi-arid River Basin under changing land use: An integrated approach of hydrologic modelling and principal component analysis. Sustainability, 8, 1133. doi:10.3390/su8111133

Khanal N (2002) Land Use and Land Cover Dynamics in the Himalaya: A Case Study of the Madi Watershed, Western Development Region, Nepal. Tribhuvan University, Kirtipur, Nepal. p 297

Khanal, N. R., & Watanabe, T. (2008). Landslide and debris flow in the Himalayas: A case study of the Madi Watershed in Nepal. Himalayan Journal of Sciences, 2(4), 180–181. https://doi.org/10.3126/hjs.v2i4.864

Khanal, Narendra & Watanabe, Teiji. (2017). Low-flow Hydrology in the Nepal Himalaya: The Madi Watershed. Geographical Studies. 92. 6-16. 10.7886/hgs.92.6

Kiros, Gebremedhin & Shetty, Amba & Nandagiri, Lakshman. (2015). Performance Evaluaion of SWAT Model for Land Use and Land Cover Changes in Semi-arid Climatic Conditons: A Review. Journal of Waste Water Treatment & Analysis. 06. 10.4172/2157-7587.100216.

Munoth, Priyamitra; Goyal, Rohit (2019). Impacts of Land Use Land Cover Change on Runoff and Sediment Yield of Upper Tapi River Sub Basin, India. International Journal of River Basin Management, (), 1–37. doi:10.1080/15715124.2019.1613413

Neupane, Ram P.; Kumar, Sandeep (2015). Estimating the effects of potential climate and land use changes on hydrologic processes of a large agriculture dominated watershed. Journal of Hydrology, (), S0022169415005569–. doi:10.1016/j.jhydrol.2015.07.050

Setyorini, A., Khare, D. and Pingale, S.M., 2017. Simulating the impact of land use/land cover change and climate variability on watershed hydrology in the Upper Brantas basin, Indonesia. Appl Geomat, DOI 10.1007/s12518-017-0193-z.

Singh, R. K., Singha, M. , Singh, S. K. , Pal, D. , Tripathi, N. & Singh, R. S. (2018). Land use/land cover change detection analysis using remote sensing and GIS of Dhanbad districtct, India. Eurasian Journal of Forest Science, 6 (2) , 1-12 . DOI: 10.31195/ejejfs.428381

Tadesse, W., Whitaker, S., Crosson, W. and Wilson, C. (2015) Assessing the Impact of Land-Use Land-Cover Change on Stream Water and Sediment Yields at a Watershed Level Using SWAT. Open Journal of Modern Hydrology, 5, 68-85. http://dx.doi.org/10.4236/ojmh.2015.53007

Wang GX, ZhangY, Liu GM, Chen LL (2006) Impact of land-use change on hydrological processes in the Maying River basin, China. Science in China Series D: Earth Sciences 49 (10): 1098-1110.DOI: 10.1007/s11430-006-1098-6

Prediction of Bank Erosion and Channel Migration of Koshi River Using Remote Sensing

Mukesh Raj Kafle[1]

[1]Assistant Professor, Department of Civil Engineering, Institute of Engineering Pulchowk Campus, Tribhuvan University, Nepal

† Corresponding author. Email: mkafle@pcampus.edu.np

Abstract

This paper presents results of morphological phenomenon of Koshi River, Nepal. Sequential satellite images covering periods from 1972 – 2011 were used to study the process. The satellite images were geo-referenced by collecting ground control points (GCP) from previously geo-referenced satellite images using UTM projection and WGS 84 datum. River channels, chars and sandbars were extracted by classification of satellite images in the ERDAS Imagine software. Channel change maps were prepared to study the pattern of temporal changes of secondary channels of the river. The river channels of each year were extracted by supervised classification of satellite images. The channel change maps were prepared by overlaying the datasets of two consecutive years. After 1980, it shifts to the left bank, where it essentially stays until 2007 and for the upper reach the channel pattern remains along the left bank even till now. In addition, downstream of Koshi barrage, the braided channel pattern is along the right bank and in the middle. In 1980, the channel pattern was along the left bank. In 2000, the pattern was again along the right bank. However, in 2010 the channel patterns were again reverted to the left bank.

Keywords

Morphology, satellite images, river channels, sand bars, Koshi River

1. Introduction

Rivers attain their stability by changing its course. Because of its dynamic characteristics, during the process of gaining such stability, rivers plan form; morphology and other features change to cope with it. Effects of such changes are replicated in plan form and channels. The most common outcome of such adaptation in plan form is bank erosion. Stream bank erosion is a dynamic natural geomorphic process. It occurs during or immediate after floods resulting in meandering of rivers as well as alteration of channel course. Such erosion affects a range of physical, ecological management issues in the fluvial environment. It is also important from the geomorphological aspect as it also induces changes in the river channel course and in the development of the floodplain (Hooke, 1979; Bridge, 2003). Studies have shown that sediment from stream bank can account for as much as 85% of watershed sediment yields bank retreat rates as high as 1.5 to 110 m/year have been documented (Trimble, 1997). A combination of three processes - sub aerial processes erosion, bank failure and fluvial erosion retreats stream bank (Lawler, 1995). Erosion rates can be quantified by the soil critical shear stress (τc). The critical shear stress is defined as the stress at which soil detachment begins or condition that initiates soil detachment. If the critical stress is higher than the effective stress, the erosion rate is zero (Osman and Thorne, 1998).

Significant parameters affecting erosion are vegetation index (stability), the presence or absence of meanders, bank material (classification) and stream power (Atkinson et al., 2003). Other factors such as bank height, riverbank slope, river cross-section width, riverbed slope and water velocity have also been reported to affect the erosion rate (Hooke, 1979; Abam, 1993; Winterbottom and Gilvear, 2000; Rinaldi et al., 2008; Luppi et al., 2009). Therefore, identification of riverbanks, which are vulnerable to erosion, is of utmost importance, either for their protection or restoration. Though riverbank erosion is a usual phenomenon, it's difficult to predict and locate the extent of riverbank erosion. To overcome this difficulty, researchers have developed and tested a number of approaches and methods. For the prediction of changes in the river channel form, identification of the areas vulnerable to bank erosion is the most important issue. Different methods such as historical maps, sequential aerial photographs have been used to predict erodibility. However, a combination of bank stability methods and hydrodynamic models is commonly used to predict the vulnerable areas and estimate the erosion rate (Nardi et al., 2013).

2. Rationale

The most important rivers in the Terai region of Nepal required for flood control and bank protection are - Mahakali, Karnali, West Rapti, Gandaki, Narayani Bagarmat, Kamla, Koshi, and Mechi (Mahananda). These are trans - boundary rivers, most of which originate in Tibet (China), flow through Nepal and enters to Indian Territory through Terai plains. These rivers have almost the same morphological characteristics. During the monsoon, floods and related flooding are common in Nepal. However, the Koshi flood of 2008 was unique in terms of its magnitude and the extent of devastation it created. The flood magnitude was less than the long-term average monsoon flood. However, damage it created in Sunsari district (Nepal) and northern Bihar (India) was catastrophic. Similarly, the 2008 flood also hit hard the Far-Western districts of Kailali and Kanchanpur. The main reason behind this was the bank erosion. In this context, to reduce annual loss of lives and property due to flooding, proper prediction of bank erosion and channel migration is important. This prediction will allow the local authority and planners to apply necessary measures for bank protection works. In such scenario, this study may be useful.

3. Study Area

The Koshi basin is roughly located between 85˚ to 89˚ east longitude and 25˚ to 29˚ north latitude. Koshi is a trans-boundary river, originating in Tibet, flowing through the Himalaya, through the eastern part of Nepal and the flat plain of Indian north territory. Out of total 69,300 km^2 catchment area of Koshi River, it drains 29400 km^2 in China; 30,700 km^2 in Nepal and 9,200 km^2 in India (Fig.1). The Koshi River flows with seven major tributaries namely Sunkoshi, Tamakoshi, Dudhkoshi, Indravati, Likhu, Arun and Tamur. At Tribeni (Nepal), these rivers combine and become Saptkoshi, literally known as "Seven Koshis". Downstream of Tribeni, the Saptkoshi crosses almost 10 km middle mountains or Mahabharat Range in a narrow gorge and emerges from mountains. The River is unable to transport sediment all the way to Ganges resulting huge deposition below foothills (Fig.1).

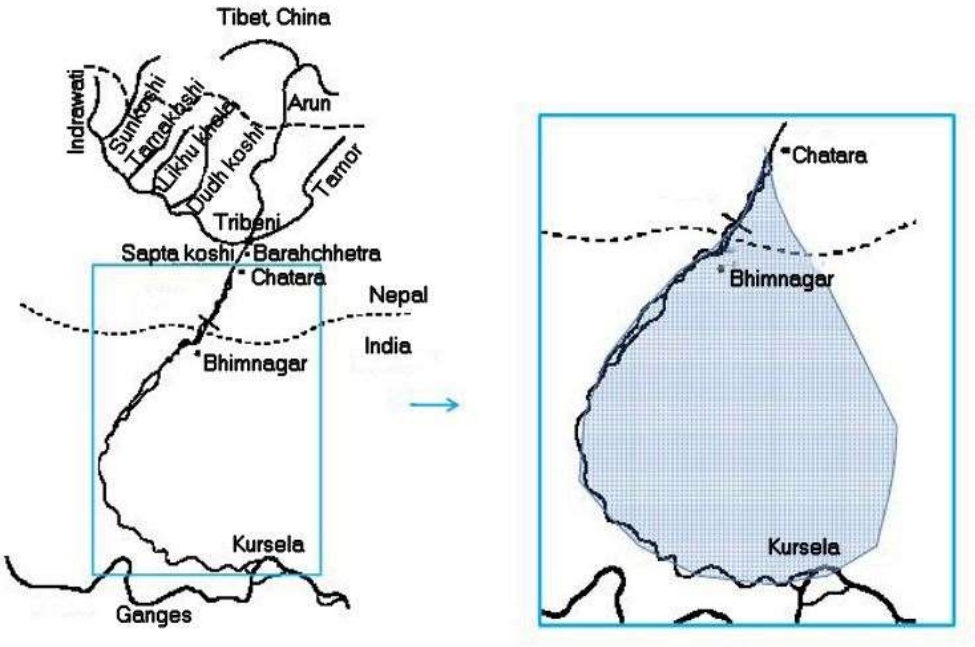

Figure 1. Koshi River with tributaries and alluvial fan (adopted: Hooning 2011)

4. Materials and Methods

Materials Sequential satellite images were used to study t detailed morphological phenomenon in the Koshi River. This approach has proven to be very valuable in maintaining the embankment system and in planning of bank protection works in Jamuna River, Bangaladesh. To increase the understanding of detailed morphological phenomenon, satellite imagery was used covering periods from 1972 – 2011 (Table 1). The earlier satellite images have a low resolution (Landsat 1 200 m), but the more recent images have a much higher accuracy. Landsat 7 images for example have an accuracy of 20 m. A low accuracy does not allow to identify yearly bank erosion rates less than say 100 m, but even this might be acceptable for the present analysis, where the width first and second order channels is in the order of 1 km. It can be observed that the minimum levels at Chatra have been varying over the years (Fig.2a). Hence, the gauge reading itself was not used for an evaluation of how well the selected image fulfilled the criterion that it should correspond to low water conditions. Instead, the level difference between the date of image acquisition and the minimum gauge reading in that particular year was used. This difference is plotted and it is observed that only for two years the water level difference is in the order of 1 m, notably the years 1999-2000 and 2005. In other years it is less than 0.5 m and hence quite acceptable (Fig.2b).

Table 1. Satellite images used

Low water season	Planform	Date of imagery	Gauge reading (m)			
			I	II	III	Average
1972-73	Landsat 1	13-Dec-72				
1975-76	Landsat 2	20-Nov-75				
1976-77	Landsat 2	26-Oct-76				
1978-79	Landsat 2	6-Jan-79	1.06	1.06	1.07	1.06
1979-80	Landsat 3	18-Jan-80	0.86	0.86	0.87	0.86
1987-88	Landsat 5	8-Feb-88	1.78	1.78	1.78	1.78
1988-89	Landsat 4	17-Jan-89	1.76	1.76	1.76	1.76
1989-90	Landsat 4	25-Mar-90	1.48	1.48	1.48	1.48
1999-00	Landsat 7	29-Nov-99	1.99	1.99	1.98	1.99
2000-01	Landsat 7	7-Mar-01	0.83	0.82	0.8	0.82
2001-02	Landsat 7	6-Feb-02	0.81	0.81	0.82	0.81
2003-04	Landsat 7	27-Jan-04	0.7	0.7	0.68	0.69
2005-06	Landsat 7	5-Nov-05	1.5	1.52	1.51	1.51
2007-08	Landsat 7	5-Dec-07	1.08	1.08	1.08	1.08
2007-08	Landsat 5	6-Jan-08	0.73	0.73	0.73	0.73
2008-09	Landsat 5	2-Dec-09	0.9	0.91	0.92	0.91
2009-10	Landsat 5	20-Feb-10	0.26	0.26	0.26	0.26
2011-12	Landsat 5	6-Nov-11				
2011-12	Landsat 5	18-Feb-12				

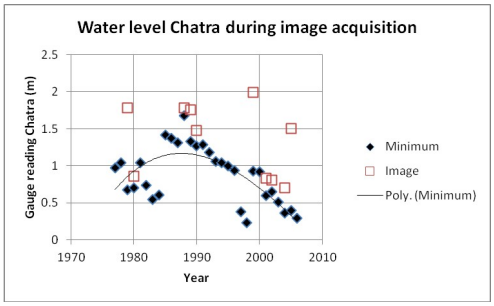

(a) Gauge readings

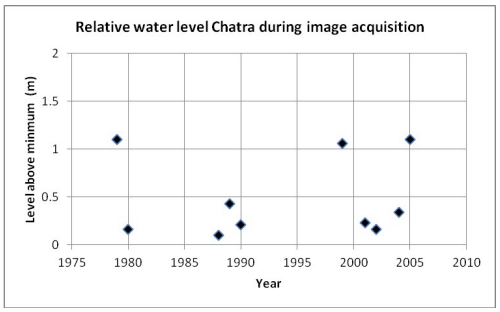

(b) Difference water level image and minimum

Figure 2 Gauge reading date image acquisition and minimum gauge reading

Satellite images of different years were to be compared. To allow this, images need to be geometrically corrected (often referred to as geo-referencing). The satellite images were geo-referenced by collecting ground control points (GCP) from previously geo-referenced satellite images using UTM projection and WGS 84 datum. In a further step, satellite images of each dry season were mosaicked to get an image of entire area. Arc GIS and ERDAS Imagine software were used for carrying out geo-referencing and mosaicking.

5. Results and Discussions

River channels, chars and sandbars were extracted by classification of satellite images in the ERDAS Imagine software. Channel change maps were prepared to study the pattern of temporal changes of secondary channels of the river. The river channels of each year were extracted by supervised classification of satellite images. The channel change maps were prepared by overlaying the datasets of two consecutive years. The younger river channel of two consecutive years is kept at the bottom of the overlay. The middle layer of the overlay is composed of common portions of the water channels present in satellite images of both the years. The top layer represents the river channel in the older (previous) year. Channel change maps were prepared for a period from 1973 through 2012, though many not on a year-by-year basis (Fig.3). In total 19 images have been classified over a period of almost 40 years (Table 2).

Table 2. Year-to-year and longer period differential maps

Previous image	Later image	Time interval (years)
13-Dec-72	20-Nov-75	3
20-Nov-75	26-Oct-76	1
26-Oct-76	6-Jan-79	2
6-Jan-79	18-Jan-80	1
18-Jan-80	8-Feb-88	8
8-Feb-88	17-Jan-89	1

Previous image	Later image	Time interval (years)
17-Jan-89	25-Mar-90	1
25-Mar-90	29-Nov-99	10
29-Nov-99	7-Mar-01	1
7-Mar-01	6-Feb-02	1
6-Feb-02	27-Jan-04	2
27-Jan-04	5-Nov-05	2
5-Nov-05	5-Dec-07	2
5-Dec-07	6-Jan-08	<1
6-Jan-08	20-Oct-08	<1
20-Oct-08	2-Dec-09	1
2-Dec-09	20-Feb-10	<1
20-Feb-10	6-Nov-11	2
6-Nov-11	Feb18-2012	<1

However, only 7 pairs of images are available where the time difference is in the order of 1 year. All the other differential maps cover longer periods (5 of 2 years interval, 1 of 3 years interval, 1 of 8 years and 1 of 10 years interval). Plan form changes in the period 2007-2008 through 2010-2011, may be the best series (Fig.3). Unfortunately in this period the 2008 Koshi breach did occur, and this means that this period is not representative for the period before 2007.

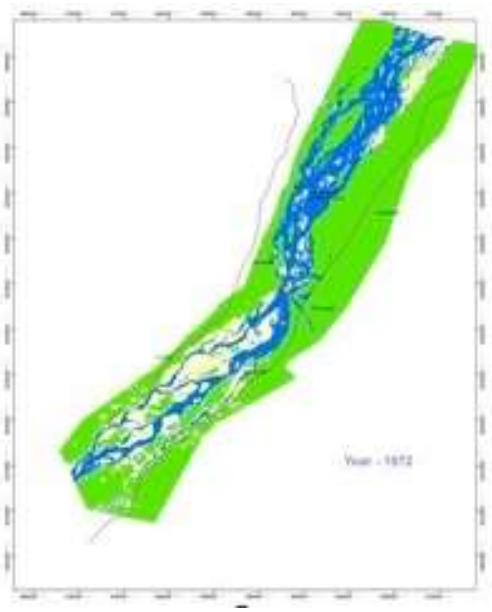

(a) 1972-1973

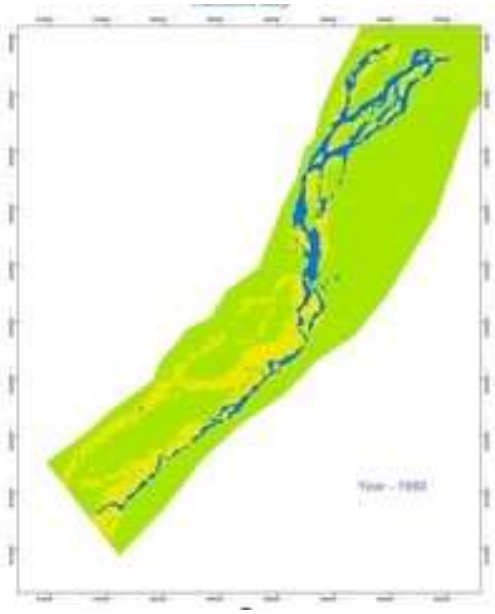

(b) 1980

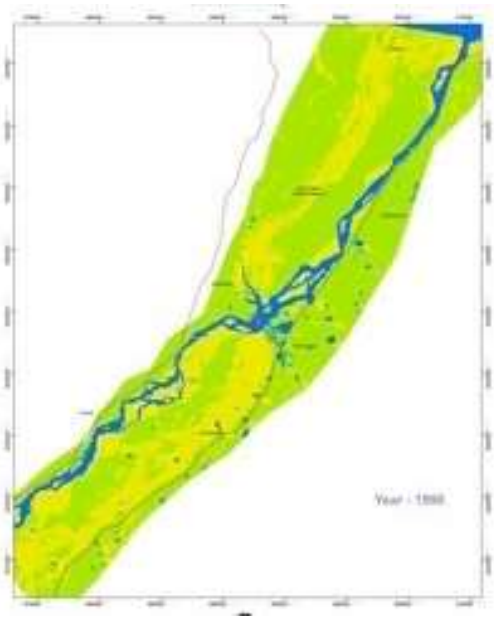

(c) 1990

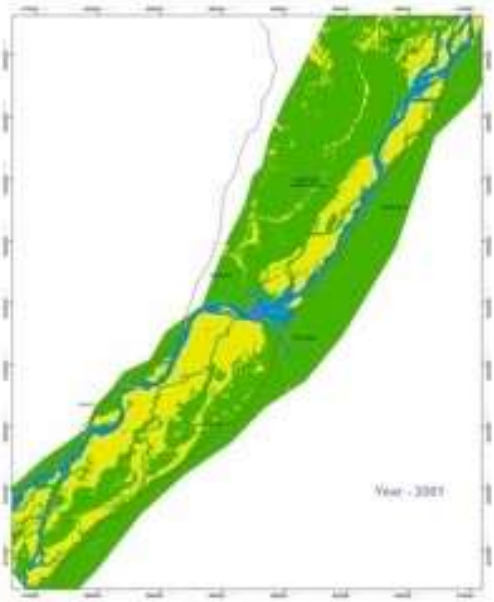

(d) 2001

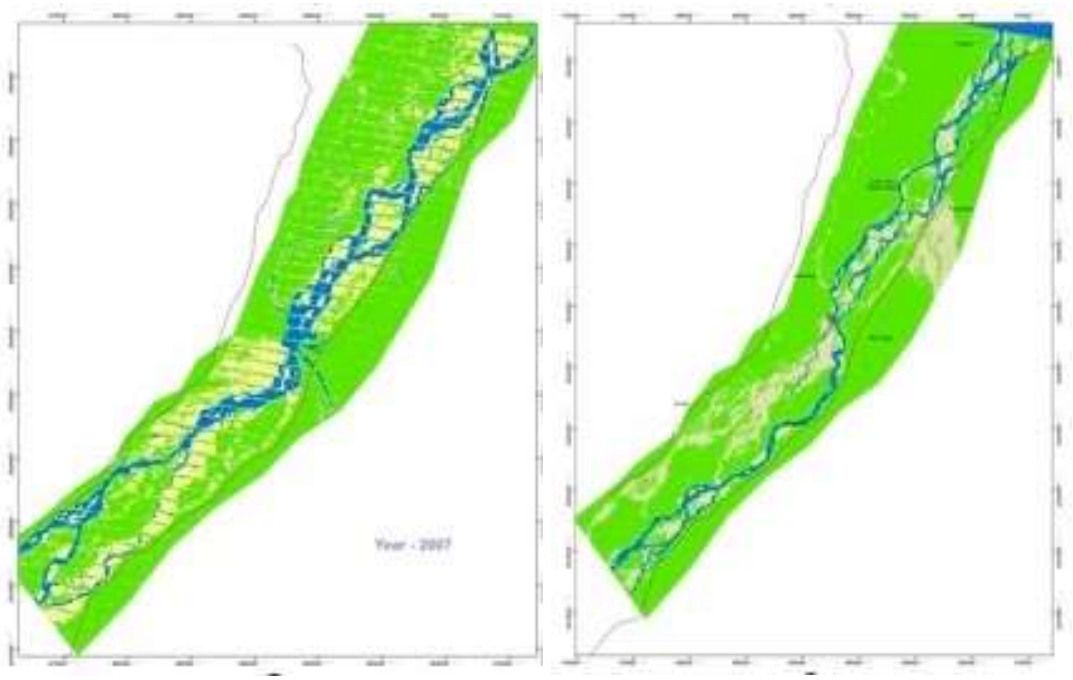

(e) 2007-2008 (f) 2010-2011

Figure 3. Change in planform (classified maps) of the Koshi River in period 1973-2011

The differential maps (Fig.4) indicate that the channel pattern is not filling the whole riverbed. The low water bed can occupy different courses (roughly speaking on the right, in the middle and on the left). Moreover, in quite some years, the bank protection works seem to attract the channels. Upstream of Koshi barrage, the braided channel initially is located along the right bank. However, after 1980 it shifts to the left bank, where it essentially stays until 2007 and for the upper reach the channel pattern remains along the left bank even till now. In addition, downstream of Koshi barrage, the braided channel pattern is along the right bank and in the middle. In 1980, the channel pattern is along the left bank, but about 20 years later the pattern is again along the right bank, and 10 years later again the channel pattern is back to the left bank.

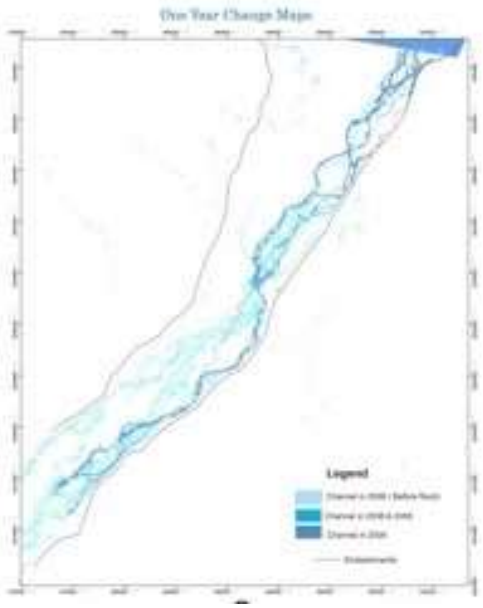

(a) Difference 2007-2008 and 2008-2009

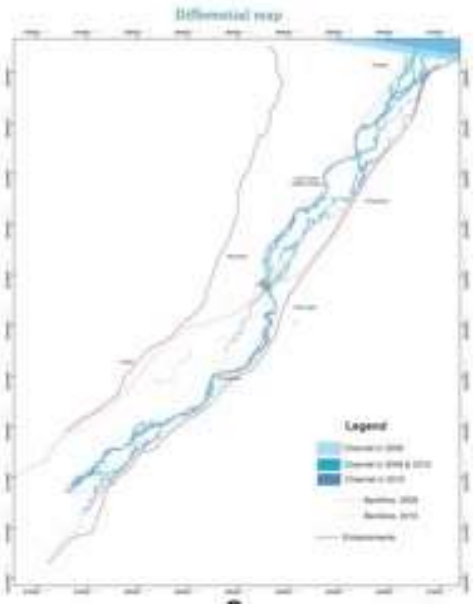

(b) Difference 2008-2009 and 2009-2010

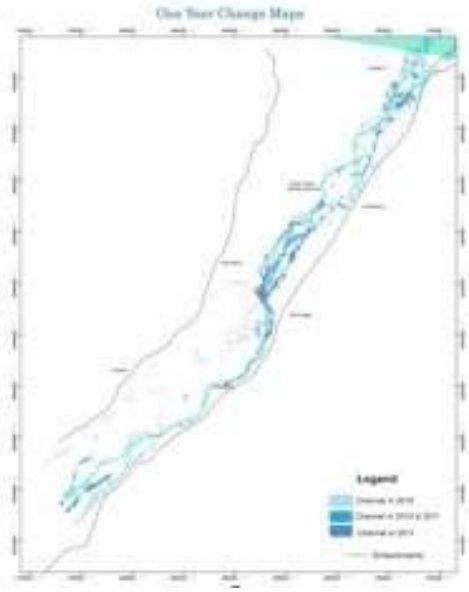

(c) Difference 2009-2010 and 2010-2011

(d) Difference 2010-2011 and 2011-2012

Figure 4. Change maps for period 2007-2008 through 2011-2012

6. Conclusions

Differential images provided a good insight into the morphological changes occurring in the Koshi River over the decades. The study shows channel pattern is shifting from right to back and vice versa with a time scale of a number of days. There appears limited correlation between the location upstream and downstream. A possible influence of the barrage operation

cannot be identified, as the operation of the barrage is not known. The reason of shifting of the channel pattern might be the aggradation of the channel due to avulsion. It has been observed that, the right part of the channel is filled in first and then the river shifts to the other bank, which is relatively low-lying to continue the deposition of sediment along that bank. This study demonstrates how remote sensing techniques can help in prediction of bank erosion and channel migration in the Terai Rivers. This study is only a first step towards the development of a year-to-year prediction of bank erosion along the Terai rivers in Nepal, in due time to be used as a management tool for decisions regarding investments in bank protection works

.

References

Abam, T. K. S (1993). Factors affecting distribution of instability of river banks in the Niger delta. Eng. Geol., 35, 123–13.,

Atkinson, P. M., German, S. E., Sear, D. A., and Clark, M. J (2003). Exploring the relations between riverbank erosion and geomorphological controls using geographically weighted logistic regression. Geogr. Ana. 35, 58–82.

Bridge, J. S (2003). Rivers and floodplains: forms, processes, and sedimentary record. Blackwell, Malden, Mass., USA.

EGIS (2002). Developing and updating empirical methods for predicting morphological changes of the Jamuna River, Dhaka. EGIS Technical Note Series 29.

Hooke, J. M (1979). An analysis of the processes of river bank erosion. J.Hydrol., 42, 39–62.

Lawler D.M (1995).The impact of scale on channel side sediment supply: A conceptual Model, In effects of scale on interpretation & management of sediment & water quality. IAHS Pub-226.

Luppi, L., Rinaldi, M., Teruggi, L. B., Darby, S. E., and Nardi, L (2009). Monitoring and numerical modelling of riverbank erosion processes: A case study along the Cecina River (central Italy). Earth Surf. Proc. Land., 34, 530–546.

Nardi, L., Campo, L., and Rinaldi, M (2013). Quantification of riverbank erosion and application in risk analysis. Nat. Hazards, 69, 869887.

Osman, A. M., and C. R. Thorne (1998). Riverbank stability analysis: I. Theory. J. Hydraulic Eng.114(2): 134-150.

Rinaldi, M., Mengoni, B., Luppi, L., Darby, S. E., and Mosselman, E (2008). Numerical simulation of hydrodynamics and bank erosion in a river bend. Water Resour. Res., 44, W09428, doi:10.1029/2008WR007008.

Trimble, S. W (1997). Contribution of stream channel erosion to sediment yield from an urbanizing watershed. Science. 278(5342):pp: 1442-1444.

Winterbottom, S. J. and Gilvear, D. J (2000). A GIS-based approach to mapping probabilities of river bank erosion: Regulated River Tummel, Scotland. River Res. Appl., 16, 127–140.

Flow and Stress Analysis of Penstock Trifurcation of Dordi Khola HPP (27MW)

Bharat Chand[1]†

[1]Global Civil Consult Pvt. Ltd., Kathmandu, Nepal
† Corresponding author. Email: bharatchand.100@gmail.com

Abstract

The research was studied with the help of a 3D model in ANSYS CFX and APDL. This study presents the results of a computational fluid dynamics (CFD) study and a review of fluid flow modelling and stress analysis in ANSYS Mechanical APDL on trifurcation of penstock pipe of Dordi Khola Hydropower Project. ANSYS CFX is a high-performance Computational Fluid Dynamics (CFD) software tool that delivers reliable and accurate solutions quickly and robustly across a wide range of CFD and multi-physics applications. ANSYS Mechanical APDL is software that delivers accurate solutions. The geometry was created and the flow field was analysed under different conditions and analysed the von-misses stress on the trifurcation.

Keywords

Dordi Khola HPP; Computational fluid dynamics; Stress analysis; Trifurcation

1. Introduction

A power tunnel is provided to connect the intake structure to the powerhouse in any hydropower project. Usually, the power tunnel is branched into several penstocks in order to feed the individual turbines of the powerhouse. Penstock is the pressure conduit between the turbine inlet valve and the first open water upstream from the turbine. The open water can be a surge tank, forebay, or reservoir. The penstock is mostly made up of welded carbon steel. The branching may be made by providing a trifurcation with abrupt entry or conventional Wye arrangement or trifurcation with the suitable transition. Whatever the manner of branching, the objective of the planning should be to get the most efficient system of branching (Adamkowski & Kwapisz, 2004; Zhou & Bryant, 1992). The flow analysis through a pipe under pressure is simple and can be described by the one-dimensional and two-dimensional flow equations precisely. However, the flow near the junction of the branches is difficult or sometimes impossible to describe by the closed-form mathematical solution (O'Brien, Ehrlich, & Friedman, 1976; Xuan, Li, & Tu, 2006). In such a case either model analysis will capture the flow pattern or the Computational fluid dynamics (CFD) can best model the flow (Thapa, Luintel, & Bajracharaya, 2016). The most famous CFD algorithm uses finite element modelling. The finite element model of the control volume just replaces the water volume by the discrete tetrahedral or hexahedral elements. The flow parameters are assigned to each node. The nodal parameters known at the boundary are known as boundary conditions. Mathematically this process converts the flow differential equations by the set of simultaneous linear equations for each fluid element. The coefficient matrix of the linear equations of each element is well known by the element stiffness matrix. The elemental stiffness matrixes of all elements are assembled to form a global stiffness matrix. The matrix is solved to obtain the nodal parameter at each node. All of these tasks can be done easily with the help of the available

CFD tools (Aguirre & Camacho, 2014; Kandel & Luitel, 2019; Koirala, Chitrakar, Neopane, Chhetri, & Thapa, 2017). ANSYS CFX and FLUENT are the strong CFD tools for modelling of the flow in any boundary conditions and flow load (Alligne, Rodic, Arpe, Mlacnik, & Nicolet, 2014; Anand, Jawahar, Bellos, & Malmquist, 2021; Židonis, Benzon, & Aggidis, 2015).

Introduction to Computational Fluid Dynamics and Mechanical APDL

Computational fluid dynamics (CFD) is a branch of fluid mechanics that uses numerical analysis and data structures to analyse and solve problems that involve fluid flows. Computers are used to perform the calculations required to simulate the free-stream flow of the fluid, and the interaction of the fluid (liquids and gases) with surfaces defined by boundary conditions. With high-speed supercomputers, better solutions can be achieved, and are often required to solve the largest and most complex problems. Ongoing research yields software that improves the accuracy and speed of complex simulation scenarios such as transonic or turbulent flows. Initial validation of such software is typically performed using experimental apparatus such as wind tunnels. In addition, previously performed analytical or empirical analyses of a particular problem can be used for comparison. Final validation is often performed using full-scale testing, such as flight tests.

CFD is applied to a wide range of research and engineering problems in many fields of study and industries, including aerodynamics and aerospace analysis, weather simulation, natural science and environmental engineering, industrial system design and analysis, biological engineering, fluid flows, and heat transfer, and engine and combustion analysis.

CFD has increased in importance and inaccuracy; however, its predictions are never completely exact. Because many potential sources of error may be involved, one has to be very careful when interpreting the results produced by CFD techniques. The key to various numerical methods is to convert the partial differential equations that govern a physical phenomenon into a system of algebraic equations. Different techniques are available for this conversion. CFD is merely a tool for analysing fluid-flow problems. If it is used correctly, it can provide useful information cheaply and quickly. ANSY Mechanical APDL has become a powerful tool for finite element analysis to solve an enormous range of mechanical engineering applications. It has capabilities to solve problems ranging from simple, linear, static analysis to a complex, nonlinear, transient dynamic analysis, in the fields of stress analysis, fluid and heat transfer, etc.

ANSYS Mechanical provides solutions for many types of analyses including structural, thermal, modal, linear buckling, and shape optimization studies. ANSYS Mechanical is an intuitive mechanical analysis tool that allows geometry to be imported from a number of different CAD systems. It can be used to verify product performance and integrity from the concept phase through the various product design and development phases. The use of ANSYS Mechanical accelerates product development by providing rapid feedback on multiple design scenarios, which reduces the need for multiple prototypes and product testing iterations.

2. Methodology

The Modelling process consists of first taking the real-world fluid geometry and replicating this in the virtual environment. From here, a mesh can be created to divide the fluid into the discrete section. Boundary conditions then must be entered into the model to designate parameters such as the type of fluid to be modelled or the detail of any solid edges or flow inlets/outlets. The simulation is then ready to be run and when a converged solution is found, it must be carefully analysed to establish whether the mesh is appropriately modelling flow conditions. Generally, some form of mesh refinement will be necessary to put in further detail around the areas of interest.

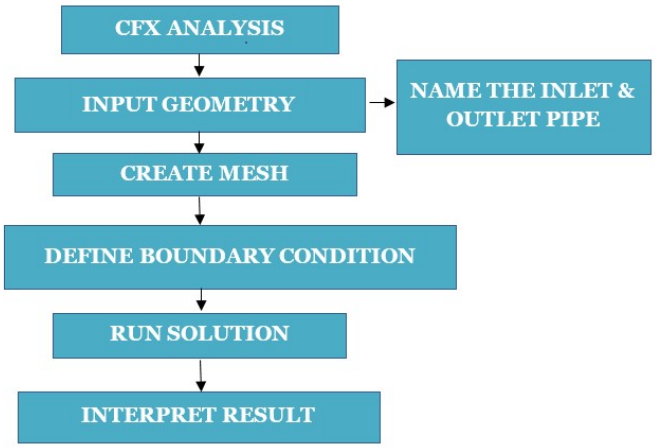

Figure 1. Flow chart of CFX numerical modelling

Building the model for CFX analysis

The 2D sketch is converted into 3D solids using the software like solid works, AutoCAD, ANSYS etc. The study considers the flow modelling of following option for manifold layout. The scope of work is to observe the flow pattern distribution.

1. Symmetrical, Equilibrium with diverging angle of 45 degree for each manifold.

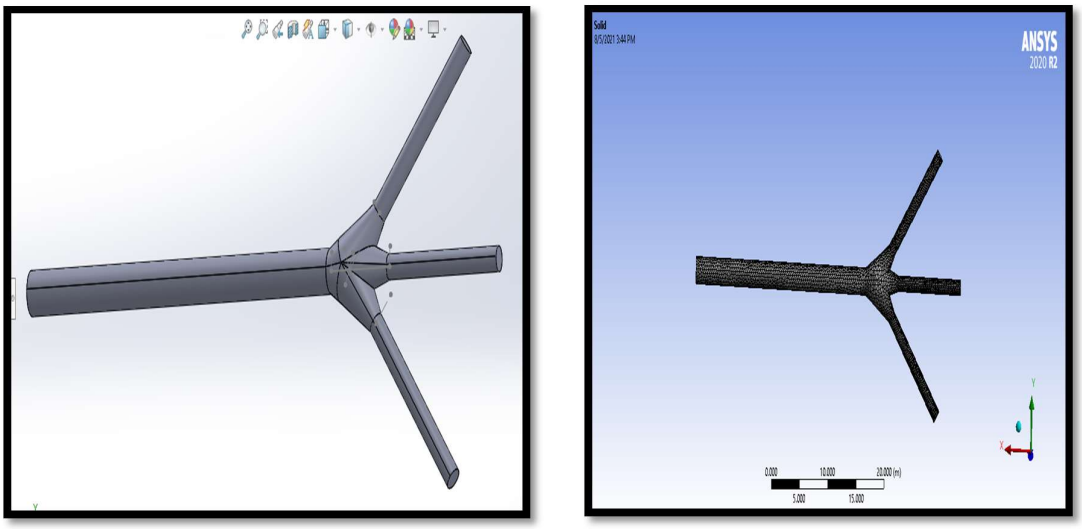

Figure 2. Model preparation for CFX analysis

Analysis Criteria

Computational Fluid Dynamics is used for the analysis of the velocity and pressure distribution in penstock pipes with branches. The velocity and pressure distribution can be used as criteria for choosing the best option to get maximum possible efficiency. The option with minimum loss or maximum discharge carrying capacity with same head loss should be selected for the recommendation.

CFX and FLUENT features of the ANSYS v1 is used for the mathematical modelling of the flow through the profile. The tetrahedral mesh is imported to ANSYS CFX for the analysis. Wall is considered to be smooth wall in order to reduce the computational requirement. As the wall length is small this loss can be estimated analytically. Reference pressure is assumed to be 0 atm. The pressures indicated in the pressure diagram are relative to this pressure. Flow is assumed to be incompressible without heat transfer. K-ε turbulence model is used to model the flow turbulence. High resolution solver option with convergence criteria of 10^-4 is selected. All the calculations are conversed within maximum inner loop iteration limit of 100.

The analysis for current scenario was done for three cases as follows:

1. All 3 turbines are running at inlet pressure 2 Mpa.
   Mass flow rate at outlet 1,2,3 = 5000kg/s.
2. One turbine is closed and two are running at inlet pressure 2 Mpa.
   Mass flow rate at outlet 1= 0, outlet 2,3 =5000kg/s.
3. Only one turbine is running at inlet pressure 2 Mpa.
   Mass flow rate at outlet1,2= 0, outlet 3= 5000kg/s.

Modelling Process in Mechanical APDL

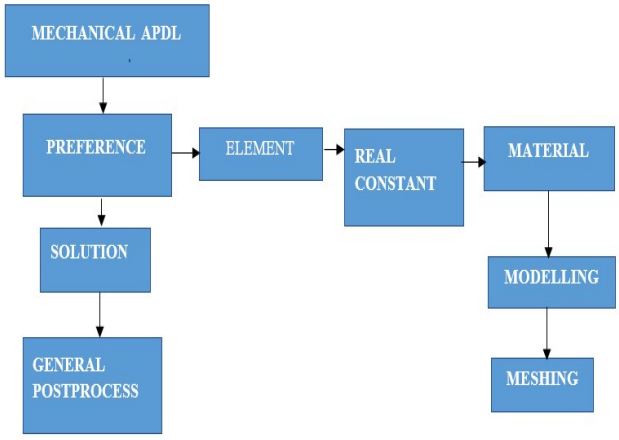

Figure 3. Flow chart for Mechanical APDL numerical modelling

Building the Model for Stress Analysis

The 2D sketch are converted into 3D solids using solid work. The created 3D solid converted into .IGES file and then this file is imported in ANSYS mechanical APDL for the stress analysis.

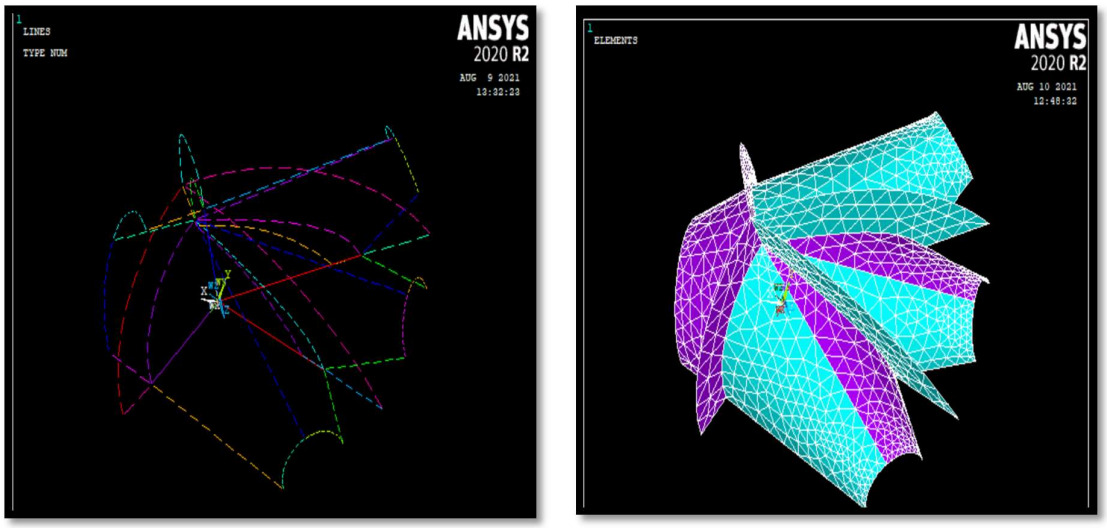

(a) (b)

Figure 4. The 3-D model (a) and meshing of the model (b)

Boundary Condition

The analysis takes advantage of the existing symmetry conditions by modelling only one half of the trifurcation. Hence, all nodes located on the symmetry plane are held against translations normal to and rotations parallel to this plane. In addition to all nodes located at the end faces

of the pipes are held against translations normal to and rotations parallel to the respective end planes.

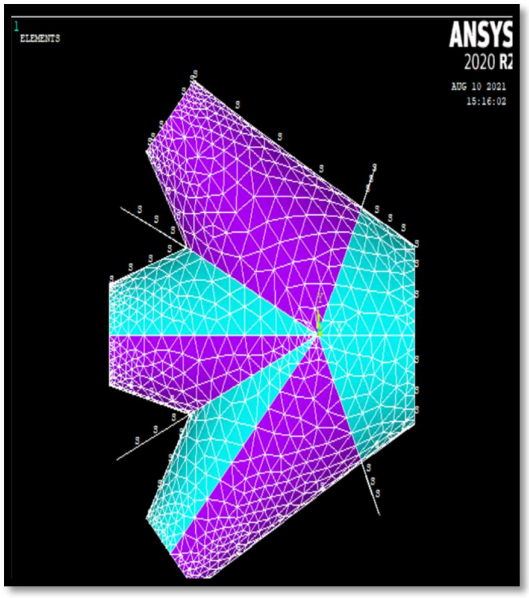

Figure 5. Boundary condition of the model

Design Premises

Loads	**Trifurcation**
Design Pressure	2 N/mm^2
Trifurcation dimensions	
Diameter of inlet	2300 mm
Diameter of outlet-1	1300 mm
Diameter of outlet-2	1300 mm
Diameter of outlet-3	1300 mm
Trifurcation angle	45 degree
Height of main rib	300 mm
Height of side ribs	300 mm
Proposed plate thickness	
Downstream pipe in front of trifurcation	50 mm
Downstream pipe at rear of trifurcation	50 mm
Main ribs	50 mm
Left and right ribs	50 mm
Material properties	
Elastic modulus	2e7 N/mm^2
Poisson's ratio	0.3
Yield stress	460 MPa

Basis for Analysis

The cone parts of the trifurcation are modelled and analysed. In addition, the model also consists of the upstream and downstream cylindrical pipes. The figure shows the design pressure of 2 Mpa which is applied as surface loads to all nodes except for those solely belonging to the ribs.

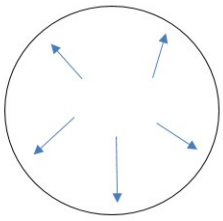

Figure 6. Internal pressure

3. Results

3.1. CFX Analysis

1. Case I: All three turbines are running

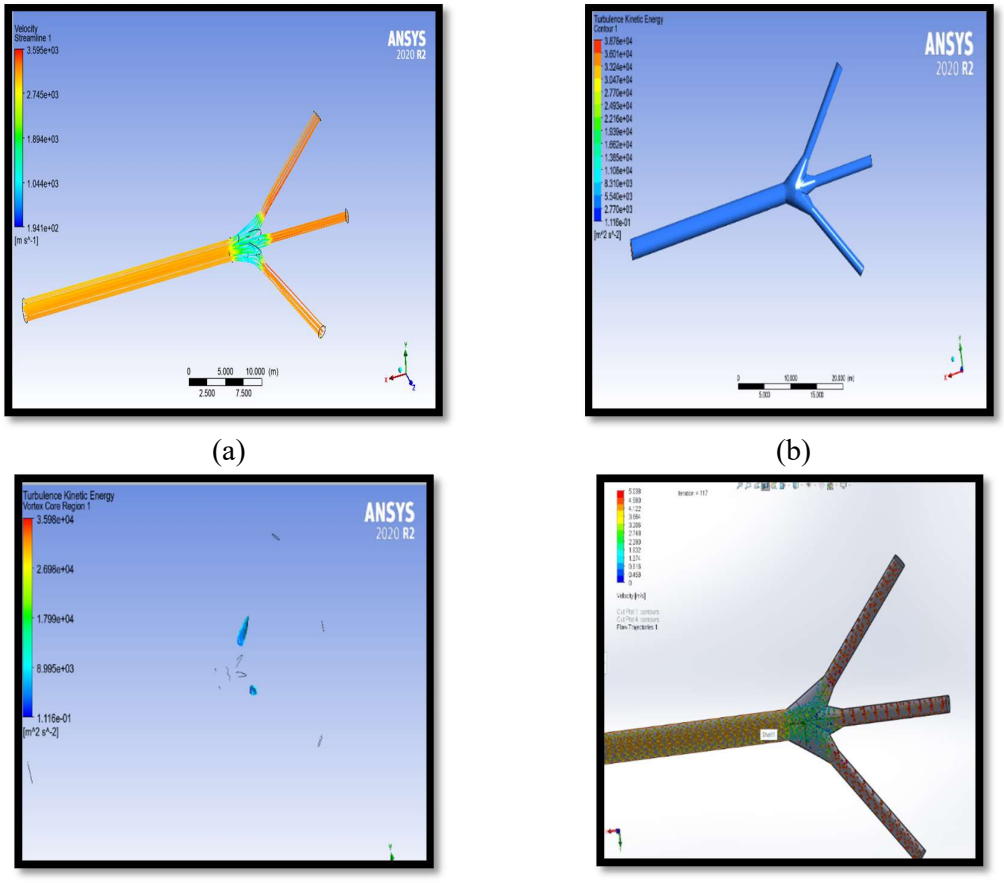

Figure 7. Velocity streamline (a), Turbulence kinetic energy contour (b), Turbulence kinetic energy vortex core region (c), and Flow particle tracking for case I

2. Case II: One turbine is closed and other two are running

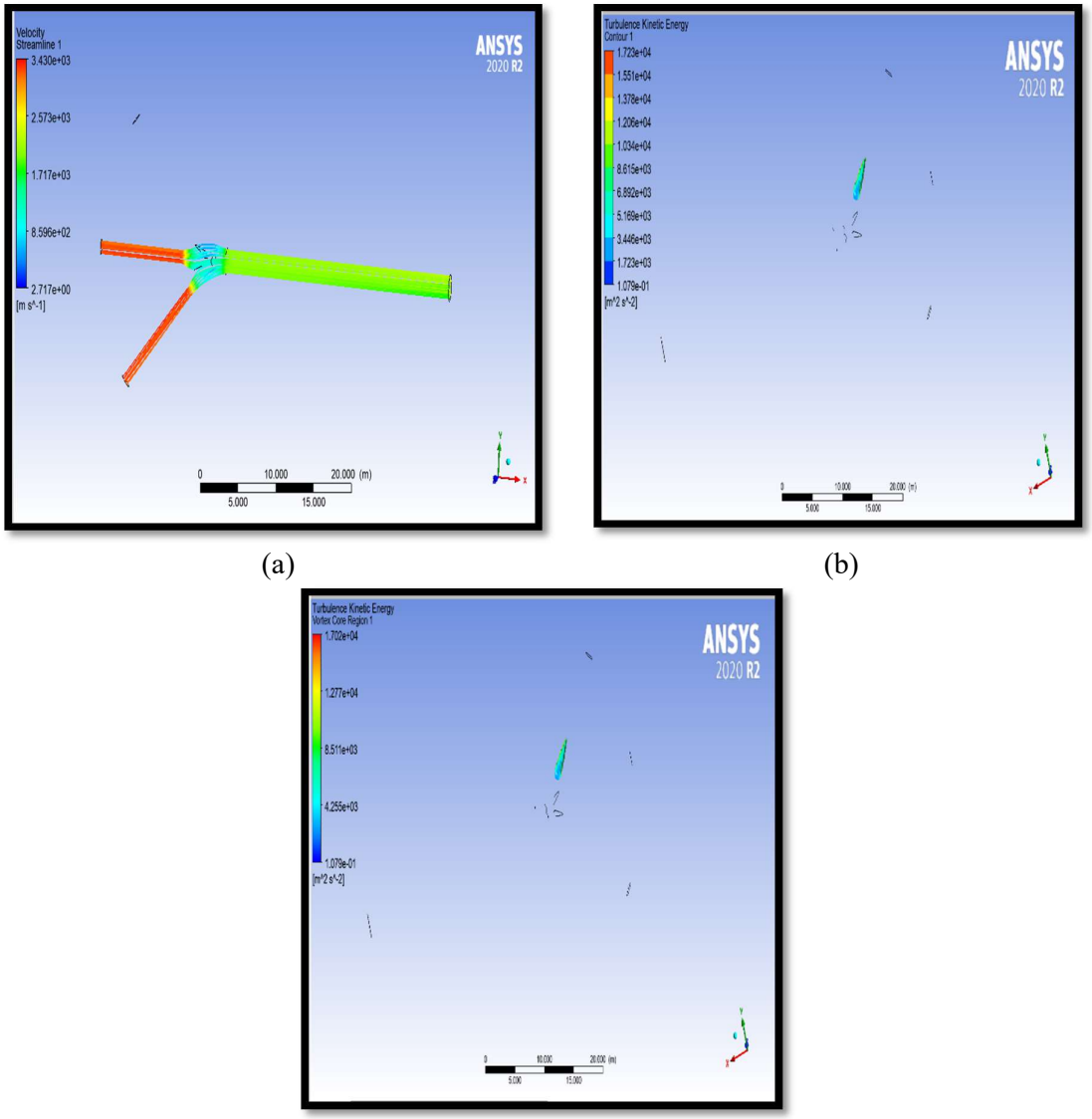

Figure 8. Velocity streamline (a), Turbulence kinetic energy contour (b), and Turbulence kinetic energy vortex core region (c) for case II

3. Case III: Only one turbine is running and the other two are closed

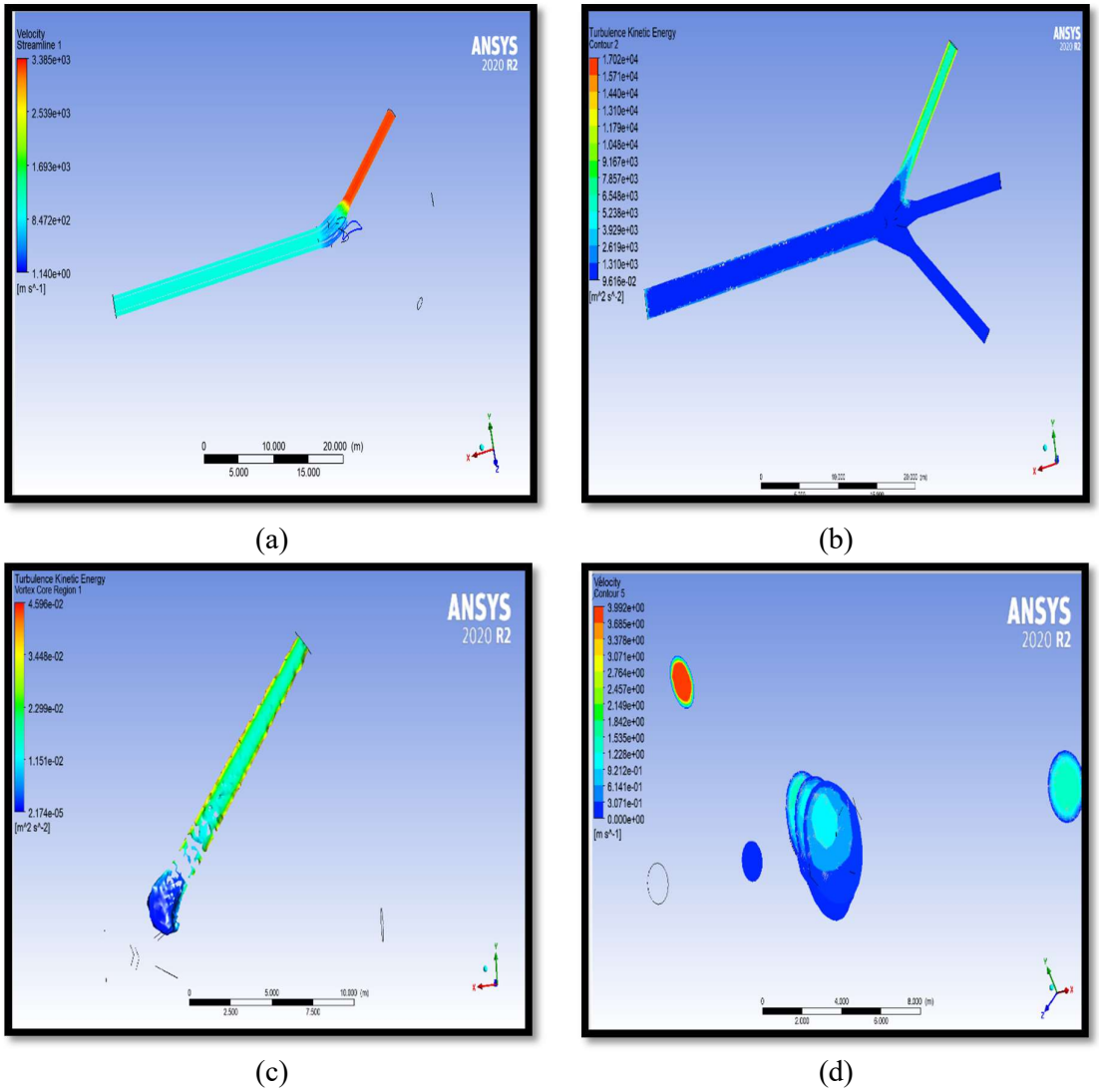

Figure 9. Velocity streamline (a), Turbulence kinetic energy contour (b), Turbulence kinetic energy vortex core region (c), and Velocity contour at centre, 10 m towards the outlet 3 and 10 m towards inlet, for case III

3.2. Stress Analysis

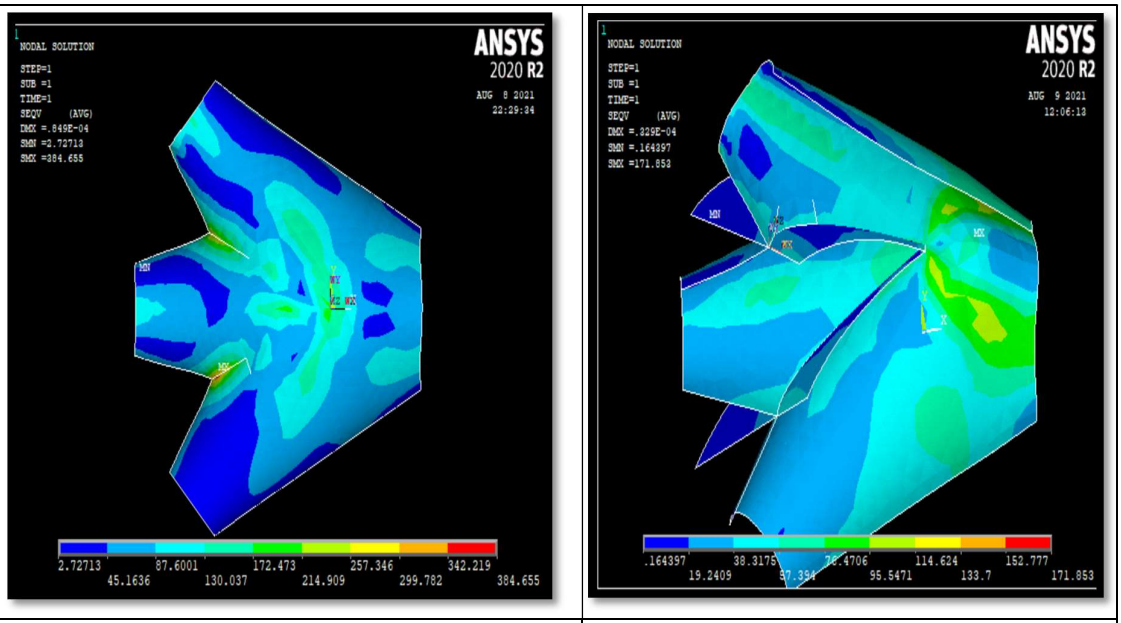

(a) (b)

Figure 10. Von-Mises stress without stiffener (a), and with stiffener (b)

The von Mises equivalent stresses at the cylinder and cone parts as shown in the figure above. The values are bound at the bottom of the shell elements, where the highest stress levels are observed. The figure further points out those regions where the stress levels exceed the given limits. These regions are strictly concentrated along the cone intersections and are completely covered within the width of the suggested ribs. The stress levels in the areas adjacent to the ribs are within the limits, thus the cylinders and cones fulfil the given stress criteria.

4. Conclusions

It was observed that the value of turbulence kinetic energy vortex core region is 2.14e-5, which is negligible. Therefore, no problem occurs during the fluid flow.

The stress accumulated without the stiffener is 384.653 N/mm^2, which exceeds the safer allowable stress (240 N/mm^2).

The stress accumulated with the stiffener is 171.853 N/mm^2, which does not exceed the safer allowable stress (240 N/mm^2).

Thus, with the help of stiffener, we can reduce stress.

Reference

Adamkowski, A., & Kwapisz, L. (2004). Strength analysis of penstock bifurcations in hydropower plants. *Transactions of the Institute of Fluid-Flow Machinery*, *115*, 113–124.

Aguirre, C. A., & Camacho, R. G. R. (2014). Head losses analysis in symmetrical trifurcations of penstocks—High pressure pipeline systems CFD. *CamachoInstituto de Engenharia MecâNica, Universidade Federal de Itajubá*.

Alligne, S., Rodic, P., Arpe, J., Mlacnik, J., & Nicolet, C. (2014). Determination of Surge Tank Diaphragm Head Losses by CFD Simulations. https://doi.org/10.1007/978-981-4451-42-0

Anand, R. S., Jawahar, C. P., Bellos, E., & Malmquist, A. (2021). A comprehensive review on Crossflow turbine for hydropower applications. *Ocean Engineering*, *240*, 110015.

Kandel, B., & Luitel, M. C. (2019). Computational Fluid Dynamics Analysis of Penstock Branching in Hydropower Project. *Journal of Advanced College of Engineering and Management*, *5*, 37–43.

Koirala, R., Chitrakar, S., Neopane, H. P., Chhetri, B., & Thapa, B. (2017). Computational design of bifurcation: a case study of Darundi Khola hydropower project. *International Journal of Fluid Machinery and Systems*, *10*(1), 1–8.

O'Brien, V., Ehrlich, L. W., & Friedman, M. H. (1976). Unsteady flow in a branch. *Journal of Fluid Mechanics*, *75*(2), 315–336.

Thapa, D., Luintel, M. C., & Bajracharaya, T. R. (2016). Flow Analysis and Structural Design of Penstock Bifurcation of Kulekhani III HEP. In *Proceedings of IOE Graduate Conference* (pp. 271–276).

Xuan, F.-Z., Li, P.-N., & Tu, S.-T. (2006). Limit load analysis for the piping branch junctions under in-plane moment. *International Journal of Mechanical Sciences*, *48*(4), 460–467.

Zhou, Y., & Bryant, R. H. (1992). The optimal design for an internal stiffener plate in a penstock bifurcation.

Židonis, A., Benzon, D. S., & Aggidis, G. A. (2015). Development of hydro impulse turbines and new opportunities. *Renewable and Sustainable Energy Reviews*, *51*, 1624–1635.

Determination of Geomorphic Indices for Jure Landslide

Roshan Shrestha[1], Ram Chandra Tiwari[2]

[1]M.Sc. Student, Department of Civil Engineering, Institute of Engineering Pulchowk Campus, Tribhuvan University, Nepal
[2]Assistant Professor, Department of Civil Engineering, Institute of Engineering Pulchowk Campus, Tribhuvan University, Nepal

†Corresponding author. Phone: +977-49847367311, Email: rctiwari1975@gmail.com

Abstract

Landslide damming is a complex process which is why it is difficult to predict them. This research aims to determine the geomorphic indices namely MOI (Morphological Obstruction Index) and HDSI (Hydromorphological Dam Stability Index). These values define the possibility of any landslide resulting in the formation of natural dams and also determine the stability of resulting natural dams. These indices are gaining popularity all over the world to determine the possibility of damming phenomenon of rivers due to landslides as well as the stability of these naturally formed dams. The Jure landslide is taken as the study area. The parameters required for their calculation are derived from the related works of literature. The value of these indices concludes that there is the possibility of damming of Sunkoshi River due to the Jure landslide. Additionally, it is also found that the result natural dam would be unstable on its own.

Keywords

Jure Landslide, Geomorphic indices, Landslide Damming,

1. Introduction

1.1 Background

Nepal is a country where there is the occurrence of natural hazards in the form of earthquakes. Landslide, flood, avalanche, GLOF (Glacial Lake Outburst Flood), and many more. Among them, a landslide is one of the most frequent and devastating hazards. These landslides have the possibility to dam the rivers when they reach the river section. These landslides also commonly block rivers, which results in the construction of landslide dams. When these dams are prevalent, flooding is frequently caused in the upstream areas, and flooding is caused when they fail in the downstream areas.

According to Evans et al. (2011), landslide damming is a typical geomorphic phenomenon that occurs in confined river valleys and is frequent in steep terrain (Costa and Schuster, 1991). Depending on the size, material, stream power, upstream catchment area, and valley breadth of the dam, the duration of the damming operation before it breaches may range from days to years (Li et al., 1986; Costa and Schuster, 1987). These dams may develop as a result of avalanches, rock falls, or debris flows.

To determine the likelihood of landslide damming, it is essential to consider the landslide volume, stream power, and morphological setting of the valley. Geomorphic indices are the best option to incorporate them. There is widespread use of the geomorphic indices Morphological Obstruction Index (MOI) and Hydromorphological Dam Stability Index (HDSI) to predict the possibility of landslide dam development and their temporal stability (Costa and Schuster, 1987; Ermini and Casagli, 2002; Carlo Tacconi Stefanelli, Segoni, Casagli, & Catani, 2016).

1.2 Geomorphic Indices

Two geomorphic indices namely MOI (Morphological Obstruction Index) and HDSI (Hydromorphological Dam Stability Index) are used to determine the possibility of landslide dam formation. Carlo Tacconi Stefanelli, Segoni, Casagli, & Catani, (2016) derived these equations on the basis of 300 cases which are as follows:

i. Morphological Obstruction Index (MOI)

$$\mathbf{MOI = \log (V_l/W_v)} \quad \ldots\ldots\ldots\ldots\ldots\ldots\ldots\ldots\ldots\ldots \quad (1)$$

ii. Hydro-morphological Dam Stability Index (HDSI)

$$\mathbf{HDSI = \log (V_d/A_b * S)} \quad \ldots\ldots\ldots\ldots\ldots\ldots\ldots\ldots \quad (2)$$

Where, Vd (dam volume) = Vl (landslide volume, m3), Ab is the upstream catchment area (km^2), Wv is width of the valley (m) and S is local slope gradient of river channel ($m\ m^{-1}$). Dam volume is assumed to be equal to landslide volume for the worst case.

By utilizing the comprehensive dataset of 300 landslide dams of Italy, Carlo Tacconi Stefanelli, Segoni, Casagli, & Catani, (2016) have classified the MOI into

a. non-formation domain (MOI<3.00),
b. uncertain evolution domain (3.00<MOI>4.60),
c. Formation domain (MOI>4.60).

By utilizing the same dataset, Carlo Tacconi Stefanelli, Segoni, Casagli, & Catani, (2016) defined the HDSI into following categories:

a. Instability domain (HDSI<5.74)
b. Uncertain determination domain (5.74<HDSI>7.44)
c. Stability domain (HDSI>7.44).

Many literatures were reviewed in the process of this research. Most of the literatures revealed that the volume of Jure landslide was between 50 to 60 million cubic metres. Hence, the dam volume that is required for the estimation of these indices is taken as the landslide volume i.e 55 million cubic metres (MOI, 2014).

The average of the entire run of the river valley, which is taken to be 30m, is used to calculate the river's width. According to the river's profile, which was collected from Google Earth, the river's slope is assumed to be 5%. With the use of ArcGIS software, the upstream catchment that would contribute to the flow up to the place of landslide occurrence is computed. The graphic below depicts the upstream catchment area:

2. Study Area

2.1 Study Area

The research region is situated in Nepal's Sindhupalchowk district. It is situated between latitudes of 27°45'19.75" and 27°47'29.75"N and longitudes of 85°54'15.37" and 85°51'39.77"E, 70 km northeast of Kathmandu Valley. The study area has a river running through it and is primarily mountainous in nature. The Araniko highway, which follows the Sunkoshi River and links to the Chinese border at Kodari, passes through the region. The climate there is subtropical, temperate, and alpine. There is 3604.3 ml of rainfall, of which 80 percent falls during the monsoon season, and temperatures range from 28.5° to 4.0° C. (Nepal Tourism Board, 2008). The Kuncha formation, which includes phyllitic quartzites, meta-sandstones, and uncommon basic rock types, is made up of fine-grained quartz-conglomerates.

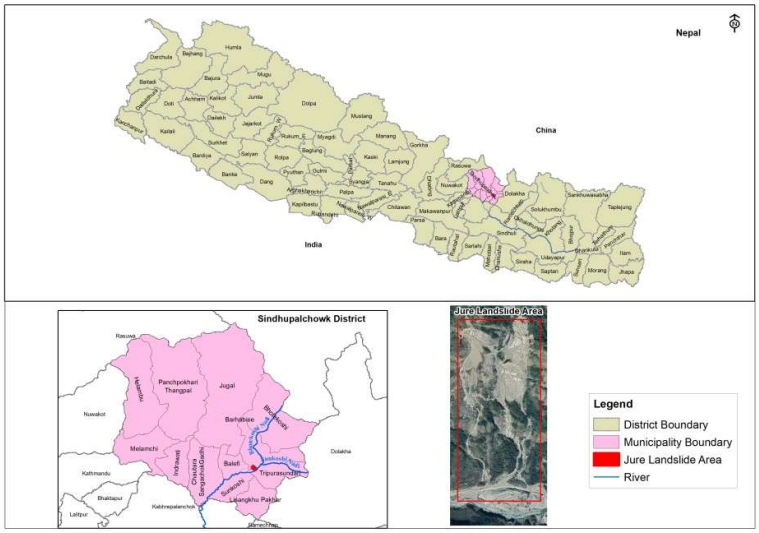

Figure 1: Location Map of Study Area

2.2 Study Event

On August 2, 2014, at roughly 2:36 am, a landslide with a solid volume of 5 to 7 million cubic meters occurred in Jure, which is located around 80 km northeast of Kathmandu, the capital of Nepal. The coordinates of its location are 27°46'1.55"N and 85°52'17.10"E, respectively. (Panthi, 2021). The landslide had large rock fragments, sand, and dirt, and it was a typical slope collapse. It blocked the Sunkoshi River's waterway by dumping a

significant amount of material there. It took over 12 hours for the lake to fill, overflow the debris dam, and perhaps cause a Lake Outburst flood. By blasting away a portion of the landslide blockage, the lake was made accessible and the water's discharge was facilitated. The slide resulted in the deaths of 156 individuals who were sleeping in their homes, the displacement of 436 people, the destruction or burial of 120 homes, partial damage to 37 homes, and complete damage to a section of the Araniko highway of about 2 km.

3. Methodology

The study started with desk study where different literatures were studied thoroughly. The detail geology of the place along with the climatic condition and the seismicity of the area were studied. The data required for the calculation of these indices were gathered after detail study of related literature.

The volume of landslide is taken as 5 million cubic metres. The width of the river is determined by taking average of the whole reach of the river valley and is taken is 30m and also verified through literatures.(Khanal & Gurung (ICIMOD), 2014) The slope of the river is taken as 5% which is determined from the profile of the river obtained from Google Earth. The upstream catchment which would contribute to the flow up to the point of landslide occurrence is calculated with the help of ArcGiS software. Area upto China in the North contributes to the catchment area up to the landslide area. The upstream catchment area is as shown in the figure below:

Figure 2: Upstream Catchment Area

The pink portion represents the area of China (1997.72 sq. km) which contributes to the catchment area up to landslide whereas the yellow portion represents the area of Nepal (492.85 sq. km) contributing to the catchment area to the same point.

The data thus required and used for the calculation are presented in table below:

Table 1- Parameter Required for Determining Geomorphic Indices

Volume of Landslide($m^{3)}$	Width of the valley(m)	Upstream catchment Area(km^2)	Local Slope Gradient of River Channel (mm^{-1})
55,00,000	30	2490.57	0.05

4. Results

The values of geomorphic indices thus obtained are as follows:

Table 2- Results of Geomorphological Indices

Morphological Obstruction Index(MOI)	Domain	Hydro morphological Dam Stability Index(HDSI)	Domain
5.38	Formation Domain	4.65	Instability Domain

The results indicate that the value of MOI is 5.38 which is greater than 4.6 which is why there is possibility of damming of Sunkoshi River due to Jure landslide. Furthermore, the value of HDSI is 4.65 which is greater than which is less than 5.74 which indicates that the resulting natural dam thus formed due to Jure landslide will be unstable in its own.

This is supported by the fact that the Sunkoshi River was dammed in 2014 as a result of the Jure landslide. After 36 days, the natural dam that was created at that period was breached.

5. Conclusions

This study concludes that the geomorphic indices can be used as a measure to determine the possibility of damming of any river due to landslide. These indices can further be used to check the initial stability of the resulting natural dam. This study can be useful for a country like Nepal where this phenomenon occurs time and again. These indices can further be used to develop early warning systems, mitigation models, and resettlement of population and preparation of land use maps. This simple preliminary estimation can be used to relocate the population and their possession well in advance before the occurrence of such catastrophic event.

Acknowledgement

The authors are thankful to the co-ordinator of Department of Geo-Technical Engineering, Pulchowk Campus. The authors are thankful to Mr. Uddhab Lal Karki for providing assistance related to the use of Arc Gis.

References

Costa, J. E., & Schuster, R. L. (1987). *The Foramtion and Failure of Natural Dams*. US Geological Survey Open-File Report 87-392, 39.

Costa, J. E., & Schuster, R. L. (1991). *Documented historical landslide dams from around the world*. Open-File Report (United States Geological Survey), 494. Retrieved from https://pubs.er.usgs.gov/publication/ofr91239%0Ahttp://pubs.er.usgs.gov/publication/ofr91239

Ermini, L., & Casagli, N. (2003). Prediction of the Behaviour of Landslide Dams using a Geomorphological Dimensionless Index. 47(October 2002), 31–47. https://doi.org/10.1002/esp.424

Evans, S.G., Delaney, K.B., Hermanns, R.L., Strom, A., Scarascia-Mugnozza, G., (2011). *The formation and behaviour of natural and artificial rockslide dams; implications for engineering performance and hazard management*. In: Evans, S.G., Hermanns, R.L., Strom, A., Scarascia-Mugnozza, G. (Eds.), Natural and Artificial Rockslide Dams. Springer Verlag Berlin Heidelberg, pp. 1e75. https://doi.org/ 10.1007/978-3-642-04764-0.

Khanal, N. R., & Gurung, D. R. (2014). ICIMOD rapid field investigation: Jure Landslide Dam Site, Sindhupalchowk District, Nepal. (August), 1–7.

Li, T., Schuster, R. L., and Wu, J. (1986). *Landslide dams in south-central China*. In: Proc. of the Landslide dams: processes, risk, and mitigation, ASCE Convention, Washington, 146–162,

MoI. (2014). Ministry of Irrigation Report on Jure Landslide, Mankha VDC, Sindhupalchowk District. 1–29.

Panthi, K. K. (2021). *Assessment on the 2014 Jure Landslide in Nepal - A disaster of extreme tragedy*. IOP Conference Series: Earth and Environmental Science, 833(1). https://doi.org/10.1088/1755-1315/833/1/012179

Tacconi Stefanelli, Carlo, Segoni, S., Casagli, N., & Catani, F. (2016). *Geomorphic indexing of landslide dams evolution*. Engineering Geology, 208, 1–10. https://doi.org/10.1016/j.enggeo.2016.04.024

Minimizing Disputes in the Implementation of Water Supply Projects in Nepal

Manoj Kumar Sharma[1]†

[1]Graduate Student, MSc Engineering Management, HIST Engineering College, Purbanchal University, Nepal
[1]Director, Building Design Authority Pvt. Ltd.
† Corresponding author. Phone: +977-9851043457, Email: manozkrsharma@gmail.com

Abstract

Water supply falls under priority projects of the government. The constitution of Nepal has ensured these services as a fundamental right. The long-term vision of the government is 'Prosperous Nepal, Happy Nepali' by making Nepal a high-income country by 2043 for which safe drinking water is the basic need. So far, 84% of the people of the nation have access to drinking water. However, drinking water services are not safe, reliable, and sustainable yet, as per the expectations. Due to various causes, the construction projects are seldom completed in time resulting in cost overruns, and disputes. Disputes arises from the initial stage of design and documentation to the final implementation of construction works. Poor preparation of design, bid document, technical specifications, bill of quantities, etc. during the design phase, and change in site condition, geological condition of the site, poor quality of works, etc. are some of the causes of disputes during construction works. It has been observed that due to disputes in construction, the construction works prolong for years and years. They are not completed in the stipulated timeframe, which ultimately overruns the cost of the project. The water supply sector is the most important sector as it is related to the basic needs of human beings. Delay in implementation of water supply projects affects, to a great extent, the life of the people. Due to the lack of safe drinking water, the life of thousands of people is badly affected. Hence, it is necessary to make the construction industry free from disputes, which is not possible most of the time. Nevertheless, it can be minimized. Among various impacts of disputes, cost overrun, time overrun, additional expenses in management and administration, dissatisfaction and stress, loss of company reputation, idling of resources, etc. are the major ones. The study shows that disputes are inevitable in construction water supply projects. Therefore, it is not possible to implement dispute-free construction of water supply projects. Nonetheless, it can be minimized to a great extent if the measures to minimize disputes, as identified, are followed in different stages of implementation of water supply projects.

Keywords

Water supply project; Dispute minimization; Impact analysis

1. Introduction

Drinking water and sanitation services have a multidimensional impact on human life. Therefore, the constitution of Nepal has ensured these services as a fundamental right. Moreover, specific goals have been set in the sector of drinking water and sanitation as per the Sustainable Development Goals (SDG) set internationally. Access of people to these facilities has reduced the infant mortality rate and increased life expectancy. It has also increased productive hours by improving the health status of people and positively contributed to improving the social behaviour of people as well as the school attendance of children.

In Nepal, the Department of Water Supply and Sewerage Management (DWSSM) implement most of the water supply projects, while some of the water supply projects are implemented by other departments like the Department of Urban Development and Building Construction (DUDBC), Nepal Water Supply Corporation (NWSC), Kathmandu Upatyaka Khanepani

Limited (KUKL), etc. However, the study focuses on the water supply project implemented by DWSSM as they are the ones who are implementing water supply projects on a large scale.

With the increase in construction, disputes are also increasing day by day. Thus, the study is focused on how to implement dispute-free construction, especially in the water supply sector. For this, the main causes of disputes during the implementation of construction works of water supply projects have been found out and then necessary measures for minimization of those disputes have been identified. The study has also found the impact of disputes on the construction of water supply projects. The design problem starts from the poorly detailed engineering survey. When there is an error in the engineering survey then that is carried over to detailed engineering design. This causes disputes during construction works. Also, most of the time, the detailed designs are not reviewed by experts, and errors in design are found during the construction work that may result in a dispute.

Disputes require resolution and therefore, are associated with distinct justifiable issues. The resolution process may lend itself to third-party intervention. 10–30% of construction projects experience serious disputes. The dispute is not because a claim has been submitted but because it has not been admitted (Tayeh, Alaloul, & Muhaisen, 2019). The complexity of construction projects is continuously increasing which increases the complication of contracts and the disputes probability that might arise at any stage in the project lifecycle. Therefore, disputes are almost unavoidable in construction projects. It is normally trusted that owners' initial choices regarding the selection of delivery methods, procurement methods, and contract types influence the recurrence and seriousness of project disputes. In this context, the construction projects are the fertile seedbeds for disputes (Alaloul, Liew, Zawawi, & Mohammed, 2018).

Disputes are one of the main factors which prevent the successful completion of the construction project. Thus, it is important to be aware of the causes of disputes to complete the construction project in the desired time, budget, and quality (Cakmak & Cakmak, 2014). Several factors contribute to developing disputes in construction projects, among these are the adversarial nature of contracts, poor communication between the parties, ineffective communication on site, inability to understand the terms of the contract, different expectations of the parties, fragmented nature of the industry, improper contractual documentation, tender systems and government policy on tendering, inability or reluctance to pay, and unforeseen effect of third party interests (Karthikeyan & Manikandan, 2017; Shash & Habash, 2021; Younis, Wood, & Malak, 2008).

The main areas causing disputes are contract, defective work, variations or extra works, delays, an extension of time, latent conditions, failure to adequately document the works, and failure to adequately document the daily events (Eilenberg, 2003). The most important eight factors that convert claims into disputes which are identified as: delayed interim payment from client, qualification of teamwork, an extension of time, incomplete drawings and specification, poorly written contracts clauses, change orders, cooperation and communication nature among project team, and late supply of equipment and materials (Mohamed, Ibrahim, & Soliman, 2014).

The impact on construction works due to disputes are damaged business relationships, increased project costs, project delays, undermining team spirit, damaged company reputation, dispute escalation, poor client satisfaction, and delay in project completion (Equbal, Banerjee, Khan, & Dixit, 2017). The main effects of conflicts are disputes, arbitration, time overrun, quality of work, wasted resources, lack of new idea, idling of resources, decreased productivity, poor quality of work due to hurry, negative social impact, poor decision making, cost overrun, dissatisfaction and stress, increased costs and litigation (Aryal & Dahal, 2018).

The various strategies to prevent disputes in construction projects are designing contract conditions that are fair to all parties (allocating projects risks fairly to all parties), understanding contractual documents before proceeding into an agreement, proper planning and organization of payment and schedule, payment as at when due, maintaining a good relationship between the clients, professionals, and workers, engaging the organization professionals, engaging the organization trained artisans/labors (Ramonu et al., 2018). The most significant factors for 'no-dispute' performance, which are: owners need thoroughly understood and defined; regular monitoring and feedback by top management; adequate communication among all project participants; availability of resources as planned throughout the project; and timely and valuable decision from top management (Tabish & Jha, 2011).

Due to disputes in construction, the progress of works is likely to be hampered. Therefore, it would be desirable to implement the construction of water supply projects free from disputes, i.e., zero disputes. However, most of the time, it is not possible. As the study has endeavored in finding causes, impacts, and minimization of disputes in the implementation of water supply projects in Nepal, it would be very helpful to Employers and Engineers/Consultants to avoid possible conflicts/disputes during the construction works. This will also be helpful to the Contractors as it would save the construction time, additional overheads, reputation of the company, etc. Disputes have always had a negative impact on projects. Thus, the research on minimizing disputes in the implementation of water supply projects would be very useful to all stakeholders of projects in many ways to avoid or minimize disputes during the construction period.

2. Research Methodology

The methodology undertaken about the research paradigm, sampling process, and data collection and analysis techniques used to study minimizing disputes in the implementation of water supply projects in Nepal. After the literature review, a questionnaire was formulated to gather information from different stakeholders like employers, consultants/engineers and contractors of the projects on different relevant issues and topics. The questionnaire was of objective type - multiple choice, rating scale, yes-no, and mixed questions so that they were easy to analyze and interpret.

For this study, thirty-five (35) projects have been selected as sample projects among the population of nearly 85 projects including first (29), second (21), and third (19) small towns water supply and sanitation sector projects and urban water supply and sanitation project (16) of DWSSM. The projects are selected randomly considering the geographical location; Terai,

Mountain, and Hill, contractors, type of projects (gravity flow, underground), etc. For the purpose of the research, 19 sub-projects under TSTWSSSP and 16 sub-projects under UWSSP of DWSSM have been studied. In TSTWSSSP, the Employer had engaged 2 (two) Consulting firms, one for eastern and another for western, and a team of management Consultants named DRTAC (Design Review and Technical Audit Consultant). For each Eastern as well as Western region, Regional Project Management Office (RPMO) headed by the Regional Project Manager (RPM) had been established by PMO to manage and monitor the construction activities of the town projects. Similarly, for 16 sub-projects under UWSSP, the Employer has engaged 3 consulting firms, one for eastern, one for western, and one for the central region and a team of management consultants named PMQAC (Project Management and Quality Assurance Consultant). The Regional Project Management Offices (RPMOs) for TSTWSSSP also look after the UWSSP respectively of Western and Eastern Regions. The projects under the central region are managed and monitored by PMO. Construction of each town is being carried out by one Contractor (either single or in a joint venture). However, some Contractors have got two or more projects.

As the Employer and Consultant are the same for most of the sub-projects, calculating the target population considering the number of Employers, Consultants, Contractors, etc. involved in the projects (TSTWSSSP and UWSSP) instead of several sub-projects. Thus, the target population:

Table 1 Target Population Involved in the Project

Entity Involved in Project	Number
Contractor	24
Consultant	10
Employer (PMO-1, RPMO-2)	3
DRTAC	1
PMQAC	1
Total Population	39

There are many methods available to determine the size of the sample for the study. The following Slovin's formula (1960) can be used to calculate Sample Size if the population size is finite and known:

$$n = \frac{N}{1+Ne^2}$$

Where n = Sample size
N = Population size
e = Margin of error

Here, the Sample Size of the Population = 39
The margin of error assumed to be = 5%

Therefore, n $= \frac{39}{1+3 \times (0.05)^2} = \frac{39}{1.0975} =$ 35.54
$=$ 36 numbers

In addition to the above, to obtain independent opinions on the subject matter, some independent individual consultants, experts, specialists, adjudicators/arbitrators, etc. on water

supply projects were interviewed. Though an exact number of individual consultants, experts, specialists, adjudicators/arbitrators, etc. in the water sector is not known, information from 50% of the calculated Population was surveyed as an independent population. 50% was chosen so that it did not dominate or supersede the opinion of a calculated sample of persons involved in the projects.

50% of total population = 0.5 x 36 = 18

Thus, taking 18 individual consultants, experts, specialists, freelancers, etc. for the questionnaire survey.

Target population = 36 + 18 = 54

Thus, a questionnaire survey was conducted for 54 numbers of sample sizes.

A case study can be defined as an intensive study about a unit, which is aimed to generalize over several units. A case study has also been described as an intensive, systematic investigation of a single individual, group, community, or some other unit in which the researcher examines in-depth data relating to several variables. Hence, out of 35 sub-projects (19 TSTWSSSP and 16 UWSSP) under study, the sub-projects in which disputes (disputes which were not resolved by employer or consultant but referred to Adjudicator/Arbitrator or Litigation) had arisen were studied intensively regarding causes of disputes and impacts of disputes. This helped to validate some of the responses received through the questionnaire survey.

The formulated questionnaire was developed into Google Forms. Google Forms is online software that allows creating surveys and quizzes, and it's part of Google's web-based apps suite, including Google Docs, Google Sheets, Google Slides, and more. It's a versatile tool that can be used for various applications. Google Forms collects information from people via personalized quizzes or surveys. The information is then connected to a spreadsheet on Sheets to automatically record the answers. The spreadsheet then populates with the responses from the survey in real-time. It analyses the collected data automatically and gives the result in a pie chart, histogram, etc. as customized.

The purpose of the analysis was to establish the relative importance of the various factors identified as responsible for disputes, their impact, and the minimization or elimination of disputes. The Relative Importance Index (RII) method was applied to prioritize the causes, impacts, and minimization of dispute factors. The score for each factor is calculated by summing up the scores given to it by the respondents. The RII was calculated using the following formula (Fagbenle et al., 2004):

$$RII = \frac{\Sigma W}{\mathrm{A \times N}}$$

Where,
W is the weightage given to each factor by the respondents, which ranges from 1 to 5
A is the highest weight on the scale
N is the total number of respondents

The higher the value of RII, the more important is the cause or impact or minimization of dispute factors.

A sample example of RII calculation is shown below:

Table 2 Sample RII calculation

S.N.	Factor (Cause of dispute)	Very Low (1)	Low (2)	Moderate (3)	High (4)	Very High (5)	Total
1	Poorly written contract clauses	3	12	10	15	11	51

$$= \frac{3*1+12*2+10*3+15*4+11*5}{5*51} = 0.675$$

3. Results and Discussions

Out of 54 numbers of the sample population (respondents), 51 respondents (94.44%) responded, which was an outstanding achievement. This shows that respondents had a keen interest in the subject matter, i.e., disputes, their impact, and minimization in water supply projects. This also shows that they are well familiar with the subject matter and wanted some research outcome on it.

3.1. Causes of disputes in the implementation of water supply projects

3.1.1 Contract documents (contract, design, drawing, specification) related factors

Incomplete design, drawings, and specifications are the prime cause of disputes due to contract document-related factors in the implementation of a water supply project with RII 0.820 followed by errors and omissions in design drawings with RII 0.733. The third major cause of disputes is incomplete information in bid documents with RII 0.708. The other 8 causes of disputes due to contract document-related factors in priority wise are discrepancies/ambiguities in the contract documents, poorly written contract clauses, unfair allocation of risks, contradiction in contract documents, different interpretations of the contract provisions, errors and omissions in the contract terms, incorrect procurement/tendering method and misplacement of priority.

3.1.2 Employer-related factors

The prime cause of disputes due to employer-related factors in the implementation of the water supply project is delay in the decision by the employer with RII 0.776 followed by delay in access to the site with RII 0.769. The third major cause of disputes is interfering in the execution of the contract by the employer with RII 0.729. The other 7 causes of disputes due to employer-related factors in priority wise are supremacy of employer, unrealistic time/cost/ quality targets (by employer), delay in payment of IPC, design variations initiated by the employer, excessive change order/ change of scope, non-payment of interest on late payment and unilateral early termination of the contract.

3.1.3 Consultant/engineer-related factors

Poor site investigation (engineering survey, soil investigation, etc.) is the prime cause of disputes due to consultant/engineer-related factors in the implementation of water supply project with RII 0.788 followed by delay in decision with RII 0.765. The third major cause of disputes is errors and omission in design (default design) with RII 0.733. The other 7 causes of disputes due to consultant/engineer-related factors in priority wise are errors and omissions in BoQ, change in site conditions, errors and omissions in the specification, delay in issuing construction drawings, quality control in design, application of liquidated damages to the contractor, delay in recommending IPC.

3.1.4 Contractor-related factors

Delay in work progress (time overrun) is the prime cause of disputes due to contractor-related factors in the implementation of the water supply project with RII 0.788 followed by misuse of advance payment with RII 0.776. The third major cause of disputes is low bidding with RII 0.768. The other 11 causes of disputes due to contractor-related factors in priority wise are contractor's noncompliance with design, drawings, specifications, extension of time (EoT) and prolongation cost, technical inadequacy, lack of deployment of skilled workers, defective construction (poor quality of works), use of unauthorized sub-contractor, non-payment to sub-contractor, non-submission of as-built drawings/ O & M Manual, inadequate contract administration, delays in handing over the project site, unrealistic/exaggerated claims for variations of works.

3.1.5 Human behavior-related factors

Lack of communication is the prime cause of disputes due to human behavior-related factors in the implementation of a water supply project with RII 0.728 followed by lack of team spirit and attitude and behavior of managers towards workers with RII 0.688. The third major cause of disputes is personality traits with RII 0.628. The fourth and fifth cause of disputes due to human behavior-related factors are cultural issues and personality traits respectively.

3.1.6 External factors

Outside people interruption is the prime cause of disputes due to external factors in the implementation of the water supply project with RII 0.698 followed by force majeure with RII 0.678. The third major cause of disputes is inflation with RII 0.667. The other 3 causes of disputes due to external factors in priority wise are adverse weather condition, change in act/laws, regulations, policy and labor dispute/union strike.

3.1.7 Other factors

Differing site condition is the prime cause of disputes due to other factors in the implementation of the water supply project with RII 0.718 followed by cost overrun with RII 0.716. The third major cause of disputes is sudden increases in cost for materials and fuels with RII 0.678. The other 9 causes of disputes due to other factors in priority wise are unclear instructions from consultant/engineer, unforeseen site condition, extra item, price escalation, breach of contract

by any party, fraud act of any party, suspension of works, insurance and indemnity and acceleration of works.

3.2. Impact of disputes on the construction of water supply project

3.2.1 Major impact of disputes on the construction of water supply projects

Cost overrun is the major impact of disputes on the construction of water supply projects with RII 0.852 followed by time overrun with RII 0.827. The third leading impact of disputes is additional expenses in management and administration with RII 0.804. The other 12 impacts of disputes on the construction of water supply projects with priority wise are dissatisfaction and stress, loss of company reputation, idling of resources, loss of professional reputation, loss of profitability, damaged business relationship, loss in revenue, loss of productivity, arbitration, adverse impact on the overall national economy, litigation and abandonment of project.

3.3. Measures to minimize disputes in the implementation of water supply project

3.3.1 Design and documentation stage

Detailed and thorough site investigations is the major measure to minimize disputes in the implementation of water supply projects with RII 0.873 followed by the employment of proper expert/manpower during design as per ToR with RII 0.863. The third leading measure to minimize disputes is fixing properly (scientifically/logically) project duration with RII 0.863. The other 6 measures to minimize disputes in the implementation of water supply projects in priority wise are flawless/clear-cut (without any ambiguity) contract documents, sufficient design time, thoroughly define the scope of work, fair allocation of risks, peer review of contract documents and freeze design.

3.3.2 Tendering stage

Site visit before bidding by bidders is the major measure to minimize disputes in the implementation of a water supply project with RII 0.863 followed by understanding contractual documents before proceeding into an agreement with RII 0.836. The third leading measure to minimize disputes is detailed information about the project to bidders with RII 0.824. The other 3 measures to minimize disputes in the implementation of water supply projects in priority wise are rejection of substantially low bid, pre-bid conference and escrow bid documents (EBD).

3.3.3 Construction stage

Timely decision is the major measure to minimize disputes in the implementation of water supply projects with RII 0.898 followed by the use of quality manpower and materials by the contractor as per specification and close supervision of construction work by consultant/ engineer with RII 0.863. The third leading measure to minimize disputes is adequate communication among all project participants with RII 0.840. The other 9 measures to minimize disputes in the implementation of water supply projects in priority wise are forwarding of IPC on time, payment within the due date, use of sub-contractor with proven capacity by the contractor, engaging the organization trained artisans/labors by the contractor, avoid/minimize the change in scope/design during implementation, preparation and

implementation of 'Conflict Management Plan', close contract administration and setting up of Dispute Board (DB)/ Adjudicator before the start of construction.

3.4. Case study

Having studied all 35 sub-projects (19 under TSTWSSSP and 16 under UWSSP), one of the projects named Tamsariya Nawalparasi Town Water Supply and Sanitation Sector Project was found in disputes. Hence, a case study has been conducted in this project to verify whether real causes of disputes in the implementation of water supply projects and real impacts of disputes on the construction of water supply projects validate the causes and impacts of disputes identified through secondary data and primary data (questionnaire survey).

The case study validates the following causes of disputes in the implementation of water supply projects:

a. 'Supremacy of Employer' under employer-related factors, as it was observed that the employer did not approve the consultant's recommended extension of time. Non-approval of consultant's recommendation also justifies the causes of disputes due to 'Decisions beyond one's authority' and 'Outrightly rejection of claim'.
b. 'Delay in Payment of IPC' and 'Non-payment of Interest on Late Payment' under employer-related factors as it was observed that the employer did not pay IPCs within time as well as did not pay interest on late payment as per contract.
c. 'Delay in Decision' under consultant-related factors as it was observed that the consultant's representative (construction supervision engineer at the site) had instructed one shade and pattern of color. However, after applying such color in some structures, the higher authority of the consultant changed the shade and pattern of color.
d. 'Application of liquidated damages to the contractor' under consultant-related factors. After the non-approval of EoT-3, the consultant applied liquidated damages to the contractor.
e. 'Delay in Work Progress (Time overrun), Extension of Time (EoT) and Prolongation Cost, Technical Inadequacy, Inadequate Contract Administration' under contractor-related factors as it observed that contractor had requested time extension again and again. It was also observed that the contractor had appointed almost a fresh engineer in place of an experienced Project Manager at the site. Similarly, the contractor's contract administration and management were observed very poorly.
f. 'Outside People Interruption' under external factors as it was observed that third party damaged laid pipes at some places.

The case study validates the following impacts of disputes in the implementation of water supply projects:

a. Loss of profitability of contractor,
b. A damaged business relationship,
c. Loss of professional reputation,
d. Loss of company reputation,
e. Cost overrun,
f. Additional expenses in management and administration, and
g. Arbitration.

4. Conclusions

Sixty-eight causes of disputes identified in the literature review were categorized into seven different groups based on their nature. Different respondents had different opinions on the significance or importance of the causes. Different causes of disputes under different factors are prioritized above.

Considering sixty-eight major causes of disputes in the implementation of water supply projects as identified and respondents' opinions, it is crystal clear that the construction of water supply projects is highly prone to disputes. Any potential cause of disputes, as identified and described may arise at any time during the construction period. Thus, disputes are inevitable in construction projects. Therefore, it is not possible to implement dispute-free construction of water supply projects. Nonetheless, it can be minimized to a great extent if twenty-seven measures to minimize disputes, as identified, are followed in different stages of implementation of water supply projects.

The impacts of disputes on the construction of water supply projects are immense. It hinders the work progress resulting in cost and time overrun. Besides other, projects may be abandoned due to disputes. Hence, the success of a construction project is inversely proportional to the Dispute (Success$\propto$1/Dispute), i.e., more the disputes in a project, less the success of the project, and vice-versa.

A contingency plan is executed when the risk presents itself. The purpose of the plan is to lessen the damage of the risk when it occurs. Without the plan in place, the full impact of the risk could greatly affect the project. The contingency plan is the last line of defense against the risk. Hence, preparation and implementation of the 'Risk and Contingency Plan' by the Employer as well as the Contractor are necessary, which would help to minimize disputes during the construction of the water supply project.

The Public Procurement Act 2063 has removed the provision of Adjudication to settle disputes and provisioned directly to go for Arbitration if not settled through mutual consent. However, the study shows that the provision of adjudication in the contract is necessary prior to arbitration to settle disputes.

The DWSSM lacks its Standard Technical Specification at present. At present, different consultants employed for different projects prepare the technical specifications for different projects. Most of the time they are copied and pasted, ambiguous, contradict with different items, etc., which creates disputes during the construction of water supply projects. Hence, it is necessary to develop a standard technical specification that would help to minimize disputes to some extent during the implementation of water supply projects.

Besides provision in the contract for adjudication, adjudication or DRB are not employed at the signing of the construction contract. The employer and contractor appoint an adjudicator when a dispute arises in the contract. Appointing an adjudicator at the beginning of construction helps resolve problems/issues before they take the shape of disputes.

A single party involves in the design and construction of a project in Engineering, Procurement & Construction (EPC) Contract or Turnkey Contract. The EPC contract minimizes disputes during construction to some extent.

Partnering is about achieving the best value for all parties using a flexible approach unrestrained by contractual barriers. It describes how parties will conduct themselves and the behavioral attitudes that will be adopted. However, it is different from creating a joint venture or a partnership. It can involve any or all of the consultants, employer, main contractor, and/or subcontractors. It is an arrangement based on openness, integration, and collaboration. The concept is when partnering takes place, the relationship among the parties changes from being linear up and down to the contractual chain and to being based on a desire to solve issues on a more equal footing. This might mean that the whole supply chain becomes involved in management decisions. Partnering among Employer, Consultant and Contractor minimizes disputes during the construction phase to a great extent.

The study shows that interest in late payment is never or rarely paid by the employer which is one of the factors of disputes.

In accordance with the Contract of TSTWSSP and UWSSP, an interest-free 15% mobilization advance is given against the unconditional bank guarantee to the contractor. The advance is given as an initial resource to the contractors to start and carry out the works in a smooth way without any initial investment from their pocket. However, the study shows that misuse of advance money is the second prime cause of disputes. It is because those monies are not used for the project works. This causes a delay in the completion of the project in the stipulated time, which is a source of dispute.

References

Alaloul, W. S., Liew, M. S., Zawawi, N. A. W. A., & Mohammed, B. S. (2018). Industry revolution IR 4.0: future opportunities and challenges in construction industry. In *MATEC web of conferences* (Vol. 203, p. 2010). EDP Sciences.

Aryal, S., & Dahal, K. R. (2018). A review of causes and effects of dispute in the construction projects of Nepal. *Journal of Steel Structure and Construction*, *4*(144), 437–2472.

Cakmak, E., & Cakmak, P. I. (2014). An analysis of causes of disputes in the construction industry using analytical network process. *Procedia-Social and Behavioral Sciences*, *109*, 183–187.

Eilenberg, I. M. (2003). *Dispute resolution in construction management*. UNSW Press.

Equbal, A., Banerjee, R., Khan, Z. R., & Dixit, R. B. (2017). Construction disputes in construction work sites and their probable solutions. *International Journal of Civil Engineering and Technology*, *8*(3), 74–81.

Karthikeyan, R., & Manikandan, T. (2017). A study on causes and effects of conflicts in Indian construction projects. *International Research Journal of Engineering and Technology (IRJET)*, *4*(3), 1153–1170.

Mohamed, H. H., Ibrahim, A. H., & Soliman, A. A. (2014). Reducing construction disputes

through effective claims management. *American Journal of Civil Engineering and Architecture*, *2*(6), 186–196.

Ramonu, J. A. L., Ilevbaoje, J. O., Olaonipekun, O. A., Omotosho, A., Owamah, H. I., & Adewole, T. A. (2018). Prevention of Conflict in Construction Industry Considering; Organization, Consultancy Firm, Contractual Firm and the Professionals Personnel in Nigeria. *International Journal of Civil Engineering and Technology (IJCIET)*, *9*(12), 472–484.

Shash, A. A., & Habash, S. I. (2021). Disputes in Construction Industry: Owners and Contractors' Views on Causes and Remedies. *Journal of Engineering, Project & Production Management*, *11*(1).

Tabish, S., & Jha, K. N. (2011). Important factors for success of public construction projects. In *2nd International Conference on Construction and Project Management IPEDR. Singapore: IACSIT Press*.

Tayeh, B. A., Alaloul, W. S., & Muhaisen, W. B. (2019). Challenges facing small-sized construction firms in the gaza strip. *The Open Civil Engineering Journal*, *13*(1).

Younis, G., Wood, G., & Malak, M. A. A. (2008). Minimizing construction disputes: the relationship between risk allocation and behavioural attitudes. *Women's Career Advancement and Training & Development in the*, *728*.

Programme

B.E.
Civil Engineering

M.Sc.
Engineering Management (EM)
Information System Engineering (ISE)

New Baneshwor, Kathmandu, Nepal
Phone: 01-4794951, 01-5202726
Cell No.: 9851088422, 9841296240
E-mail: info@hist.edu.np
Facebook: www.facebook.com/histcollege/